NOTICE

AVIS

The quality of this microform is heavily dependent upon the quality of the original thesis submitted for microfilming. Every effort has been made to ensure the highest quality of reproduction possible.

La qualité de cette microforme dépend grandement de la qualité de la thèse soumise au microfilmage. Nous avons tout fait pour assurer une qualité supérieure de reproduction.

If pages are missing, contact the university which granted the degree.

S'il manque des pages, veuillez communiquer avec l'université qui a conféré le grade.

Some pages may have indistinct print especially if the original pages were typed with a poor typewriter ribbon or if the university sent us an inferior photocopy.

La qualité d'impression de certaines pages peut laisser à désirer, surtout si les pages originales ont été dactylographiées à l'aide d'un ruban usé ou si l'université nous a fait parvenir une photocopie de qualité inférieure.

Reproduction in full or in part of this microform is governed by the Canadian Copyright Act, R.S.C. 1970, c. C-30, and subsequent amendments.

La reproduction, même partielle, de cette microforme est soumise à la Loi canadienne sur le droit d'auteur, SRC 1970, c. C-30, et ses amendements subséquents.

Canada

UNIVERSITY OF ALBERTA

MODELING BIOLOGICAL DRINKING WATER TREATMENT PROCESSES

BY

SHULIN ZHANG

A thesis submitted to the Faculty of Graduate Studies and Research in partial fulfillment of the requirements for the degree of **DOCTOR OF PHILOSOPHY**

IN

ENVIRONMENTAL ENGINEERING

DEPARTMENT OF CIVIL ENGINEERING

EDMONTON, ALBERTA

SPRING 1996

ISBN   0-612-10659-4

Canadä

UNIVERSITY OF ALBERTA

LIBRARY RELEASE FORM

NAME OF AUTHOR: **Shulin Zhang**

TITLE OF THESIS: **Modeling Biological Drinking Water Treatment Processes**

YEAR THIS DEGREE GRANTED: **1996**

Permanent Address:
301-1717 12th Street S.W.
Calgary, Alberta   .
Canada T2T 3M9
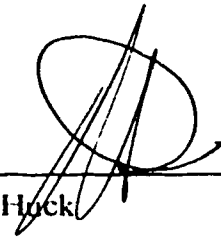
Date: January 31, 1996

UNIVERSITY OF ALBERTA

FACULTY OF GRADUATE STUDIES AND RESEARCH
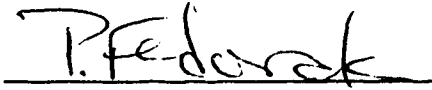
The undersigned certify that they have read, and recommend to the Faculty of Graduate Studies and Research for acceptance, a thesis entitled **MODELING BIOLOGICAL WATER TREATMENT PROCESSES** submitted by **SHULIN ZHANG** in partial fulfillment of the requirements for the degree of **DOCTOR OF PHILOSOPHY** in **ENVIRONMENTAL ENGINEERING**.

Dr. P. M. Huck
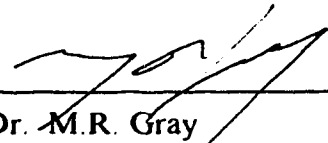
Dr. D.W. Smith
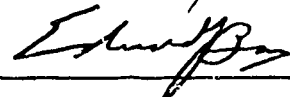
Dr. P.M. Fedorak

Dr. N.R. Morgenstern

Dr. M.R. Gray

Dr. E.J. Bouwer

Date: Jan. 31 , 1996

January 29, 1996

University of Alberta
Faculty of Graduate Studies and Research/
The University of Alberta Library

Dear Sir:

RE: Copyright Permission for Ph.D. Thesis
       by Shulin Zhang - Student ID 195604
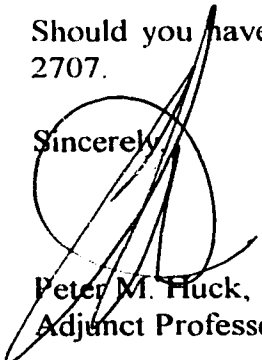
Please consider this letter as my formal permission for Mr. Shulin Zhang to use the contents of the following two articles in his Ph.D. thesis, entitled "Modeling Biological Drinking Water Treatment Processes":

> Zhang S. and Huck P.M. (1996)   Removal of AOC in biological water treatment processes: a kinetic approach. *Water Research*, in press.

> Zhang S. and Huck P.M. (1996)   Parameter estimation for biofilm processes in biological water treatment. *Water Research*, 30(20), 456-464.

Should you have any question in this regard, I can be contacted at (519) 888-4567 ext. 2707.

Sincerely,

Peter M. Huck, Ph.D. P.Eng.
Adjunct Professor

CC: S. Zhang

Dedicated to . . . . . .

My late grandmother.

Who shaped my spirit;

My Parents.

Who presented me the life to enjoy and to perceive; and

.

My wife.

Who fulfills my heart.

ACKNOWLEDGMENTS

ABSTRACT

A steady-state biofilm model was applied for modeling the removal of easily assimilable organic carbon (AOC) in biological drinking water treatment. It was found that there is an approximately linear relationship between substrate removal and influent concentration. The slope of the linear relationship, representing the approximate percentage removal of the substrate, is mainly determined by the dimensionless detention time (X^*), a quantity developed in this research. Percentage removal increases convexly with increasing X^*. Beyond a certain value of X^*, further increases achieve little improvement.

Four model parameters, kX_f (the product of the maximum specific rate of substrate biodegradation and biofilm density), K_s (the half velocity constant), S_{min} (the minimum substrate concentration for sustaining a steady-state biofilm) and D (average AOC diffusivity) were estimated using pilot and bench scale AOC data through data-fitting. The estimates for kX_f, S_{min} and D fell in the expected range of values. Both pilot and bench scale K_s estimates, although still considered reasonable, were higher than expected from the literature. Probably because of this intrinsically high K_s, kX_f and K_s estimates varied widely. A high K_s implies that AOC biodegradation kinetics can be approximated as first order.

The pseudoanalytical solution to the steady-state biofilm model used for the parameter estimation was originally derived by assuming a first-order dependence of biofilm detachment rate on biomass. In this research, the first-order relationship was found to unrealistically overestimate biofilm thickness from S_{min} estimates. This is attributed to the fact that biofilm detachment is often a complex process. A generalized definition of S_{min} was therefore proposed to accommodate many possible detachment mechanisms, whose relationship with S_{min} could be difficult to quantify. Such an S_{min} should be regarded as a distinct biofilm kinetic parameter and determined independently.

With the generalized S_{min} concept, a new solution requiring no assumption concerning biofilm detachment kinetics was devised for the steady-state biofilm model. However, the current pseudoanalytical solution should still be reasonable for describing substrate removal so long as S_{min} is independently measured *in-situ* or estimated through data-fitting.

TABLE OF CONTENTS

LIST OF TABLES

LIST OF FIGURES

NOMENCLATURE

b	sum of b_d and b_1 (T^{-1})
b'	overall first-order biofilm decay rate coefficient (T^{-1})
b_1	first-order biofilm detachment rate coefficient (T^{-1})
b_2	second-order detachment rate coefficient related to biofilm thickness $(L^{-1}T^{-1})$
b_d	endogenous-respiration decay rate coefficient (T^{-1})
b_g	biofilm detachment rate coefficient related to specific growth rate (L^{-1})
D	free liquid diffusivity $(L^2 T^{-1})$
D^*	dimentionless substrate diffusivity, $D^* = D/D_f$
D_f	diffusivity in a biofilm $(L^2 T^{-1})$
D_H	hydrodynamic dispersivity $(L^2 T^{-1})$
d_p	particle diameter of packed-bed media (L)
f	factor $f = J/J_{deep}$
f_{num}	value of factor f based on numerical solution
f_{pseudo}	value of factor f based on pseudoanalytical solution
f_{analy}	value of factor f based on analytical solution
J	substrate flux into a steady-state biofilm $(J, M_s L^{-2} T^{-1})$
J^*	dimentionless substrate flux into a steady-state biofilm, $J^* = J\tau/K_s D_f$
J_{deep}	substrate flux into a "deep" biofilm with $S_w=0$ $(J, M_s L^{-2} T^{-1})$
J_{deep}^*	dimensionless substrate flux into a "deep" biofilm, $J_{deep}^* = J_{deep}\tau/K_s D_f$
k	maximum specific rate of substrate utilization (T^{-1})
K_s	half velocity constant in Monod expression $(M_s L^{-3})$
L	thickness of effective diffusion layer (L)
L^*	dimentionless thickness of effective diffusion layer, $L^* = L/\tau$
L_f	biofilm thickness (L)

L_f^*	dimentionless biofilm thickness, $L_f^* = L_f/\tau$
Q	feeding flow rate to a completely mixed biofilm column (L^3T^{-1})
Q_r	recycle flow rate in a completely mixed biofilm column (L^3T^{-1})
Re	Reynolds number $R = vd_p\rho/\mu_w$
R	total biofilm loss rate $(M_xL^{-1}T^{-1})$
R_d	biofilm loss rate due to endogenous decay $(M_xL^{-1}T^{-1})$
R_{det}	biofilm loss rate due to detachment $(M_xL^{-1}T^{-1})$
R_g	biofilm growth rate $(M_xL^{-1}T^{-1})$
r_f	depth ordinate in a biofilm (L)
r_f^*	dimentionless depth ordinate in a biofilm (L).
S_b	bulk liquid concentration of substrate (M_sL^{-3})
S_b^*	dimentionless bulk substrate concentration, $S_b^* = S_b/K_s$
Sc	Schmidt number, $Sc = \mu_w/\rho D$
S_e	effluent concentration (M_sL^{-3})
S_e^*	dimensionless effluent concentration, $S_e^* = Se_i/K_s$
S_f	substrate concentration within the biofilm (M_sL^{-3})
S_f^*	dimensionless substrate concentration within the biofilm
S_i	influent concentration (M_sL^{-3})
S_i^*	dimensionless influent concentration, $S_i^* = S_i/K_s$
S_{min}	minimum substrate concentration for sustaining a steady-state biofilm (M_sL^{-3}).
S_{min}^*	dimentionless minimum substrate concentration, $S_{min}^* = S_{min}/K_s$
S_s	substrate concentration at biofilm outer surface (M_sL^{-3})
S_s^*	dimentionless substrate concentration at biofilm outer surface, $S_s^* = S_s/K_s$
S_w	substrate concentration at inner surface of the biofilm (M_sL^{-3})
S_w^*	dimensionless substrate concentration at substratum surface, $S_w^* = S_s/K_s$
t	time (T)
u	substrate utilization rate $(ML^{-3}T^{-1})$.

v	superficial flow velocity or hydraulic loading rate (LT^{-1})
V	volume of a biofilm reactor (L^-)
x	longitudinal distance along packed-bed biofilm column (L)
X*	dimentionless empty bed contact time
X_f	biofilm density (M_xL^{-3})
Y	biomass yield coefficient, M_x/M_s

Greek Letters

θ	empty bed contact time (T)
σ_J	standard deviation of J $(M_sL^{-2}T^{-1})$
σ_{Se}	standard deviation of S_e (M_sL^{-3})
β	$\beta = 0.5035 - 0.0257\tanh(\log S_{min}^*)$
γ	$\gamma = 1.5557 - 0.4117\tanh(\log S_{min}^*)$
ρ	density of water (ML^{-3})
τ	factor for dimentionless transformation, $\tau = (K_sD_f/kX_f)^{1/2}$ (L)
ε	porosity of packed bed
α	biofilm surface area in each unit volume of biofilm column (L^{-1})
μ_w	dynamic viscosity of water $(ML^{-1}T^{-1})$
μ	specific biomass growth rate (T^{-1})
χ	Dimensionless longitudinal distance along a biofilm column

Chapter 1

INTRODUCTION

In Europe, biological treatment has long been recognized as an important unit operation for producing biologically stable drinking water. However, it is only in recent years that the importance of biological treatment has started to be perceived by the North American water industry. Despite the fact that numerous biological water treatment facilities are in operation in Europe and that a large number of pilot scale investigations have been carried out in North America, there is still no rational basis for the design of these facilities.

The primary objective of this thesis is to present a framework to enable rational analysis and design of biological drinking water treatment processes. The background of biological water treatment processes, the specific objectives of this study and the structure of this thesis are introduced in the following sections.

BACKGROUND

Biological Drinking Water Treatment in North America

Biological treatment of drinking water is a rather new concept in North America. While in Europe biological treatment has long been recognized as an important unit operation for producing biologically stable drinking water, with few exceptions, it is not included in drinking water treatment trains in North America (Huck et al., 1991). The reasons for the European interest in drinking water biotreatment can be attributed to (1) the generally poorer surface water quality than in North America and, to some extent, (2) greater aesthetic demands of European consumers accompanied by more stringent regulatory limits on free chlorine residuals and chlorine disinfection byproducts in comparison with those in North America (Rittmann and Huck, 1989).

One of the most common problems in drinking water supply is biological instability. Substances creating biological instability can serve as electron donors in

bio-oxidation. These materials usually include biodegradable organics and ammonia. In some situations, biological instability of drinking water may also be attributed to Fe^{2+}, Mn^{2+}, NO_2^- dissolved H_2 gas, and several reduced species of sulfur. All of the components of biological instability share the common characteristic that they can be oxidized through microbiologically catalyzed reactions and provide energy and electrons for cell growth (Rittmann and Huck, 1989; Rittmann and Snoeyink, 1984).

In water distribution systems, these electron donors would provide substrate for the growth of microorganisms, which include pathogens. Bio-oxidation of these electron donors can also produce taste and odor and lead to accelerated corrosion. Traditionally, free chlorine is used in water distribution systems to suppress the biogrowth. In water treatment practice, chlorine is also used as an oxidant to oxidize those (mainly inorganic) electron donors to achieve relatively bio-stable water. Chlorine also reacts with many types of organic matter. While eliminating some bio-instability, chlorination on its own also produces some biodegradable organics. More importantly, chlorination produces chlorine-containing organic by-products, some of which, such as trihalomethanes (THMs), are suspected carcinogens. Finally, the regrowth of microorganisms attached to pipe walls or solid particles may still occur even with high free chlorine residuals (Lechevallier et al., 1987, 1988; Camper et al., 1986).

Biological treatment processes before chlorination can reduce the bio-instability and largely reduce the amount of chlorine required to achieve a certain residual of free chlorine, and therefore reducing the production of hazardous chlorination byproducts. The removal of organic carbons also help prevent the bioregrowth in distribution system by starvation, decrease the bacterial resistance to disinfectants, and thus reduce the free chlorine level required to inhibit regrowth (van der Kooij, 1990; Martin and Harakeh, 1990).

In recent years, the importance of biological treatment has been recognized by the North American water industry. Many pilot and full scale studies on biological drinking water treatment have been carried out in North America. It is believed that biological treatment will become an essential part of drinking water treatment in North America in the next decade (Rittmann, 1990). The reasons for its introduction to North American drinking water industry stem from the promulgation of more stringent

drinking water standards for THMs and other chlorination byproducts and the deterioration of surface water quality by hazardous organic compunds. Although careful control of the amount and location of chlorination might, to some degree, reduce the production of chlorination by-products, the water industry still faces strong pressure from new regulations on hazardous organic materials. Biotreatment is an attractive option for the removal of some hazardous organics (Rittmann and Huck, 1989).

Biodegradable Organic Matter

Bio-unstable compounds most commonly involved in drinking water are ammonia and organic compounds (Rittmann and Huck, 1989). Stabilization of the other inorganic bio-unstable compounds may occur in accompaniment with the biostabilization of ammonia and organics. Biological treatment of drinking water is also used for denitrification to remove high concentrations of NO_3^--N (Bouwer and Crowe, 1988). In denitrification the nitrate pollutant is an electron-acceptor. The scope of this thesis, however, is limited to organic carbon removal because elevated ammonia levels are not a general problem in North America (Huck, 1988). Another reason for the emphasis on organic carbon removal is that so called total organic carbon is a surrogate parameter which actually includes numerous types of organic compounds. The measurement of organic carbon compounds is much more complicated than either NH_4^+ or NO_3^-/NO_2^- removal.

Biodegradable organics have been generically termed biodegradable organic matter (BOM) (Rittmann and Huck, 1989). According to a surface water survey by the U.S. Geological Survey, humic substances may contribute 50% of the total dissolved organic carbon (DOC), whereas low molecular weight acids contribute 25%, hydrophilic neutrals 15%, hydrophobic neutrals 6%, neutral bases 4%, and contaminants 0.5% (Malcolm, 1990). A large percentage of these organics, such as humic substances, are largely non-biodegradable or only slowly biodegradable. Therefore, BOM could be only a small portion of total DOC and the amount of BOM may be difficult to determine against the DOC background. Many techniques have been developed to measure BOM. Most widely used two techniques are the biodegradable dissolved organic carbon (BDOC) technique (Servais et al., 1987) and

the easily assimilable organic carbon (AOC) technique (van der Kooij and Hijinen, 1984; van der Kooij et al., 1982). The portion of BOM in water which is susceptible to biodegradation is called BDOC whereas the portion of BOM which is readily biodegradable and can be converted to cell mass is termed AOC. The measured levels of BOM are highly technique dependent, which, in addition to the fact that all BOM measurements are group parameters, has important implications for modeling BOM removal in biological treatment (Huck, 1990).

As an integral part of biological water treatment systems, ozonation is usually included in the water treatment train, among other purposes, to enhance the following biological treatment. Although ozonation on its own does not mineralized a large percentage of organic carbon, it may modify otherwise non-biodegradable or slowly biodegradable organics, such as humic substances, to easily biodegradable organics, providing organic carbon for the following biodegradation in biological units (Singer, 1990). Therefore, ozonation may increase the mass percentage of AOC in the total DOC.

Biofilms in Biological Drinking Water Treatment Processes

Before the middle decades of this century, the "original" biotreatment processes, mainly slow sand filtration or bank infiltration, were commonly practiced in European waterworks to treat surface water. After the 1970s various "new" biological treatment processes were developed with the renewed emphasis on biotreatment in Western Europe (Huck, 1988). Specifically, biological water treatment processes used in practice for biostabilization can be divided into seven types, including in-situ treatment via ground passage, slow sand and rapid sand filters, granular activated carbon (GAC) contactors, fluidized beds, submerged aerated filters and unsubmerged filters. These processes are generally simple and of low cost, compared to the alternatives for achieving equivalent water quality (Huck, 1988). In fact, filters and GAC contactors in most cases are also intended for physical/chemical treatment purposes, such as filtration and adsorption. These concurrent physical/chemical processes are well known in the literature. Understanding biological behavior of filters and GAC contactors, however, remains an additional challenge.

All of the biotreatment processes in drinking water treatment are biofilm processes. In biofilm processes, biologically active matrices of microbial cells and noncellular material accumulate on the solid substratum surfaces to form layers of microorganisms, their waste products and other adsorbed and attached materials. The longer cell retention of biofilms make drinking water biotreatment feasible where the substrate concentration and thus biomass growth rate are very low. It also allows the high cell accumulation densities needed to degrade substrates in a short contact time and, therefore make biological treatment economically attractive (Rittmann and Huck, 1989).

An essential factor for biofilm versus suspended biomass to dominate in an environment is that suspended cell growth is minimized by a high dilution rate (van Loosdrecht and Heijinen, 1993). The high dilution rate provided by drinking water bioreactors coupled with low growth rate due to low BOM concentration, in turn, allows only microorganisms attached to solid surfaces to survive.

Many species of heterotrophs naturally attach to solid surfaces (Marshall, 1976). The very low concentration of BOM present in drinking waters appears to select for a population of aerobic, heterotrophic bacteria known as oligotrophs. Under oligtrophic conditions, bacteria actually benefit from being stationary in a flowing stream of water from which they can scavenge a continuous supply of nutrients.

Although oligotrophs can survive and function at extremely low substrate concentrations, there is still some threshold value which has been termed the minimum substrate concentration, S_{min} (Rittmann and McCarty, 1980). At concentrations of BOM lower than S_{min} no biofilm can be established. Even existing biofilms would decay and disappear when the low concentration remains for a long time.

BIOFILM MECHANISMS AND BIOFILM MODELING

A biofilm is a collection of microorganisms and their extracellular products bound to a solid surface (termed substratum) (Marshall, 1984). Biofilms are a natural phenomenon: most microorganisms in nature are associated with solid surfaces (Marshall, 1976). In the past decade, biofilm phenomenon has drawn broad attention

and become an interdisiplinary topic of interest to microbiologists, engineers, ecologists and chemists. Numerous research articles regarding biofilm phenomenon can be found in the literature.

Occurrence of Biofilm

It is said that 99.9% of bacteria exists within biofilms on surfaces (Costerton et al., 1987). In all aquatic ecosystems, biofilms form on literally any available surface that can support microbial growth (Lappin-Scott et al., 1993). In soil ecosystems, most bacteria adhere to a solid substratum, either in the form of soil particles, plant roots or terrestrial microfunna. In medical sector, microbial biofilm can be found on the surface of various implantable devices such as catheter or orthopedic joints, which can pose a number of serious complications (Bryers, 1987).

In engineered systems, biofilms can be either beneficial or detrimental. Detrimental biofilms in engineered systems create problems by reducing the efficiency of the transport of energy, momentum or mass, or by accelerating the corrosion of metal surfaces (Bryers, 1987, 1991). Excessive growth of biofilms has been considered to contribute to the plugging of oil-bearing strata (Geesey et al., 1987).

Traditional biofilm wastewater treatment systems, including rotating biological contactors, trickling filters, packed-bed biofilters and fluidized bed biofilm reactors, are typical examples of the beneficial use of biofilms. In-situ bioremediation techniques encourage biofilm growth in soil to mitigate soil and groundwater contamination. The mining industry has developed methods for microbially enhanced leaching of metals from ores and recovery of metals from solutions (Cunningham et al., 1991). In biochemical production processes, cells immobilized by adsorption have been applied in large scale vinegar and penicillin production (Klein and Ziehr, 1990).

Biofilm Formation

The accumulation of biofilm is the net result of a number of processes including adsorption, desorption, attachment, detachment, microbial growth and endogenous decay (Characklis, 1990a). The formation of biofilm typically follows a process of initial colonization, cell accumulation and biofilm formation.

Initial Colonization

Adsorption of measurable quantities of organic macromolecules occurs within minutes, if not seconds, of exposure of a clean surface to an aqueous environment (Peyton, 1992). Although the total mass of organics adsorbed are insignificant in terms of a mature biofilm, the adsorbed organic macromolecules serve to mediate the solid surface and form a film of organic polymers, usually called the conditioning film, bonded to the solid surface (Bryer, 1987). Although it has not been shown to be a prerequisite, the conditioning film leads to the initial attachment of bacterial cells, the first step in the colonization of surfaces for further events. Craik et al. (1992) suggested that the high substrate concentration on the surface of granular activated carbon (GAC) could be attractive for bacteria to attach on the surface of GAC particles.

The initial colonization of a clean substratum by cells is termed adsorption (Charackiis, 1990). Cells are likely transported to the substratum surface by one or a combination of the following mechanisms: gravity sedimentation within a quiescent system (Bryers, 1987), molecular diffusion (Powell and Slater, 1983), and eddy diffusion (in turbulent flow) (Bryers, 1987). The adsorption can be either reversible or irreversible (Bryers, 1987). The re-entrainment of an adsorbed cell into the bulk liquid is termed desorption (Characklis, 1990). Reversible adsorption is affected by a number of factors including momentum transport, shear stress, substratum properties, cell surface conditions and physiological state of the cells, and nutrient levels (Peyton, 1992). When the cells are attached to a surface, some specific genes are activated to produce a great amount of extracellular polymeric substances (EPS) (Davies et al., 1993). Irreversible adsorption is often associated with the binding of cells to the conditioned solid surface using the extracelluar polymers (Fletcher and Floodgate, 1973).

Biofilm Growth and Attachment

Biofilm growth is a collective process of cell growth, replication, substrate conversion, endogenous decay, the production of EPS and adsorption of other particles. Although irreversible adsorption plays a major role in net biofilm accumulation in the early stages of colonization, subsequent growth of cells is the

dominant process responsible for the accumulation of a biofilm. Following initial colonization, cell division produces sister cells, which are bonded within the matrix of EPS, and leads to the development of adherent microcolonies. EPS formation rate is associated with the growth rate of the cells (Bakke et al., 1984). The specific growth rate is a function of local instantaneous substrate concentration, which is dictated not only by the biological reaction rate but also by mass transfer resistance. As a consequence, a growth rate gradient will exist inside the biofilm (van Loosdrecht and Heijinen, 1993).

Planktonic cells in the bulk liquid may continue to be adsorbed onto the existing biofilm. The process of cells from the bulk liquid sticking to an existing biofilm is termed attachment. The eventual production of a continuous biofilm on the colonized surface is a function of cell division within microcolonies and attachment of bacteria from the bulk phase (Costerton et al., 1987). Although attachment may play a significant role in the initial stage of biofilm development, cell growth plays the dominant role in an existing biofilm.

Biofilm Detachment

The accumulation of biomass on the surface will eventually be stabilized by detachment. Detachment is the process of removal of cells and cell products from an existing biofilm into the bulk liquid, which is the primary mechanism which counter-balances the biogrowth (Stewart, 1993; Peyton and Characklis, 1993; Wanner and Gujer, 1986). van Loosdrecht and Heijinen (1993) considered detachment in biofilm processes equivalent to the dilution rate in a chemostat. Bryers (1987), indicated that biomass can be removed from the biofilm in any one of the following ways: (1) erosion, (3) abrasion, (2) sloughing, (4) predator grazing, and (5) human intervention.

Erosion is the continuous removal of small particles of biofilm, which is the most common mechanism of biofilm detachment encountered biofilm processes (Peyton and Characklis, 1993). Although the rate coefficient of erosion is believed to be affected by many factors including shear stress (Chang et al., 1991), shear forces are thought to exert erosion by moving fluid in contact with the biofilm surface. Therefore, biofilm erosion is often called shear loss. In highly turbulent hydrodynamic

conditions, increased turbulence may create forces normal to the biofilm surface and cause erosion.

Abrasion is caused by collisions of solid particles with the biofilm. In fluidized-bed biological reactors abrasion (including removal of biofilm in a filter during backwash) can be the dominant detachment process (Bryer, 1987; Chang et al., 1991). Abrasion not only contributes to the detachment of the biofilm but also affects the density of the biomass. Increased abrasion and turbulence pressure tend to make the biofilm denser (Mulcachy and Shieh, 1987).

While erosion and abrasion are continuous processes of the removal of small particles of biomass from biofilms, sloughing is an event where a large amount or entire sections of biofilm are detached from the substratum, and is a stochastic and discrete process. Few researchers have focused on detachment as a result of sloughing, and most have treated it as an annoying phenomenon which distorts and complicates biofilm research. Except for the sloughing of an entire section of biofilm, the distinction between erosion and sloughing may be arbitrary because both erosion and sloughing have been hypothesized to be exerted by moving fluid in contacted with the biofilm surface (Characklis, 1981). Stewart (1993) suggested that the detachment of relatively small particles whose characteristic size is smaller than the thickness of the biofilm itself can be categorized as erosion and particles larger than the thickness of biofilm as sloughing. Except for the sloughing of the entire section of biofilm, in fact the biofilm detachment model developed by Stewart (1993) allows the detachment to be either erosion or sloughing.

Sloughing of large section of biofilms is a very complicated phenomenon. Sloughing has been linked to a number of factors including (1) excessive biofilm thickness, (3) sudden and drastic change of nutrient condition and (2) formation of gas bubbles within the biofilm. In wastewater treatment, such as trickling filters, sloughing has been linked to the occurrence of anaerobic activity within the depth of very thick yet otherwise aerobic biofilms. Due to oxygen transfer limitations, deeper layers of biofilm may become anoxic, producing both volatile acids, which decrease pH, and insoluble gas, both of which combined may weaken the biofilm structure (Bryer, 1987). Bakke (1983) found that step increases of substrate concentration led to spontaneous sloughing of biofilms. Jansen and Kristensen (1980) had associated

sloughing with the formation of nitrogen bubbles in denitrifying biofilms. Similar sloughing is expected to occur in anaerobic systems producing methane and CO_2. Bubble formation and associated sloughing could be minimized by employing a fluidized-bed fixed film reactor, since biofilm thicknesses are less and the agitation may physically dislodge fine bubbles before they coalesce and disrupt the biofilm structure.

Predator grazing is the harvesting of biofilm mass by larger organisms such as protozoa, snails and insects. Detachment as a result of human intervention is the removal of a biofilm by chemical or physical means. These two processes are not strictly a detachment mechanism, and are of little interest to biofilm researchers.

Detachment is one of the least understood processes in term of the variables which affect the process rates yet the detachment rate coefficient is the most sensitive variable affecting the predicted rate and extent of biomass accumulation (Peyton, 1992; Wanner and Gujer, 1986). Biofilm detachment modeling has been mainly concentrated on erosion processes exerted from shear stress. Because it is difficult to distinguish attachment from the growth, net detachment of biomass as the difference between total detachment and attachment is considered in modeling biofilm detachment. Stewart (1993) has provided a comprehensive biofilm detachment model. In general, biofilm detachment rate is a function of biofilm mass and biofilm growth rate. The dependence of biofilm detachment rate on biofilm mass may range from zero to second order. The detachment rate may also be a function of several physical factors, such as shear stress, turbulence pressure and intensity of abrasion (Chang et al., 1991, Rittmann, 1982). However, the influence of these physical factors on the detachment rate is even less well understood.

Biofilm Physiology and Metabolism

In a mature biofilm, cells are entrapped within a gelatinous matrix of EPS that is directly produced from the surface associated microorganisms. The C:N ratios in some biofilms are considerably higher (approximately five times) than in microbial cells. This probably reflects the large portion of EPS (generally low in nitrogen) (Christensen and Characklis, 1990; Pappin-Scott et al., 1993), if the total carbon rather than cell organic carbon is measured. EPS plays a role in cementing cells on surfaces and in protecting cells from desiccation and toxic chemicals. However, EPS gel is not

a passive matrix but instead exhibits physical chemical and electrical responses to environmental stimuli (Costerton et al., 1987). Several genes have being found to be responsible for the production of alginate, the primary constituent of biofilm mass (Davies et al., 1993).

The predominately polyanionic, highly hydrated nature of EPS also means that it can act as an ion exchange matrix, serving to increase local concentration of ionic species, such as heavy metal, ammonium, potassium, etc., while having the opposite effect on anionic groups (Costerton et al., 1994). It may not have any effect on uncharged potential nutrients, including sugars (Hamilton and Characklis, 1989). However, bacteria are assumed to concentrate and use cationic nutrients such as amines, suggesting that EPS can serve as a nutrient trap, especially under oligotrophic conditions. Conversely, the penetration of charged molecules such as some biocides may be at least partly restricted by this phenomenon (Costerton et al., 1994).

Although the experimental evidence for this is inconclusive, it is generally considered that cells have higher activities when attached to a surface (Hamilton and Characklis, 1989). In a nutrient limited environment with a high dilution rate, such as in drinking water treatment processes, oligotrophs attached to a surface survive better. Oligotrophs adapt to the nutrient limited environment by decreasing the size and increasing surface to volume ratio (Novisky and Morita, 1978). However, some workers found that once these cells were attached they grew back to their normal size and began to multiply (Marshall, 1988).

Biofilm Modeling

Heterogeneity and Biofilm Modeling

In general, an established biofilm system is considered consisting of three compartments, the bulk solution, the biofilm and the substratum. The substratum provides support for biofilm attachment and is usually considered as impermeable and inert. The bulk liquid functions as the substrate carrier which delivers substrate to the surface of the liquid film above the biofilm, mainly through convective flow.

A biofilm can be divided into two sub-compartments: the base film and the surface film (Wilderer and Characklis, 1989). The base film is relatively dense and homogeneous. Because of the high density, the base film is considered to have a low hydraulic permeability, such that mass transport within the base film is by molecular diffusion (Wilderer and Characklis, 1989).

The surface film is of lower density and may be composed of cell clusters, microbial filaments or other irregularly shaped components. The relatively low density and high porosity of a surface film may allow flow to penetrate the biofilm. In this case, water velocity does not go to zero at the outer surface of the biofilm but at some point within the biofilm. Thus in addition to molecular diffusion mass transport into and within a surface film can also be due to advection and turbulent diffusion.

Using non-disruptive scanning confocal laser microscopy (SCLM), recent studies were able to observe surface biofilms directly (Caldwell and Lawrence, 1989). In the surface films, microbial clusters attached to the substratum and each other with polymeric material with void conduits beneath the clusters (Costerton et al., 1994; de Beer et al., 1994). The voids formed a network of channels of pores connected with each other and with the bulk liquid. The functional water channels may deliver nutrients to the bacterial cells through convective flow.

Filamentous films are the surface biofilms often observed in wastewater treatment process, such as rotating biological contactors. A surface film with filaments emerging out of the solid matrix seems presently to be beyond the possibilities of mechanistic modeling. Spatial gradients are less important for this type of biofilm. It is even not possible to define a distinct interface between the aqueous phase and the biofilm. However, there has been no report of development of filamentous biofilms in biological drinking water treatment processes.

A biofilm can be entirely of surface film or entirely of base film. Most biofilms, however, are composed of a mixture of base and surface films (Gantzer, 1989). The amounts of surface and base films can vary widely in different biofilms. The ratio of surface to base film for a biofilm defines the ease with which the fluid interface can be defined. If base film dominates, then a relatively smooth surface exists. If the surface

film component is significant, the irregular topography of the surface will make interface determination difficult.

The ratio of surface to base film can be a function of the shear stress exerted on the biofilm during development (Ganzter, 1989). A high shear stress often corresponds to a biofilm predominately composed of base film. A biofilm acclimated to a low shear stress may be predominately composed of surface film. Thus the hydraulically impermeable assumption may be more applicable to biofilm acclimated to high shear stress.

Different species display substantial difference in the ratio of surface to base film. *Pseudomonas* is one of the dominant microorganisms found in the biofilm in biological water treatment processes. *Pseudomonas aeruginosa* is often found to form relatively uniform and smooth biofilms (Siebel and Characklis, 1991; Gjaltema et al.,1994). Other species such as *Klebsiella pneumoniae* and *Thosphaera pantotropha* were found to form patchy microtowers with bare substratum between the towers, or even form filamentous structure after prolonged cultivation (Siebel and Characklis, 1991). A binary population biofilm forms a relatively smooth film with peaks extending above the base of smooth film surface.

In biofim modeling it is usually assumed that the bacterial cells and EPS form a solid matrix that is continuous throughout the biofilm. This assumption clearly contradicts the complexity and variety of observed structures. However, irregular biofilm structures and discontinuities of the solid matrix do not necessarily render mechanistic modeling impossible. An appropriate portion of biofilm volume, termed "biofilm volume element (BVE)", can always be found for which the average quantities are representative (Wanner, 1989). The solution to irregular biofilm structures and discontinuities is to choose the volume of the BVE as required by the heterogencities present in the biofilm, but to make the BVE very wide in parallel to the substratum and thin perpendicular to it. For a base film with low hydraulic permeability, convective transport along the substratum surface is negligible. Calculations with a two dimensional model indicate that it is adequate to consider only substrate diffusion along the direction perpendicular to the substratum surface (Wanner, 1989). Only if the ratio of the diameter of the patches to the distance between them is small, will the one dimensional biofilm model fail.

Multispecies versus Monospecies Modeling Approach

In water and wastewater treatment where organic substrates are usually measured by a sole surrogate parameter, such as BOD, BOM, COD, TOC, etc., it may be reasonable to treat biofilm bacteria as an undefined population even though several species may coexist in the biofilm. Sometimes, two or more distinctively different bioreactions measured by different parameters occur in the same biofilm while competing for some common substrates or for space. Biofilm modeling based on single substrate removal kinetics and uniform distributions of biofilm properties will fail in such cases. Multispecies competition has to be considered in modeling such biofilms.

The most typical example of such mixed population competition is biofilm nitrification, where autotrophic *Nitrosomonas* and *Nitrobacter* compete with heterotrophic bacteria for oxygen and space (Wanner and Gujer, 1986; Kissel et al., 1984; Rittmann, 1992). Wanner and Gujer (1986) demonstrated that the organisms with higher growth rate will be found at the outside of the biofilm, whereas slower growing or inactive organisms will be found inside. In biofilm nitrification, heterotrophic bacteria (which has a faster growth rate) would be found at outside of the biofilm which protects the slower growing *Nitrosomonas* and *Nitrobacter* at the inner layer of the biofilm from shearing loss (Rittmann, 1992). Zhang et al. (1994) have shown experimentally that competition in nitrification biofilm results in non-uniform spatial distributions of metabolically active bacteria. Siebel and Characklis (1991) found that the competition between two organisms was decided not only by the growth rates but also cell mobility.

Non-uniform spatial distribution of biotic and abiotic components in turn affects substrate transfer and substrate competition within the biofilm. In agal biofilms (Flora et al., 1993) and nitrifying biofilms (Szwerinski et al., 1986) bioreaction may result in a significant H^+ gradient within the biofilm and varied electrostatic interactions, which may also need to be considered in biofilm modeling.

In aerobic processes, oxygen can become the limiting substrate in a thick biofilm. Typical experimental values for the thickness of the aerobic active layer are about 100 to 200 μm (van Loosdrecht and Heijnen, 1993). When anoxic conditions

-14-

develop in the inner layer of thick biofilms, biofilm properties may change drastically along the depth of the biofilm. In a study of wastewater treatment with rotating drum biofilm reactors, Zhang and Bishop (1994a) found that for biofilms with thickness ranging from 1000 μm to 2000 μm that the biofilm density, porosity and the percentage of living cells changed significantly from the top to the bottom layer of biofilm. It is well known that the effective diffusion coefficient within biofilms is dependent on the cell density (Westrin and Axelsson, 1991). With the increase of biofilm density, effective diffusivity of the top layer could be almost twice as high as that of the bottom layer (Zhang and Bishop, 1994b).

These complex conditions, however, are unlikely to develop in biological drinking water treatment processes, where organic substrate concentration is relatively low. Unless biological nitrification is required, rigorous multispecies analysis would not be necessary for biological drinking water treatment.

Steady-state versus Nonsteady-state

The most compelling reason for choosing steady-state systems in biofilm studies is that their behavior remains constant for prolonged periods. It is possible against this background, therefore, to perturb one parameter at a time and to observe the response of the system unequivocally. From a modeling point of view, dynamic solutions are difficult to generalize since they change with time and incorporate the complete history of a biofilm. In water and wastewater treatment processes, it is desirable to operate biological treatment processes under steady-state conditions so as to obtain stable and controllable effluent quality. Therefore, the clearly defined (pseudo)steady-state solutions are often of more practical value.

In a steady-state biofilm all quantities, including the substrate concentrations in the bulk liquid, are assumed to be constant with time, and the net production of microorganisms is assumed to be equal to their loss to the bulk liquid. In real systems these assumptions are often limited. However, as long as they stay within reasonable boundaries, steady-state modeling may still yield valid results.

A nonsteady-state modeling approach is often employed to help understand the initial development of biofilms or the response of bioprocessing systems to a drastic

change of operating conditions. For example, Wanner and Gujer (1986) used a nonsteady-state approach to illustrate how a multispecies biofilm developed and reached a stable spatial distribution of microbial species and substrates within the biofilm. In GAC bioregeneration processes, where substrate adsorption by fresh GAC is a dynamic process, nonsteady-state approaches were employed to model the interaction between biofilm growth and GAC adsorption (Speitel and DiGiano, 1987; Chang and Rittmann; 1987). More recently, Bouwer and Holzinsky (1994) have developed a nonsteady-state modeling approach to describe the impact of backwashing on drinking water treatment biofilters.

Modeling Idealized Steady-state Biofilm

For the convenience of mathematical description, a typical biofilm is commonly perceived as a matrix of EPS with bacteria randomly entrapped in the matrix attached to the substratum surface. For such an idealized biofilm, it is assumed:

(1) There is a well defined interface between the biofilm and the liquid phase and thus a continuous and uniform biofilm thickness. Hydraulic convection at the interface and within the biofilm is negligible.

(2) The spatial distribution of biofilm properties, for example biofilm density, is homogeneous.

(3) In such a biofilm system, substrate is assumed to be transported into and within the biofilm by molecular diffusion only. The flux of substrate into the biofilm is normal to the substratum.

(4) There is a sole limiting substrate which is both diffusion and bioreaction limiting in the biofilm system

(5) Although not essential, it is often assumed that the substratum is impermeable.

The idealized biofilm growing on a planar substratum is illustrated in Figure 1-1 (Rittmann and McCarty, 1980; Sáez and Rittmann, 1988). The biofilm has a uniform thickness of L_f (L) and a uniform density of X_f ($M_x L^{-3}$). In the biofilm system,

the substrate with a concentration of S_b (M_sL^{-3}) is transported from the bulk liquid to the biofilm surface through an effective diffusion layer (an equivalent depth of liquid film through which the actual mass transport can be described by molecular diffusion alone) with a thickness of L (L). Inside the biofilm, solutes diffuse down the concentration gradient induced by the substrate consumption by the bacteria. The substrate concentration on the outer surface of the biofilm is S_s (M_sL^{-3}), within the biofilm is S_f (M_sL^{-3}), and at the inner surface of the biofilm is S_w (M_sL^{-3}).

In biochemical engineering, biofilms are considered as a subcategory of the whole cell immobilization technology (Karel et al., 1985), because many aspects of the use of artificially or naturally immobilized-cells are similar to biofilm cells. For immobilized whole cells, apparent biotransformation kinetics is considered as the result of the interactions between simultaneous physical diffusion and bioreaction. Such reaction-with-diffusion concept has been widely accepted in biochemical engineering (Karel et al., 1985). Molecular diffusion in immobilized whole cell systems is governed by Fick's law. Intrinsic bioreaction kinetics used in the literature includes zero-order, first-order, hyperbolic (e.g. Monod, Michaelis-Menten, Langmuir-Hinshelwood etc.), substrate and product inhibition, "ping-pong", and reversible enzymatic kinetics (Karel et al., 1985). Among them, empirical Monod kinetics is the most commonly used kinetics. First-order and zero-order kinetics can be considered as the approximation of Monod kinetics. Substrate and/or product inhibition is considered only when substrate concentrations are high (van Ede et al., 1993). "Ping-pong" and reversible enzymatic kinetics are applicable to multiple substrate systems.

The value of the half-velocity constant in Monod expression (K_s) for biological drinking water treatment processes is not available at present. Without prior knowledge of K_s, one would not be able to choose between the first-order and zero-order solutions. Therefore, the more generalized Monod kinetics is used in this research. For a steady-state biofilm the substrate concentration profile in the biofilm would not change with time. A second-order nonlinear differential equation describes the substrate mass balance between molecular diffusion and bioreaction within a differential segment of biofilm. For the Monod kinetics, this diffusion-with-bioreaction equation can be written as follows:

$$D_f \frac{d^2 S_f}{dr_f^2} + \frac{kX_f S_f}{K_s + S_f} = 0 \qquad\qquad 0 \le r_f \le L_f \qquad (1)$$

where D_f ($L^2 T^{-1}$) is the substrate diffusivity in the biofilm; K_s is the half-velocity constant in the Monod expression ($M_s L^{-3}$); k is the maximum specific rate of substrate utilization (T^{-1}); Y is the yield coefficient, M_x/M_s; r_f is the depth ordinate in the biofilm (L).

One primary difficulty in using equation (1) is that the equation cannot be analytically integrated because of the nonlinearity of the Monod-type reaction term. In a typical case of whole cell immobilization, the flux of substrate into a pellet of immobilized whole cells is calculated for a given volume of a pellet. A maximum possible flux into a pellet is first calculated by presuming that no diffusion resistance develops in the pellet and the substrate concentration in the whole pellet is uniform. The effect of diffusion resistance is then accounted for by an effectiveness factor for a given size of the pellet through numerical computation.

Numerical results for the effectiveness factor are either described graphically by effectiveness factor curves or described by approximate algebraic expressions (Karel et al., 1985). The graphical approach has been widely used for completely mixed reactors. However, it is difficult to use the graphical approach in plug-flow bioreactors because the effectiveness factor changes along the depth of the column. Algebraic approach was initially used by Atkinson and Daoud (1968) to express substrate flux into a biofilm as a pseudoanalytical function of substrate concentration and biofilm thickness. This approach has the potential for modeling plug-flow bioreactors.

In more than two decades, a variety of pseudoanalytical solutions have been developed for eqaution (1) with improving accuracy and applicable domain (Atkinson and Davies, 1974; Rittmann and McCarty, 1981; Karel et al., 1985; Suidan and Wang, 1985). In developing these pseudoanalytical solutions, biofilm thickness was used as the quantity similar to the pellet size and therefore was considered as a controllable variable.

However, the growth of the cells in biofilms is different than immobilized cells entrapped in an artificial matrix. In artificially immobilized pellets (e.g. alginate beads), because of restriction by the artificial matrix, the growth of cells mainly results in the increase of living cell density. On the other hand, because of the protection of the matrix, loss of cells from the pellets by detachment is insignificant and the size of the pellets is rather stable (van Loosdrecht and Heijinen, 1993). In a biofilm, biogrowth results in mainly the expansion of the biomass volume or biofilm thickness (van Loosdrecht and Heijinen, 1993). The thickness of the biofilm is mainly limited by the detachment process. Biofilm thickness is the result of the dynamic balance between net biogrowth and net detachment. In other words, in biofilm processes, biofilm thickness itself is not an independent variable to be controlled as may be in the case of immobilized cells.

In wastewater treatment, high substrate concentrations support to thick and thus easily measurable biofilms. This allows to couple substrate degradation with biomass accumulation (or biofilm thickness). In biological drinking water treatment processes, however, the biofilm is very thin because of low substrate concentration while the surface of the supporting media, such as anthracite or GAC, may be highly irregular. Such a combination makes the measurement of biofilm thickness very difficult. Probably because of this, biofilm models have not been widely applied for modeling drinking water treatment. In addition, for typical plug-flow type packed-bed columns in biological drinking water treatment, the substrate concentration may vary substantially along the depth. As a result, biofilm thickness changes along the depth of the column. This makes it even more difficult to include the biofilm thickness in model calibration.

Rittmann and McCarty (1980) proposed a steady-state biofilm model, which introduced the concept of S_{min}, the minimum substrate concentration capable of sustaining a steady-state biofilm, which reflects the dynamic balance between biofilm growth and loss. Sáez and Rittmann (1988, 1992) later demonstrated explicitly that the substrate flux into a biofilm (J, $M_sL^{-2}T^{-1}$) is only a function of S_s and S_{min}. Because the balance between biofilm growth and loss has been accounted for by S_{min}, the pseudoanalytical solution of Sáez and Rittmann (1988, 1992) does not require the

knowledge of biofilm thickness and thus is more appropriate for modeling biofilm processes in drinking water treatment.

OBJECTIVES AND OUTLINE OF THESIS

Although biological drinking water treatment has been widely used in Europe for a long time, current designs of biological processes are solely empirical or based on trial-and-error experimentation for particular sites. Design of reliable and cost-effective biological treatment, however, must be based on a rational foundation of biofilm kinetics. Although much research has been done in the field of biofilm kinetics since the late 1960s, until recently most research has focused on wastewater treatment.

Heath et al. (1990) developed a family "normalized loading curves", based on the pseudoanalytical solution for the steady-state biofilm model (Sáez and Rittmann, 1988), to describe the relationship between standardized substrate flux (or loading) and standardized substrate concentration. Rittmann (1990) used the "normalized loading curve' approach to analyze biological drinking water treatment processes. But the analysis was only applicable to completely or nearly completely mixed biofilm reactors, whereas the majority of biofilm processes used in biological drinking water treatment, such as slow sand filters, rapid sand filters and biological GAC filters are of plug-flow type. In addition, the parameter analyzed by Rittmann (1990) was chemical oxygen demand (COD) rather than the BOM parameters commonly used in biological drinking water treatment. The inherent uncertainty in BOM measurement, as discussed later in this thesis, will substantially complicated the process analysis. Application of biofilm kinetics in process design and process analysis for BOM removal in biological drinking water treatment, therefore, remains a prime challenge.

Objectives of Thesis

The main objective of this thesis study is to establish a framework based on the steady state biofilm model to enable mechanistic understanding and rational analysis of the performance of biological drinking water treatment processes.

-20-

In an earlier work co-authored by the author (Huck et al., 1994), using data from three pilot or full scale biological water treatment facilities, it was found that there is an approximate linear relationship between the AOC removal rate and the influent concentration. In the present research, further development of the steady-state biofilm model was undertaken to apply it to plug-flow bioreactors. An attempt was then made to fit the steady state biofilm model to AOC data from a pilot scale study (Huck et al., 1991). The steady state biofilm model was then used as a framework to link process performance in terms of the slope of the linear relationship (which represents approximate percentage AOC removal) to process operating conditions and biodegradation kinetics. The pseudoanalytical solution developed by Sáez and Rittmann (1988, 1992) was used for the data fitting and the process analysis.

Initial assessment of the data fitting results identified two major problems: (1) the estimated K_s values were much higher than expected and varied in a relatively wide range; and (2) biofilm thickness calculated from estimated S_{min} values, based on the first order biofilm detachment kinetics used in Sáez and Rittmann (1988, 1992), was unrealistically high. Three secondary objectives were then derived in an attempt to clarify the two problems. These secondary objectives were:

(1)   to confirm that K_s value is intrinsically high through well controlled bench-scale experiments,

(2)   to demonstrate that the relationship between S_{min} and biofilm detachment mechanism can be very complex and the high biofilm thickness was an artificial result of the first order detachment assumption used in the original steady state model, and

(3)   to confirm that the use of the pseudoanalytical solution of Sáez and Rittmann (1988, 1992) for data fitting was reasonable despite the fact that the first order assumption predicted unrealistically high biofilm thickness.

Outline of Thesis

Chapter 2 describes the development of a methodology for using the steady state biofilm as a framework to connect process performance with process operating

conditions and biodegradation kinetics. AOC data from a previous pilot scale study by Huck et al. (1991) are used to demonstrate the methodology. It is first demonstrated that the steady-state biofilm model can be fit to these pilot-scale AOC data with reasonable goodness-of-fit. It is shown that the empirical linear relationship between AOC removal rate and influent AOC concentration, first presented by Huck and Anderson (1992) and developed further in an earlier work co-authored by the author (Huck et al., 1994), is to expected from the steady state biofilm model. Kinetic parameters estimated through data fitting are then used to illustrate a dimensionless process analysis approach.

Chapter 3 presents a bench scale technique for the determination of kinetic parameters and AOC diffusivity which are required for the rational process design and process analysis described in Chapter 2. This chapter includes a detailed experimental protocol and an advanced parameter estimation algorithm. Since bench scale experiments can be carried out under well controlled conditions, the K_s values estimated in this chapter should help to clarify the uncertainty surrounding the higher-than-expected K_s estimates obtained in Chapter 2.

Another major concern raised in Chapter 2 is that the biofilm thickness calculated from the estimated S_{min} (which is based on a first order detachment assumption) was found to be unrealistically high. Chapter 4 reviews various biofilm detachment kinetics proposed in the literature and demonstrates that the relationship between S_{min} and biofilm detachment kinetics and thus biofilm thickness can be very complex. The artificially high prediction of biofilm thickness does not suggest that S_{min} estimates are unrealistic; it rather reflects the fact that the biofilm detachment is not a simple first order process. A generalized definition of S_{min} is proposed in this chapter to provide a framework for describing the complex relationship.

The pseudoanalytical solution for the steady-state biofilm model (Sáez and Rittmann, 1992) used in Chapters 2 and 3 was derived on the basis of first order biofilm detachment kinetics. Chapter 5 presents a new solution for substrate flux into a biofilm (J) as a function of S_s and S_{min} which requires no presumption concerning biofilm detachment kinetics. It is demonstrated that the impact of different biofilm detachment mechanisms on J is solely reflected through S_{min}. When S_{min} is treated as an independent biofilm kinetic parameter and determined through in-situ measurement

and data fitting, instead of being calculated using biofilm detachment kinetics, the biofilm detachment mechanism is "detached" from and thus have little impact on the function of J versus S_s and S_{min}. This provides the justification for the use of the pseudoanalytical solution of Sáez and Rittmann (1992) in Chapters 2 and 3 despite the unrealistic calculated biofilm thicknesses based on S_{min} estimates.

Finally, major conclusions and recommendations for further studies are presented in Chapter 6.
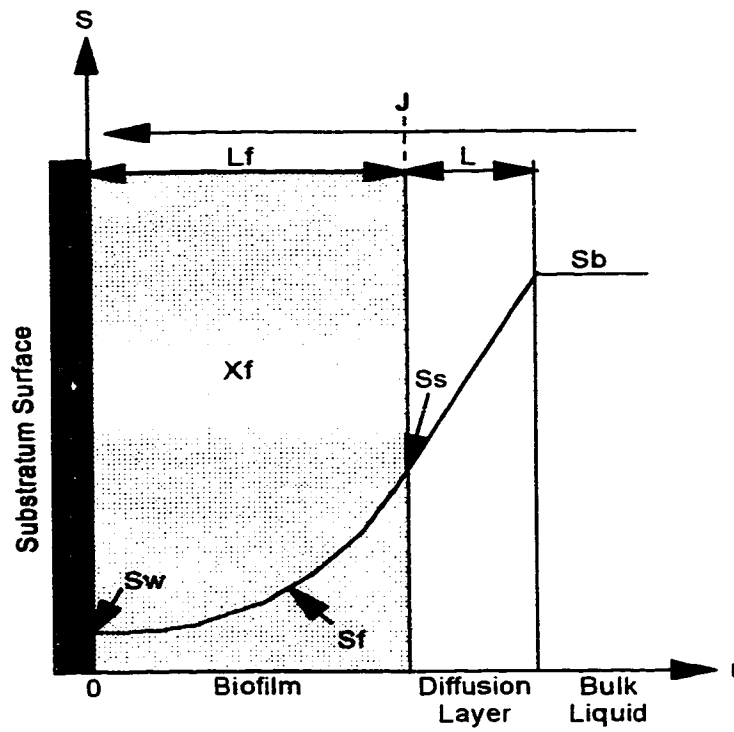
Figure 1-1. Physical concept of a biofilm system (after Sáez and Rittmann, 1988).

REFERENCES

Atkinson B. and Daoud I.S. (1968) The analogy between microbial "reaction" and heterogeneous catalysis. *Trans. Inst. Chem. Engrs.* **46**, T19-24.

Atkinson B. and Flower H.W. (1974) The significance of microbial film fermenters. *Adv. Biochem. Engng.* **3**, 224-277.

Bakke R. (1983) *Dynamics of Biofilm Processes: Substrate Load Variations*. Master Thesis, Montana State University, Bozman, MT.

Bakke R., Trulear M.G., Robinson J. A. and Charackils W. G. (1984) Activity of *Pseudomonas aeruginosa* in biofilms: steady state. *Biotechnol. Bioengng.* **26**, 1418-1424.

Bouwer E.J. and Crowe P.B. (1988) Assessment of biological processes in drinking water treatment. *J. Am. Wat. Wks. Ass.* **80**(9), 82-93.

Bower E.J. and Holzinsky R. (1995) Nonsteady-state or dynamic modeling. In *Design of Biological Processes for Organic Control* (Edited by Huck P.M.), in press. AWWARF Technical Report, AWWA, Denver.

Bryers J. D. (1987) Biologically active surfaces: processes governing the formation and persistence of biofilms. *Biotechnol. Prog.* **3**(2), 57-68.

Bryers J. D. (1991) Understanding and controlling detrimental bioreactor biofilms. *Trends Biotech.* **9**, 422-426.

Caldwell D.E., Korber D.R. and Lawrence J.R. (1992) Confocal laser microscopy and digital image analysis in microbial ecology. *Adv. Microbial. Ecol.* **12**, 1-67.

Caldwell D.E. and Lawrence J.R. (1989) Microbial growth and behavior within surface microenvironments. In *Recent Advances in Microbial Ecology* (Edited by Hattori T., Ishida Y., Maruyama Y., Morita R.Y. and Uchida A.), pp. 140-145. Japan Scientific Societies Press, Tokyo.

Camper A.K., Lechevallier M.W., Broadway S.C. and McFeters G.A. (1986) Bacteria associated with granular activated carbon particles in drinking water. *Appl. Envir. Microbiol.* **54**, 434-438.

Chang H.T. and Rittmann B.E. (1987) Verification of the model of biofilm on activated carbon. *Biotechnol. Bioengng.* **21**, 280-288.

Chang H.T., Rittmann B.E., Amar D., Heim R., Ehlinger O. and Lesty Y. (1991) Biofilm detachment mechanisms in a liquid-fluidized bed. *Biotechnol. Bioengng.* **38**, 499-506.

Characklis W.G. (1981) Bioengineering report, fouling biofilm development: a process analysis. *Biotechnol. Bioengng.* **23**, 1923-1960.

Characklis W.G. (1990) Biofilm processes. In *Biofilms* (Edited by Characklis W.G. and Marshall K.C.), pp. 195-231. Wiley, New York.

Christensen F.R. and Characklis W.G (1990) Physical and chemical properties of biofilms. In *Biofilms* (Edited by Characklis W.G. and Marshall K.C.), pp. 93-130. Wiley, New York.

Costerton J.W., Lewandowski Z., DeBeer D., Caldwell D., Korber D. and James G. (1994) Biofilms, the customized microniche. *J. Bacteriol.* **176**, 2137-2142.

Costerton J.W., Cheng K.W., Geesey G.G., Ladd T.I. and Michel T.J. (1987) Bacterial biofilms in nature and disease. *Ann. Rev. Microbiol.* **41**, 113-119.

Craik S.A., Fedorak P.M., Hrudey S.E. and Gray M.R. (1992) Kinetics of methanogenic degradation of phenol by activated-carbon-supported and granular biomass. *Biotechnol and Bioengng.* **40**, 777-786.

Cunningham A. B., Characklis W. G., Abedeen F. and Crawford D. (1991) Influence of biofilm accumulation on porous media hydrodynamics. *Envir. Sci. Technol.* **25**, 1305-1311.

Davies D.G., Chakrabarty A.M. and Geesey G.G. (1993) Exopolysaccharide production in biofilms: Substratum activation of aglinate gene expression by Pseudomonas aeruginosa. *Appl. and Envir. Microbiol.* **59**, 1181-1186.

de Beer D., Stoodley P., Roe F. and Lewandowski Z. (1994) Effects of biofilm structure on oxygen distribution and mass transport. *Biotechnol. Bioengng.* **43**, 1131-1138.

Drury W.J., Stewart P.S., Characklis W.G. (1993) Transport of 1 mm latex particles in *Pseudomonas aeruginosa* biofilms. *Biotechnol and Bioengng.* **42**, 111-117.

Fletcher M. and Floodgate G.D. (1973) An Electron-microscopic demonstration of an acidic polysaccharide involved in the adhesion of a marine bacterium to solid surfaces. *J. Gen. Microbiol.* **74**, 325-334.

Flora R. J., Suidan M.T., Biswas P. and Sayles G.D. (1993) Modeing substrate transport into biofilms: role of mutiple ions and pH effects. *J. Environ. Engng. Div.* **111**, 908-930.

Gantzer C.J. (1989) Group report: exchange processes at the fluid-biofilm interface. In *Structure and Function of Biofilms* (Edited by Wilderer P.A. and Charachlis W.G.), pp. 73-89. Wiley, Dahelm.

Geesey G.G., Mittelman M.W. and Lieu V.T. (1987) Evaluation of slime-producing bacteria in oil field core flood experiments. *Appl. Environ. Microbiol.* **53**, 278-281.

Gjaltema A., Arts P.A., van Loosdrecht J.G. Kuenen J.G. and Heijin J.J. (1994) Heterogeneity of biofilms in rotating annular reactors: occurrence, structure and consequences. *Biotechnol and Bioengng.* **44**, 194-204.

Hamilton W.A. and Characklis W.G. (1989) Relative activities of cells in suspension and in biofilms. In *Structure and Function of Biofilms* (Editerd by Wilderer P. A. and Charachlis W.G.), pp. 135-47. Wiley, New York.

Heath M. S., Wirtel S. A. and Rittmann B. E. (1990) Simplified design of biofilm processes using normalized loading curves. *Res. J. Wat. Pollut. Control Fed.* **62**, 185-192.

Huck P.M. (1988) European advances in biological treatment of drinking water, present at *Ontario Section AWWA Conf.*, London, Ontario, May, 1988.

Huck P.M. (1990) Measurement of biodegradable organic matter and bacterial growth potential in drinking water: a review of methods and their application. *J. Am. Wat. Wks. Ass.* **82**(7), 78-86.

Huck P.M., Fedorak P.M. and Anderson W.B. (1991) Formation and removal of assimilable organic carbon during biological treatment. *J. Am. Wat. Wks. Ass.* **83**(12), 69- 80.

Huck P.M., Zhang S. and Price M.L. (1994) BOM removal during biologial treatment: a first order model. *J. Am. Wat. Wks. Ass.* **86**(6), 61-71.

Jansen, J. and Kristensen, G.H. (1980) Fixed film kinetics: denitrification in fixed films. *Prog. Wat. Technol.* **12**, 253-261.

Karel S.F., Libicki S.B. and Robertson C.R. (1985) The immobilization of whole cells: engineering principles. *Chem. Engng Sci.*, **40**, 1321-1354.

Kissel J.C., McCarty P.L., Street R.L. (1984) Numerical simulation of mixed-culture biofilm. *J. Environ. Engng. Div.* **110**, 393-411.

Klein J. and Ziehr H. (1990) Immobilization of microbial cells by adsorption. *J. Biotechnol.* **16**, 1-16.

Kugaprasathan ., Nagaoka H., Ohgaki S. (1992) Effect of turbulence on nitrifying biofilm at non-limiting substrate conditions. *Wat. Res.* **26**, 1629-1638.

Lappin-Scott H.M., Jass J. and Costerton J.W. (1993) Microbial biofilm formation and characterization. In *Microbial Biofilms: Formation and Control* (Edited by Denyer S.P., Gorman S.P. and Sussman M.), pp. 109-131. Blackwell Scientific, Oxford.

LeChevallier M. W., Babcock T. M., and Lee R. G. (1987) Examination and characterization of distribution system biofilms. *Appl. Envir. Microbiol.* **53**, 2714-2724.

LeChevallier M.W., Cawthon C.D. and Lee R.G. (1988) Factors promoting survival of bacteria in chlorinated water supplies. *Appl. Envir. Microbiol.* **54**, 649-654.

Lewandowski Z., Altobeli S.A. and fukushima E. (1993) NMR and microelectrode studies of hydrodynamics and kinetics in bioifms. *Biotechnol. Prog.* **9**, 40-45.

Malcolm R.L. (1990) Factors to be considered in the isolation and characterization of aquatic humic substances. *Proc. Humic Substances Conf.* 1990, Atlanta.

Marshall K.C. (1976) *Interfaces in Microbial Ecology*, Harvard University Press.

Marshall K.C. (1984) *Mcicrobial Adhension and Aggregation*, Dahlem Konferenzen, Spring-Verlag, Berlin (1984).

Marshall K.C. (1988) Adhension and growth of bacteria at surfaces in oligtrophic habitis. *Can. J. Microbiol.* **17**, 1413-1416.

Martin A. and Harakeh S. (1990) Effect of starvation on bacteria resistance to disinfectants. In *Drinking Water Microbiology* (Edited by McFeters G.A), pp 88-110. Springer-Verlag , New York.

Mulcachy L.T. and Shieh W.K. (1987) Fluidization and reactor biomass characteristics of the denitrification fluidized bed biofilm reactor. *Wat. Res.* **21**, 451-458.

Novisky J.A. and Morita R.Y. (1978) Possible strategy for the survival of marine bacteria under starvation conditions. *Marine Biology*, **48**, 289-295.

Peyton B.M. (1992) *Kinetics of Biofilm Detachment.* Ph.D. Thesis, Department of Chemical Engineering, Montana State University, Bozeman, USA.

Peyton B.M. and Characklis W.G. (1993) A statistical analysis of the effect of substrate utilization and shear stress on the kinetics of biofilm detachment. *Biotechnol. Bioengng.* **41**, 728-735.

Powell M.S and Slater N.K.H. (1983) The deposition of bacterial cells from laminar flows onto solid surfaces. *Biotechnol and Bioengng.* **25**, 891-895.

Rittmann B.E. (1992) Development and experimental evaluation of a steady-state, multispecies biofilm model. *Biotechnol. Bioengng.* **39**, 914-922.

Rittmann B.E. and Huck P.M. (1989) Biological treatment of public water supplies. *CRC Crit. Rev. Envir. Control*, **19**, 119-184.

Rittmann B.E. (1990) Analyzing biofilm processes in biofilm processes used in biological filtration. *J. Am. Wat. Wks. Ass.* **82**(12), 62-66.

Rittmann B.E. and McCarty P.L. (1980) Model of steady-state-biofilm kinetics. *Biotechnol. Bioengng.* **22**, 2343-2357.

Rittmann B.E. and Snoeyink V.L. (1984) Achieving biological stable drinking water. *J. Am. Wat. Wks. Ass.* **76**(10), 106-114.

Sáez P.B. and Rittmann B.E. (1988) Improved pseudo-analytical solution for steady-state biofilm kinetics. *Biotechnol. and Bioengng.* **32**, 379-385.

Sáez P.B. and Rittmann B.E. (1992) Accurate pseudo-analytical solution for steady-state biofilms. *Biotechnol. Bioengng.* **39**, 790-793.

Servais P., Billen G. and Hascoët M.C. (1987) Determination of the biodegradable fraction of dissolved organic matter in waters. *Wat. Res.* **21**(4), 445-50.

Siebel M.A. and Characklis W.G. (1991) Observstion of binary population biofilms. *Biotechnol. Bioengng.* **37**, 778-789.

Singer P.C. (1990) Assessing ozonation research needs in water treatment. *J. Am. Wat. Wks. Ass.* **82**(10), 78-88.

Speitel Jr. G.E. and DiGiano F.A. (1987) The bioregeneration of GAC used to treat micropollutants. *J. Am. Wat. Wks. Ass.* 79(1), 64-73.

Stewart P. S. (1993) A model of biofilm detachment. *Biotechnol.Bioengng.* 41, 111-117.

Szwerinski H., Arvin E. and Harremoes P. (1986) pH decrease in nitrifying biofilms. *Wat. Res.* 20, 971-976.

van der Kooij D., Visser A. and Hijnen W.A.M. (1982) Determining the concentration of easily assimilable organic carbon in drinking water. *J. Am. Wat. Wks. Ass.* 74(10), 540-545.

van der Kooij D. (1990) Assimilable organic carbon (AOC) in drinking water. In *Drinking Water Microbiology* (Edited by McFeters G.A.), pp. 57-87. Springer-Verlag, New York.

van der Kooij D. and Hijinen W.A.M. (1984) Substrate ultilization by an oxalate consuming *Spirillum* species in relation to its growth in ozonated water. *Appl. Envir. Microbiol.* 47, 551-559.

van Ede C.J., Bollem A.M. and Beenackers A. (1993) Analytical effectiveness calculation concerning the degradation of an inhibitive substrate by a steady-state biofilm. *Biotechnol. Bioengng.* 42, 267-278.

van Loosdrecht M.C.M. and Heijinen S.J. (1993) Biofilm reactors for wastewater treatment. *Trends Biotech.* 11, 117-121.

Wanner O. (1989) Modeling population dynamics. In *Structure and Function of Biofilms* (Edited by Characklis W. G. and Wilderer P. A.), pp. 91-110. Wiley, New York.

Wanner O. and Gujer W. (1986) A multispecies biofilm model. *Biotechnol. Bioengng.* 28, 314-328.

Westrin B.A. and Axelsson A. (1991) Diffusion in gels containing immobilized cells: a critical review. *Biotechnol. Bioengng.* 38, 439-446.

Wilderer P.A. and Charachlis W.G. (1989) Structure and function of biofilms. In *Structure and Function of Biofilms* (Editerd by Wilderer P. A. and Charachlis W.G.), pp. 1-13. Wiley, Dahelm.

Zhang T.C. and Bishop P.L. (1994a) Density, porosity, and pore structure of bioiflms. *Wat. Res.* **28**, 2267-2277.

Zhang T.C. and Bishop P.L. (1994b) Evaluation of tortuosity factors and effective diffusivities in bioiflms. *Wat. Res.* **28**, 2279-2287.

Zhang T.C. Fu Y.C. and Bishop P.L. (1994) Competition in biofilms. *Wat Sci. Technol.* **29**(10/11), 263-270.

Chapter 2
REMOVAL OF AOC IN BIOLOGICAL DRINKING WATER TREATMENT PROCESSES: A KINETIC MODELING APPROACH[1]

INTRODUCTION

In Europe, biological treatment has long been recognized as an important unit operation for producing biologically stable drinking water to prevent bacterial regrowth in water distribution systems and thus reduce the dose of chlorine required to suppress the regrowth. However, it is only in recent years that the importance of biological treatment has started to be perceived by the North American water industry. Despite the fact that numerous biological water treatment facilities are in operation in Europe, there is still no rational basis for the design of these facilities.

As first presented by Huck and Anderson (1992) and developed further in an earlier work co-authored by the author (Huck et al., 1994), it was found that there is an approximate linear relationship between BOM removal and influent concentration. Although this relationship, to some extent, meets the urgent need of the water industry for a practical tool for the preliminary design of biofilters, the linear relationship was derived on a strictly empirical basis. The empirical approach falls short of providing the connection between removals and process operating conditions and biodegradation kinetics.

Biological processes in drinking water treatment are basically of the biofilm type (i.e. biofilms grow on the surfaces of various filter or adsorptive media). In this chapter, it is first demonstrated that the steady-state biofilm model can be fit to the same pilot-scale AOC data used in Huck et al. (1994), with reasonable goodness-of-fit. At the end of the chapter, it is shown that the approximate linear relationship is not an empirical phenomenon but can be expected from the steady state biofilm model. The steady state biofilm model is then used as a framework to link process

---

[1]A version of this chapter has been accepted for publication. *Zhang and Huck 1996. Water Research.*

performance (represented by the slope of the linear relationship) with process operating conditions and biodegradation kinetics.

One of the difficulties of using the kinetic approach to associate process performance with operating conditions is that the kinetic parameters for BOM in drinking water are not available in the current literature. For providing reasonable values for the biofilm kinetic parameters as well as for demonstrating the goodness-of-fit, a parameter estimation technique specifically suitable for analyzing pilot scale AOC data is developed based the steady state biofilm model developed by Rittmann and McCarty (1980) and improved by Sáez and Rittmann (1992).

Since the pilot study was not originally designed for parameter estimation, the values estimated for the biofilm kinetic parameters should be considered as merely semi-quantitative indications of the ranges of these parameters rather than precise estimates. Likewise, the data fitting is not intended to show that the steady-state biofilm model is the best model for the AOC data because these AOC data, which were not collected for model discrimination, would not be sufficient for that purpose. The reasons for choosing this steady state biofilm for the kinetic modeling has been discussed in Chapter 1. In fact, experimental verification of a biofilm model or statistical discrimination among competing models for drinking water biofilters is at present a very difficult, if not impossible, proposition. This is due to experimental uncertainties in assessing, for instance, the *in-situ* activity of biomass and the effective diffusivity and to the intrinsic scatter of AOC data.

The objective of this chapter is to present a framework which brings together the physical settings of a biofilm column with the operating conditions and biofilm kinetics to enable mechanistic understanding and rational analysis of the performance of biological drinking water treatment processes. The results from this chapter will help bring into focus areas requiring further study. Areas of concern identified in this chapter are addressed in Chapters 3 to 5.

Steady-State Biofilm Model

According to Sáez and Rittmann (1992), the flux (J, $M_sL^{-2}T^{-1}$) of biodegradable substrate into a steady-state biofilm can be expressed as a function of the substrate concentration at the biofilm outer surface (S_s, M_sL^{-3}) and the minimum substrate concentration for sustaining the steady-state biofilm (S_{min}, M_sL^{-3}). In dimensionless form,

$$J^* = \{2[S_s^*-\ln(1+S_s^*)]\}^{1/2} \times \tanh[\gamma(S_s^*/S_{min}^* - 1)^\beta] \qquad (1)$$

where $\gamma = 1.5557-0.4117\tanh(\log S_{min}^*)$ and $\beta = 0.5035 -0.0257\tanh(\log S_{min}^*)$.

This is the continuous pseudo-analytical solution to the nonlinear differential equation of diffusion-with-bioreaction (Eq. [1] in Chapter 1) in the so-called "steady-state biofilm model", which also includes the following three equations proposed by Rittmann and McCarty (1980):

$$S_b^* = S_s^* + J^*L^*/D^* \qquad (2)$$

$$S_{min}^* = b/(Yk - b) \qquad (3)$$

$$L_f^* = \frac{1+S_{min}^*}{S_{min}^*} J^* = J^*kY/b \qquad (4)$$

with $S_b^* = S_b/K_s$ $S_s^* = S_s/K_s$ $S_{min}^* = S_{min}/K_s$

$J^* = J\tau/K_sD_f$ $L_f^* = L_f/\tau$ $L^* = L/\tau$

$D^* = D/D_f$ $\tau=[K_sD_f/kX_f]^{1/2}$

where S_b is the bulk liquid concentration of the substrate (M_sL^{-3}); D is the free liquid diffusivity (L^2T^{-1}); D_f (L^2T^{-1}) is the diffusivity in the biofilm; K_s is the half-velocity constant in the Monod expression (M_sL^{-3}); k is the maximum specific rate of substrate utilization (T^{-1}); Y is the yield coefficient, M_x/M_s; b denotes the overall biofilm decay rate coefficient (T^{-1}), which is the sum of the biofilm decay rate coefficient of endogenous-respiration (b_d, T^{-1}) and the first-order rate coefficient for the net

hydrodynamic biofilm shearing loss (Rittmann, 1982; Sáez and Rittmann, 1988); X_f is the biofilm density $(M_x L^{-3})$; L_f is the biofilm thickness (L) and L denotes the thickness of the effective diffusion layer (L); τ $(=[K_s D_f/k X_f]^{1/2})$ is the standard biofilm depth dimension (L) (Rittmann and McCarty, 1980).

Steady-State Biofilm Model for Packed-Bed Bioreactors

Under steady-state conditions, the mass balance in a small segment (dx) of a packed biofilm column can be described as (Bailey and Ollis 1986 p. 569)

$$v\frac{dS_b}{dx} - D_H\frac{d^2S_b}{dx^2} + \alpha J = 0 \qquad (5)$$

where v is the superficial flow velocity or hydraulic loading rate (LT^{-1}); x is the longitudinal distance along the column (L); D_H is the hydrodynamic dispersivity (L^2T^{-1}); and α denotes the specific surface area which is the biofilm surface area in each unit volume of the bioreactor (L^{-1}).

Usually, the hydraulic loading rates for the filters and GAC contactors in biological water treatment processes are relatively high and the effect of axial hydrodynamic dispersion is negligible. The importance of mass transport by dispersion relative to convective mass transport is usually measured by the axial Peclet number, Pe, defined as

$$Pe = vX/\varepsilon D_H \qquad (6)$$

where X is the total depth of the packed column and ε denotes the porosity of the column.

To calculate Pe, hydrodynamic dispersivity, D_H, can be estimated by the Hiby correlation (Bear 1988 p. 602):

$$D_H = 0.67D + 0.65d_pv/(1+6.7[D/d_pv]^{1/2}) \qquad (7)$$

As an example, we take the lower hydraulic loading rate v = 4 m/h of GAC Contactor 3 in the pilot study described by Huck et al. (1991) with an average particle size of 1206 µm. By using the diffusivity of oxalate $(D=1.61 \times 10^{-9}$ m^{2}s^{-1}, Perry, 1983,

p. 3259), which is probably the most common AOC component in ozonated water (van der Kooij and Hijnen, 1984) and would also probably have as high a diffusivity as any AOC component, D_H is 8.66×10^{-7} m^2s^{-1}.

For this D_H value, Pe is calculated to be 8000. According to Bailey and Ollis (1986, p. 572), as a general rule of thumb, a bioreactor can be regarded as being plug-flow when Pe is greater than 40. Thus, the biological filters and GAC contactors used in the pilot study can be regarded as plug-flow reactors and the effect of axial hydrodynamic dispersion is negligible. Equation (5) can be simplified as

$$v\frac{dS_b}{dx} + \alpha J = 0 \qquad (8)$$

For a column with a total depth of X, dimensionless longitudinal distance along the column can be defined as $\chi = x/X$, $0 \leq \chi \leq 1$. By using the definitions for S_b^* and J^*, equation (8) can be transformed as

$$\frac{dS_b^*}{d\chi} = -\frac{\alpha X D_f}{v\tau}J^* \qquad (9)$$

In equation (9), $\frac{\alpha X D_f}{v\tau}$ is a dimensionless quantity, the significance of which is discussed later. By introducing $X^* = \frac{\alpha X D_f}{v\tau}$, equation (9) becomes

$$\frac{dS_b^*}{d\chi} = -X^* J^* \qquad 0 \leq \chi \leq 1 \qquad (10)$$

BC: at $\chi = 0$, $S_b^*(\chi) = S_{bo}^* = S_{bo}/K_s$

Analytical integration of the right hand side of equation (10) is not possible. However, it can be integrated numerically using, for example, the Runge-Kutta method. The numerical solution can be obtained by dividing χ into small segments. For a given influent substrate concentration, S_{bo} (M_sL^{-3}), and thus $S_{bo}^* = S_{bo}/K_s$, J_o^* and thus J, the flux at the inlet end of the column $(M_sL^{-2}T^{-1})$, can be found using equations (1) and (2) through root searching. This quantity is used in equation (10) to calculate S_b^* for the next segment. The process repeats until $\chi = 1$ and the resulting S_b^* is the dimensionless effluent concentration $S_{be}^* = S_{be}/K_s$.

To avoid the time-consuming root searching computation for each segment during numerical integration, equation (10) can first be partially integrated as

$$\int_{S_{bc}^*}^{S_{bo}^*} \frac{dS_b^*}{J^*} = X^* \int_1^0 d\chi = X^* \tag{11}$$

where S_{bc}^* is an unknown value at $\chi=1$. To determine the value of S_{bc}^*, equation (11) can further be transformed by substituting equation (2) into equation (11):

$$X^* = \int_{S_{sc}^*}^{S_{so}^*} \frac{dS_s^*}{J^*} + \frac{L^*}{D^*} \ln\frac{J_o^*}{J_c^*} \tag{12}$$

In equation (10), $J^* = J^*(S_s^*) = \{2[S_s^* - \ln(1+S_s^*)]\}^{1/2} \times \tanh[\gamma(S_s^*/S_{min}^* - 1)^\beta]$, $J_c^* = J^*(S_{sc}^*)$ and $J_o^* = J^*(S_{so}^*)$. Although dS_s^*/J^* cannot be analytically integrated, it can be integrated using a general-purpose numerical integrator, such as the multipoint Gauss-Kronrod algorithm (IMSL, 1987). For a given S_{so}^* determined for a given S_o by using equations (1) and (2), S_{sc}^* and thus S_{bc}^* can be determined for a given X^* through root searching using equation (12).

In $X^* = \frac{\alpha X D_f}{v\tau} = (\frac{X}{v})/(\frac{\tau}{\alpha D_f})$, $\theta = X/v$ is the average detention time of water passing through the biofilm column (T). According to Rittmann and McCarty (1980), τ $(=[K_s D_f/kX_f]^{1/2}$, L) is the standard biofilm thickness dimension. Thus $\frac{\tau}{\alpha D_f}$ represents the standard time dimension for a biofilm to intercept or "adsorb" substrate from the surrounding liquid phase. This standard interception time is a function of the contact area (α), the substrate diffusivity (D_f) and the biodegradation kinetics (K_s and kX_f). As the ratio of the average detention time and the standard biofilm time dimension, X^* can be termed the dimensionless detention time.

In practical terms, for a given biofilm column and the same substrate, average detention time would be the parameter which determines the performance of the biofilm column in terms of substrate removal. For the same detention time, different combinations of hydraulic loading rate (v) and the length of the column would result in the same performance, as strongly supported by a pilot-scale study reported by Servais et al. (1992). Conversely, when comparing among studies, even if the average

detention times are the same, differences in specific area (α), substrate diffusivity (D_f) and biodegradation kinetics (K_s and kX_f) could result in substantially different performance. The dimensionless detention time (X^*) is thus a better parameter than the simple average detention time for making comparisons among studies. Further practical impact of X^* is discussed in detail later in this chapter.

BASIC ASSUMPTIONS FOR MODELING AOC REMOVAL

Using equation (12) to model the removal of AOC in biological water treatment requires that the removal of AOC is attributable only to biodegradation, that the biofilm reactors are operated under steady-state conditions and that the AOC represents the whole energy and carbon source contributing to and limiting the biogrowth. Because of the first requirement, the application of the model in this paper applies to situations where the adsorptive capacity of the GAC has been essentially exhausted.

Since a pilot or full-scale plant is only pseudo-steady-state in nature, we should also assume that in the several days before each sampling, the AOC level following each treatment step is relatively stable and that the sample represents this value. For the data considered in this chapter, this is a reasonable assumption, except for occasions when water quality changes related to spring runoff or significant rainfall events occurred (Huck et al., 1991). However, this would likely have introduced transients and influenced the results on only one sampling day. Lu (1993) showed that the response time of the biofilm to an increase in influent substrate concentration was in the order of several days. Temperature fluctuations could also have a significant impact on the steady-state assumption because both diffusivity and kinetic parameters are temperature-dependent. However, for the data involved in the following analysis, temperature changes were relatively minor. Temperature fluctuation is therefore considered of secondary importance and is not considered in the following analysis in this chapter.

Although it is very unlikely that AOC represents exactly the whole biodegradable organic material (BOM) and thereby the sole energy and carbon source, it is argued that AOC can be regarded as, at least, a surrogate for the overall BOM.

-39-

AOC and BDOC (Biodegradable Organic Carbon [Servais et al., 1987]) are the two parameters widely accepted as measures of BOM. Whereas BDOC has often been regarded as the parameter representing the whole BOM, it is not uncommon that AOC is considered a small portion of the BOM. This is largely because AOC, when expressed as acetate carbon equivalents, has a much lower value than BDOC expressed directly as organic carbon. However, AOC is not an absolute measure of organic carbon concentration such as DOC and BDOC. It is a measure of biogrowth potential of the subject water sample. In other words, it is an indirect measure of the biologically available energy that the organics in the water contain. Merely for convenience, the energy is expressed as acetate carbon equivalents. van der Kooij et al. (1989) indicated that AOC-NOX (the AOC measured by strain NOX) expressed as oxalate carbon equivalents was about four times the value expressed as acetate equivalents. In other words, the yield factor of strain NOX for acetate was approximately four times of that for oxalate. Accordingly, for a solution of oxalate with 1 mg/L oxalate carbon, the expected BDOC concentration is 1 mg organic carbon/L whereas the expected AOC concentration is 0.25 mg acetate carbon/L. Too easily, the difference between "acetate carbon" and "organic carbon" is ignored and AOC is concluded to be a small portion of BDOC. Therefore, any comparison of a specific AOC value with its corresponding BDOC without the knowledge of the qualitative nature (or the redox state) of the organic carbons is not meaningful. Consequently, such comparison between AOC and BDOC should not suggest that AOC represents only a small portion of BOM.

On the other hand, an investigation by Kaplan et al. (1992) provides solid evidence that AOC can be the primary portion, if not the whole, of BOM. In a recent survey involving rigorously controlled sampling of 79 drinking water facilities over North America, Kaplan et al. (1992) found that, when AOC-NOX was expressed as oxalate C equivalents and AOC-P17 as acetate C equivalents, total AOC tended to exceed BDOC although AOC totally expressed as acetate C equivalents was more frequently less than BDOC. Even totally in acetate C equivalents AOC represents 2.4 to 44.0% of DOC to compare with a not much higher percentage of 0.4 to 52.8% for BDOC. The investigation of Kaplan et al. (1992) is the first large scale comparative survey over numerous and diversified water sources for different BOM measures. Whereas a simple comparison of an individual pair of AOC and BDOC data is not

meaningful, the large number of water samples and the diversified nature of the water sources allow the statistical comparison by presuming an "average" qualitative nature of BOM. If BDOC can be considered as a measure of the whole BOM, the survey results of Kaplan et al. (1992) certainly pronounce that AOC represents the bioregrowth potential attributable to the primary portion of BOM. This is especially true for ozonated water because the shift from P17 to NOX in the AOC bioassay following ozonation is well known (Kaplan, 1992), which would make the same value of total AOC in acetate C equivalent represents more organic carbon for ozonated water than for non-ozonated water. The bioreactors analyzed in this chapter were all preceded by ozonation. Therefore, it is reasonable to assume that AOC can be regarded as a surrogate for the sole energy and carbon source for the biofilm even though AOC is unlikely exactly the whole BOM.

MODELING APPROACH

Preliminary Data Evaluation

The pilot study conducted by Huck et al. (1991) included conventional coagulation, flocculation and sedimentation followed by ozonation and two stages of biological treatment (bioactive filters and biological GAC contactors) (Figure 2-1). The measure of BOM was total AOC, consisting of AOC-NOX and AOC-P17, expressed as μg acetate C eq/L. The complete data set published by Huck et al. (1991), tabulated in Appendix 1, was used in the present analysis, with the exceptions discussed below. Data for the first two sampling dates were omitted because AOC-NOX measurements were not started until the third date (July 12, 1989). As of that date the GAC contactors had been in operation for approximately 2 months, and the dual-media filters for approximately 4 months, providing reasonable steady-state conditions. Because GAC contactor 1 broke during the study, data for this contactor were incomplete and, therefore, were excluded.

For many AOC data presented in Appnedix 1, total AOC values following the dual-media filters were higher than the corresponding values following the ozone contactors. In other words, the AOC removals through the filter were negative. There are two possible reasons for such a phenomenon. First, by jointly examining

AOC and ozone residual data (see Huck et al. 1991) it was found that most of the negative AOC removals could be related to high ozone residuals entering the filters. Therefore, some AOC might have been produced in the filters by continued reaction with ozone. The second reason, although hypothetical, is also related to high ozone residuals. While a high ozone residual will depress the bioactivity of the biofilm, a high ozone dose, perhaps in combination with residual polyaluminum chloride (Huck et al. 1990), may also produce substances which inhibit the growth of P17 and/or the NOX strain and therefore interfere with the AOC measurement. These substances might be removed physically or biologically in the filters, therefore, only a few negative removals occurred in the following GAC contactors. As shown in Table 1, most of the substantial negative removals occurred in Filters 3 and 4 following Ozone Contactor 2 which had the higher ozone dosage and therefore higher ozone residual. Because this research targets the bioactivity of the biofilm but not ozonation reactions or ozonation by-products, the data for AOC removal (ΔAOC) by Filters 3 and 4 are not included in further analysis. Although there were still several negative removals for Filters 1 and 2 and the GAC contactors, some small negative values can be expected from normal variation of AOC measurements, particularly when influent AOC concentrations and therefore removals are low. These values are therefore not arbitrarily excluded.

For Filters 1 and 2 and GAC contactors 2, 3 and 4, Pearson correlation analysis was carried out using the SYSTAT® statistics program (SYSTAT, 1992) to examine whether a functional relation can be expected between influent and effluent AOC concentrations. The outputs of the Pearson correlation analysis are presented in Appendix 2. It was found that the correlation was significant at at least the 1% level in all five columns. In other words, there is indeed a strong functional relationship between influent and effluent AOC concentrations.

Physical Parameters

Among all the physical parameters involved in equation (12), the only unknown physical parameter is the substrate diffusivity, D, which needs to be estimated simultaneously with the three kinetic parameters, k, K_s and S_{min}, through nonlinear optimization. Other physical parameters can either be assigned or

calculated, as discussed in the following paragraphs. The values of these parameters are summarized in Table 2-1. The assignment or calculation of the physical parameters could be somewhat arbitrary. Among the physical parameters in Table 2-1, the specific surface area of the media (α) and the ratio of D_f/D were considered least certain. A sensitivity analysis is thus presented later in this chapter to assess the impact of these two parameters on the outcome of parameter estimation.

For a specific column, the total depth of the column (X) is given. The hydraulic loading rate (v) is usually recorded as a routine operating condition. The specific surface area (α) of the media can be calculated directly for a given bed porosity (ε) and particle diameter (d_p) if the particles are exactly spherical. Values of $d_{p\text{-}60\%}$ and $d_{p\text{-}10\%}$ were available for the filter media and GAC. While $d_{p\text{-}60\%}$ may well represent the average size of the particles and therefore can be used for calculating the thickness of the effective liquid diffusion layer, neither $d_{p\text{-}10\%}$ nor $d_{p\text{-}60\%}$ is representative for calculating the average specific surface area. The average of $d_{p\text{-}10\%}$ and $d_{p\text{-}60\%}$ was therefore used to calculate the specific surface area.

Roberts et al. (1985) found that for irregular GAC particles of 300 μm diameter, the measured external mass-transfer rate was 1.44 to 2.04 times that predicted by assuming a spherical shape. In this case, the specific external surface area (α), was assigned a value 1.5-times that calculated for spherical particles. Moreover, electron photomicrographs from the pilot experiments indicated that neither the GAC nor the sand surface was fully covered by biomass, in part because of the irregular shape of the particles (Lu, 1993). For calculation of biofilm surface area, 90% coverage was assumed. Consequently, the specific surface area is obtained by the following formu'a:

$$\alpha = 0.9 \times 1.5 \times 6 \times (1-\varepsilon)/[(d_{p\text{-}60\%} + d_{p\text{-}10\%})/2] \tag{13}$$

Since several factors involved in equation (13) are rather arbitary, α is subject to further sensitivity analysis.

The thickness of the effective liquid diffusion layer (L) is a function of superficial flow rate (v) and can be calculated with Gnieliski's correlation (Roberts et al. 1985):

$$L = \frac{d_{p-60\%}}{(2 + 0.644\,Re^{1/2}\,Sc^{1/3})[1 + 1.5(1 - \varepsilon)]}$$ (14)

where Sc is the Schmidt number ($\mu_w/\rho D$), with ρ denoting the density of water (ML^{-3}), and μ_w denoting the dynamic viscosity of water ($ML^{-1}T^{-1}$); and Re is the Reynolds number ($vd_p\rho/\mu_w$).

The diffusivity in the biofilm (D_f) is generally lower than the free liquid diffusivity (D). D_f decreases with increased biomass density (X_f) (Fan 1989, p.552). Rittmann et al. (1986) measured the density of biofilm growing on 3-mm glass beads under oligotrophic conditions. The value ranged from 13.1 to 58.0 kg-biomass/m^3-biofilm among several biofilm columns fed with different substrates. In our case, presuming X_f is 30 kg-biomass/m^3-biofilm, D_f/D is assigned a value of 0.5, according to the D_f/D versus X_f curve in Fan (1989, p.552). Mathematically, X_f can be combined with k and kX_f will be treated as a single constant to be estimated in our modeling. The actual value of X_f is, therefore, not important in parameter estimation except for its impact on the D_f/D ratio. The assignment of the D_f/D ratio as 0.5 is rather arbitary and therefore was subject to sensitivity analysis.

Parameter Estimation

With the physical parameters given in Table 2-1, there are now only four unknowns, D, kX_f, K_s and S_{min}, left in equation (12) to be determined through parameter estimation. These four parameters are, therefore, regarded as model constants. The influent AOC concentrations are used as the independent variable whereas the effluent AOC concentrations are regarded as the dependent variable. A FORTRAN 77 computer program was devised for the complicated computations involved in the parameter estimation.

The method of least squares is the most widely used parameter estimation procedure, in which the sum of squared residuals (SSR) is the function to be minimized, called the "objective function". However, the objective function SSR has optimal statistical properties only when the errors of the observations are uniformly randomized and normally distributed (Bard, 1974). Because the bioassay procedure used for the AOC measurement (van der Kooij and Hijnen, 1984) involves dilutions, it

is the relative, rather than the absolute errors of AOC data which are constant. A logarithmic transformation of the AOC data prior to parameter estimation is therefore appropriate. Furthermore, the AOC data in this study range over more than an order of magnitude for any given sampling point with only one high value for each column but quite a number of values close to or below the S_{min} estimated later in this paper. Since the high AOC point for each column occurred during the spring runoff, the steady-state assumption required for using the biofilm model might have been violated for this data point because of rapid water quality changes. Using squared residuals as the objective function would likely make the worst observation dominate the parameter estimation.

'Robust' procedures of data fitting are commonly used in enzyme kinetic parameter estimation (Cornish-Bowden and Endreny, 1981). These procedures moderate the impact of atypical values which may or may not be 'outliners' with unknown weights. The least absolute deviation procedure, which uses the sum of absolute residuals (SAR) as the objective function, is the most common robust procedure that produces estimates less influenced by outliners than the classic least square estimates (SYSTAT, 1992). Consequently, the objective function used for this study was the SAR of the logarithms of the observations:

$$F = SAR = SUM\ ABS[ln(S_{obs})-ln(S_{pred})] \qquad (15)$$

Nonlinear estimation is required because of the model form. Most nonlinear optimization techniques are based on evaluation of the gradient or derivative of the objective function. The limitations of these methods are: (a) the derivative of the objective function should be continuous; (b) when the partial derivative of the objective function with respect to one parameter is proportional to that for another parameter, so-called 'ill conditioning' occurs and these techniques fail to converge.

In this case, the objective function is subject to both limitations. The seemingly continuous equation (12) is actually discontinuous because in the searching process the optimization algorithm may choose a value of the parameter S_{min} greater than S_{bo} and thus greater than S_{so} whereas, according to equation (1), the value of S_s/S_{min} cannot be less than unity. In addition, the steady-state biofilm model is based upon the Monod expression:

$$u = kX_fS/(K_S+S) \tag{16}$$

where u is the substrate utilization rate ($ML^{-3}T^{-1}$).

When K_s is substantially higher than S, which is the situation we will encounter later, du/dk (=$X_fS/[K_s+S]$) is approximately proportional to du/dK_s (=$-kX_fS/[K_s+S]^2$) by a factor of $-k/K_s$ despite any change in S. Using gradient based techniques, one will be trapped in "ill-conditioning".

The Simplex algorithm devised by Nedler and Mead (1965) does not depend on gradient evaluation, nor does it require a continuous function. A Simplex is a geometric figure having one more vertex than the space in which it is defined has dimensions. The algorithm involves evaluating the objective function (F) at the vertices and then using a set of rules to locate a new vertex with a lower value of F. Iteration continues until a minimum value of F is obtained. The algorithm will never diverge and it allows the handling of non-continuous functions. Therefore, an algorithm called Complex (IMSL, 1987) based on the Simplex approach was chosen.

For each bioreactor, the computation procedure was initiated with initial guesses of the four parameters. For a given set of guesses, the SAR value was calculated through the following procedure: (a) For each influent AOC (S_{bo}), influent S_s^* (S_{so}^*) was determined by balancing equation (2). (b) For a given S_{so}^*, S_{sx}^* was determined for a given empty bed contact time (X^*) by balancing equation (10). The integration was carried out by a numerical integrator (IMSL, 1987). (c) The predicted effluent AOC concentration (S_{pred}) was then calculated by substituting S_{sx}^* back into equation (2). (d) When the whole set of predicted effluent AOC concentrations was determined for a set of given influent AOC concentrations, the SAR was calculated using equation (13).

The Complex subroutine was able to adjust the four model constants and then the main program returns to Step (a) to calculate the SAR value for the adjusted model constants until it finds a set of model constants with a lower SAR value to replace the initial guesses. The iteration continued until the Complex subroutine finds that the improvement was less than or equal to a preset convergence criterion. The parameter values corresponding to the least SAR value were then the best estimates

for the parameters. A FORTRAN77 program was devised to facilitate the large amount of calculation. A printout of the FORTRAN77 program and a sample of the output from the program are included in Appendix 3.

It should be noted that the mathematical treatment of the influent AOC data as the independent variable required that the influent AOC concentration was error-free or at least have negligible error in comparison with the dependent variable, the effluent AOC concentration. Given the nature of the AOC measurement, the error of the influent AOC values was very likely not negligible. As will be shown in Chapter 3, the error associated with the independent variable could be accounted for using the error-in-variables model (EVM) (Reilly and Patino-Leal, 1981). However, EVM involves partial derivatives of the constraint equation (12), which require numerical differentiation of that equation. As discussed earlier, the numerical computation will be trapped in "ill-conditioning" or "round-off error" when minimization searching moves into the region where K_s is substantially higher than S. This makes it virtually impossible to implement the EVM algorithm. In this chapter, the error in influent AOC concentration is arbitrarily assumed to be negligible despite the fact that such an assumption would impact the parameter estimates. However, the purpose of this chapter, as mentioned previously, is to establish the general range rather than to provide exact values of the kinetic parameters. This problem along with other concerns pertaining to experimental uncertainties will further be addressed in Chapter 3.

RESULTS AND DISCUSSION

Goodness of Fit

The predictions of effluent versus influent AOC concentration are plotted in Figures 2-2 (a to e) in comparison with the experimental data. The fits appear to be without systematic bias although the scatter of the experimental data from the prediction curve is evident. This scatter is likely primarily attributable to the intrinsic variability of AOC measurement and also in part due to the pseudo-steady-state conditions.

According to Bard (1978), the goodness of fit of the model can be evaluated by testing the residual errors in each experiment (e_i), $e_i=[\ln(S_{obs})-\ln(S_{pred})]$, using the statistic

$$T^2 = \frac{n(n-1)\bar{e}^2}{\sum_{i=1}^{n}(e_i - \bar{e})^2}$$ (17)

where $\bar{e} = \frac{1}{n}\sum_{i=1}^{n}e_i$.

T in equation (17) has a student t-distribution with (n-1) degrees of freedom where n denotes the number of observations. If T is less than $t_{0.05/2}$ the average of the residuals is considered not significantly different from zero, in other words, the model is considered not significantly biased. The values of the T statistic and the corresponding $t_{0.05/2}$ values are summarized in Table 2-2. For all the five columns, T values are much less than the $t_{0.05/2}$ values.

To test the randomness of the residuals, a procedure suggested by Bard (1974) was used. For each filter or GAC column, the residuals of effluent concentration were sorted against influent concentrations. The number of residuals with positive signs was counted as n_+ and negative signs as n_-. The number of runs, a run being a sequence of residuals with the same sign, was counted as n_r. For given n_+ and n_-, the expected distribution of n_r (on the assumption of complete randomness) as a cumulative probability (P_r) was derived and tabulated by Swed and Eisenhart (1943). If P_r for an n_r with given n_+ and n_- is lower than a preassigned probability, say $P_r=0.05$, the randomness of the residuals is suspected (Bard, 1974). n_r, n_+ and n_- along with P_r are also summarized in Table 2-2. The residuals appear to be highly random because P_r values for all the five columns are much higher than 0.05.

The results of both the bias and randomness tests strongly suggest that the objective function chosen for this study is appropriate and the data are not inconsistent with the model. However, it should be stressed that a good fit does not prove that the model is correct; it merely establishes the fact that there is no reason to reject the model on the basis of the data at hand. As Bard (1974) indicated, "no amount of data can ever prove a model; all we can hope is that it does not disprove it".

Parameter Estimates

The values of the four parameters estimated through nonlinear optimization are given in Table 2-3. Because of the uncertainties pertaining to the physical parameters in Tables 2-1 and the experimental design which was not originally intended for the parameter estimation, the estimates in Table 2-3 are only to be discussed semi-quantitatively. The values of the estimates in Table 2-3 are only reported to two significant digits.

There is no AOC diffusivity value reported in the literature. According to Toor's law, "all diffusion coefficients in liquid are equal" (in comparison with the variation in the gas phase) (Cussler, 1976, p.14). The average diffusivity of AOC will therefore be considered as ranging from $0.1D_{oxalate}$ to $D_{oxalate}$. Oxalate is probably the most common AOC component in ozonated water (van der Kooij and Hijnen, 1984) and has the highest diffusivity in water among all likely AOC components because it is the most polar small carboxylic acid. Oxalate diffusivity at $25°C$ is taken from Perry and Green (1984 p.#3259) and adjusted to the average temperature of $8°C$ using the relationship that D is directly proportional to T/μ (Perry and Green, 1984, p.1214). This gives a value of 8.4×10^{-5} m^2d^{-1}. The average diffusivity (D) estimated for AOC ranges from 3.1×10^{-5} m^2d^{-1} for GAC Contactor 2 to 4.2×10^{-5} m^2d^{-1} for Filter 2. These values are $0.37D_{oxalate}$ and $0.5D_{oxalate}$ respectively, which is reasonable.

kX_f estimates in Table 2-3 vary over a relatively narrow range for all five columns, from 290 g acetate C/m^3-d for Filter 1 to 440 g acetate C/m^3-d for GAC Contactor 4 which is equivalents to 4,500 g COD/m^3-d to 7,100 g COD/m^3-d after being adjusted from acetate C equivalents to COD and from the average temperature of $8°C$ to room temperature of $22°C$ (using a θ value of 1.135, Metcalf and Eddy, 1991). Rittmann et al. (1986) determined the kX_f value of a biofilm growing on glass beads under oligotrophic conditions. The values determined with the aid of the dimensionless J^* vs S_s^* relationship ranged from 2,000 to 84,000 g COD/m^3-d. Our estimates fall at the lower end of this range.

S_{min} estimates for the five columns are very similar (see Table 2-3), ranging from 4.5 to 6.5 mg acetate-C/m^3 for the GAC contactors and from 6.3 to 10 mg acetate-C/m^3 for the filters. Because of the high K_s estimates, S_{min}^* values are far less

than unity, which, according to Heath et al. (1990), implies that the biofilm growth rate is much higher than the biofilm decay rate. If a low S_{min}^* value is further confirmed, it would explain why the biomass can be sustained (and even develop) under the oligotrophic conditions of drinking water treatment processes. The small ($<<1$) L^*/D^* values in Table 2-3, on the other hand, suggest that external mass transport resistances are not important (Heath et al., 1990). In other words, in biological drinking water treatment, allowing for the accumulation of biomass is more critical for BOM removal than minimizing mass transport resistances.

When S_{min} is known, biofilm thickness can be calculated using equation (4) which assumes that biofilm detachment rate is a first order function of biofilm mass (Rittmann, 1982; Sáez and Rittmann, 1988). As shown in the sample output for Filter 2 in Appendix 3, biofilm thickness calculated based on the first order detachment assumption can be as high as 37 mm, which is certainly not realistic for media with a $d_{p-60\%}$ of 0.88 mm. The high estimates largely reflect the fact that the biofilm detachment mechanism is more complicated than a simple first-order relationship. It should be noted that the pseudoanalytical solution of Sáez and Rittmann (1988, 1992) (equation [1]) was derived on the basis of the first order assumption. Chapter 4 will demonstrate that the relationship between S_{min} and the biofilm detachment mechanism and thus the biofilm thickness can be very complex. Chapter 5 will further demonstrate that the first order assumption has little impact on the relationship between substrate removal flux and substrate concentration so long as S_{min} is treated as an independent parameter measured *in-situ* or, as in this chapter, estimated through data fitting. Therefore, the parameters estimated in this chapter using Sáez and Rittmann's pseudoanalytical solution should not be impacted by the first order detachment assumption despite the fact that the model based on this assumption predicts artificially high biofilm thickness.

The half-velocity constant, K_s, represents substrate affinity to the enzyme system. The lower the K_s value, the higher the affinity. As shown in Table 2-3, it seems that the estimate for K_s can vary in a relatively wide range. It is interesting but not surprising that the K_S values for Filters 1 and 2 and GAC Contactor 4 are lower than those for GAC Contactors 2 and 3. Because the affinities of various AOC components can be very different, the species with relatively higher affinity would be

removed in the filters and those with lower affinity would be left for the downstream GAC contactors. Consequently, the K_s value appears to increase along the stages of biological treatment. With respect to GAC Contactor 4, it should be noted that, as described in Huck et al. (1991), Filter 4, upstream of GAC Contactor 4, achieved limited biodegradation because of its high influent ozone residual and short contact time. It is therefore not surprising that the K_s value for GAC Contactor 4 was more similar to that for the two filters than to the value for the other two GAC contactors.

For all five columns, however, the K_s values are three to four orders of magnitude higher than expected. In general, under oligotrophic conditions K_s tends to be lower than under normal substrate levels. For instance, in an oligotrophic biofilm system, the K_s value for acetate was 18 mg sodium acetate/m^3 (Rittmann et al., 1986), which is equivalent to 5.27 mg acetate-C/m^3. van der Kooij and Hijnen (1984) reported a K_s value of 15.2 mg oxalate-C/m^3 for oxalate which is equivalent to 3.8 mg acetate-C/m^3 (van der Kooij et al., 1989).

On the other hand, it should be noted that our expectation of the correct range of K_s is based only upon the two papers mentioned above. There is still no directly comparable case which provides a K_s value for AOC. Typical K_s values for domestic wastewater are 25 to 100 mg BOD_5/L (Metcalf and Eddy, 1991, p.394), which is equivalent to 18.75 to 75.0 g acetate-C/m^3. The K_s values estimated in this paper fall in or below the lower end of the range, which probably reflects the oligotrophic conditions present in biological water treatment. In fact, recent investigations by others have shown that the K_s value, calculated for biological water treatment processes on the basis of BDOC measurements, was on the order of 1g acetate-C/m^3.

One possible reason for the high estimates is that the pilot plant was not designed for the determination of kinetic parameters. The relatively long biofilm columns used in the pilot plant made the response of effluent AOC very insensitive to the change of influent AOC. For kinetic parameter estimation, future research should use relatively short columns to obtain a more sensitive response in the effluent.

However, a more fundamental reason for the uncertainties in the high and uncertain estimates of K_s may be attributed to the high K_s itself. If K_s is indeed intrinsically high, say in the order of 1000 mg-C/m^3, whereas the AOC concentration

is the order of 100 mg-C/m^3, it would be very difficult to obtain precise estimation for K_s in numerical computation. In the situation of "ill-conditioning", K_s along with kX_f can "drift" to higher magnitude with little impact on the prediction.

On the other hand, if it is true that K_s is as high as estimated here, the intrinsic kinetics of AOC utilization would be reduced to first order because influent AOC rarely exceeds 1000 mg acetate-C/m^3. For first-order biodegradation kinetics, an analytical solution is available for packed-bed biofilm (Skowlund and Kirmse, 1989), which would then provide a much simpler solution for process analysis and parameter estimation. Further confirmation of the range of K_s is therefore important for modeling biological water treatment processes.

Sensitivity Analysis

Confidence intervals were unable to be estimated for the parameters in Table 2-3 because of mathematical complexity discussed previously. To provide some indication of the reliability of the parameter estimation, a sensitivity analysis was performed for Filter 2, because it has the shortest detention time and thus would be more sensitive than the other bioreactors. The results of sensitivity analysis for kX_f, K_s, and D are illustrated in Figure 2-3. By adjusting each of these three model constants by 50% (while keeping the other three unchanged), the predicted effluent concentration changed by not more than 18%. While this is encouraging from the perspective of model application, it also suggests that the confidence intervals for kX_f, K_s and D could be rather wide. The change in the three parameters has no impact in the vicinity of S_{min} whereas the impact of the change of S_{min} is limited to the vicinity of S_{min}. In other words, estimates of S_{min} are very much independent of the estimates of the other three parameters.

Because the calculation of the surface area (α) and the assignment of D_f/D as 0.5 is rather arbitrary, another kind of sensitivity analysis was performed. The α value for Filter 2 in Table 2-1 was varied by $\pm50\%$ and a D_f/D ratio of 0.8 as suggested in Rittmann et al. (1986) was used. The results of this sensitivity analysis are summarized in Table 2-4. For a given set of data, an arbitrary change of the surface area (α) would have to be compensated for by the kinetic parameters (k and K_s), and the diffusivity (D), whereas a change of D_f/D would be compensated for by k and K_s.

-52-

However, k seemed to be little affected by the changes in α and D_f/D. The kinetic part of the compensation was essentially realized through the change in K_s, which varied by a factor of two or three. This tends to support the results in Table 2-3, where the kX_f values for the five columns varied in a rather narrow range whereas K_s values varied by more than a factor of five. A change of the ratio D_f/D from 0.5 to 0.8 had only a minor impact on the estimate of D. The change did produce a more than 50% increase in K_s, which supports the earlier discussion that the biofilm process is controlled by bioreaction rather than by external transport resistance. It is worth noting that even though the variation due to the change of α and D_f/D is substantial, the order of magnitude of K_s estimates does not change. This excludes the wary that the arbitrariness in choosing the values of physical parameters could have artificially distorted the order of magnitude of K_s.

It is worth noting that the S_{min} estimates are almost completely independent of the changes in the physical parameters α and D_f/D and the three other model constants kX_f, K_s and D. Recalling the close S_{min} estimates in Table 2-3, the robustness of S_{min} estimates suggests the existence of S_{min} in terms of AOC. This in turn supports the fundamental assumption that AOC can be the surrogate for the whole substrate, because S_{min} only exists for the substrate parameter which represents the whole carbon and energy source (Rittmann and McCarty, 1980).

Process Analysis

Heath et al. (1990) found that for a completely mixed biofilm system there should a "boomerang" shape curve of $log(S_b/S_{min})$ vs $log(J/J_{deep})$ for a primary substrate, where J_{deep} is the J defined by $J^* = \{2[S_s^* - \ln(1 + S_s^*)]\}^{1/2}$. The curve was called a "normalized loading curve". Although the "boomerang" shape of the normalized loading curve explains why biofilm processes can provide consistent and low effluent BOM in biological drinking water treatment, this process analysis approach is not applicable for analyzing pilot/full scale AOC data for the following reasons.

First, because of nature of the AOC measurement, AOC data intrinsically contain large variations. When the influent AOC level is low (and thereby close to S_{min}), effluent AOC is expected to be approximately equal to influent AOC. In this situation, the large inherent variation associated with AOC measurement could mean

that the measured influent AOC is less than the measured effluent AOC. This could lead to a negative J value and makes logarithmic plotting impossible. In a pilot-scale study, the influent substrate concentration may vary slightly during sampling. The sample collected at the outlet may actually have a higher concentration than the sample collected at the inlet, resulting in a negative removal even without the large variation in AOC measurement. Therefore, the plots of effluent AOC concentration (S_e) versus influent AOC concentration (S_o) rather than the plots of $\log(S_b/S_{min})$ vs $\log(J/J_{deep})$ are used in this study. Such plotting in turn substantially moderates the convexity of the "boomerang" shaped curve.

Secondly, the "boomerang" shaped curve is only applicable for the segment where influent substrate concentration is higher than S_{min}. For S_i less than S_{min}, the steady state biofilm model predicts that the biofilm would disappear and S_e equals S_o, which results in a straight line with a slope of unity. Combining this segment of straight line with the moderated "boomerang", the curve of S_e vs S_o predicted from the steady state biofilm model could be roughly a straight line rather than a "boomerang". Such behaviour is seen in Figure 2-2(b). It is therefore essentially impractical to illuminate a "boomerang" for AOC data in biological drinking water treatment.

Indeed, as shown in Figure 2-4(a), plots of S_e vs S_o for Filter 2 suggest that there may be a simple linear relationship between the effluent AOC and the influent AOC. (Statistical significance cannot be tested because the influence concentration is not error free or negligible.) The plot in Figure 2-4(b) for GAC Contactor 2, on the other hand, indicates that the linearity, if any, can be very weak. No matter how the AOC data are modelled, given their large intrinsic variability it is unrealistic to expect precise prediction of process performance. However, from the viewpoint of bioregrowth prevention, it is also unnecessary to be able to pinpoint a specific effluent AOC for a specific influent AOC. To suppress bioregrowth in a water distribution system, what matters is the intermittent to long term treatment plant effluent AOC concentration rather than the AOC concentration for a specific sample at a specific moment. Therefore, predicting an average percentage removal rate would be of much more practical meaning than predicting a specific effluent AOC concentration for a given influent AOC concentration.

The average percentage AOC removal rate is approximately the slope of AOC removal ($\Delta S = S_o - S_e$) vs influent AOC concentration when the x-intercept is small. Examples of such plots are presented in Figure 2-5 for Filter 2 and GAC Contactor 2, where the straight line passes very close to the origin. The advantage of the transformation from simple S_e vs S_o plots to ΔS vs S_o plots is that the latter tends to enhance the correlation because of the confounding of ΔS and S_o, which is evident when comparing in Figure 2-5 with Figure 2-4. Very often the S_e vs S_o correlation is not so obvious. In many pilot/full scale studies the quality of AOC data (and other BOM measurements) may not be as good as the AOC data presented in this study. A quite check of the enhanced linear relationship between AOC removal and influent AOC concentration provides a fast but valuable preliminary assessment of AOC data quality. More extensive discussion of the enhanced linear relationship between the AOC removal rate and influent AOC concentration, on a strictly empirical basis, has been presented in a previous article (Huck et al., 1994). The lowest linear correlation coefficient (for GAC Contactor 2) for the linear relationship among the five columns discussed in this chapter was 0.88, significant at the 1% level.

In fact, such a linear relationship between AOC removal and influent AOC concentration can be expected from the steady state biofilm. Based on equation (12), a FORTRAN77 program was written to demonstrate the linear relationship between dimensionless substrate removal (ΔS^*) and dimensionless influent concentration (S_o^*), inherent in the steady state biofilm model. Figure 2-6 illustrates the linear relationship of ΔS^* vs S_o^* for S_o^* ranging from 0 to 0.036 and for a range of dimensionless EBCT (X^*). The values of the dimensionless parameters were chosen based on the estimates in Table 2-3 with $S_{min}^* = 0.001$ ($K_s = 10^4$ mg acetate-C/m^3) and $L^*/D^* = 0.025$. The FORTRAN77 program is given in Appendix 3.

The beauty of the slope of the ΔS vs S_o relationship is two-fold. On one hand, as an approximate percentage removal, it is the process performance parameter with the most practical importance, as discussed previously. On the other hand, it is physically dimensionless and thus can be directly related to the dimensionless kinetic model: dimensionless ΔS^* vs S_o^* is equivalent to dimensional ΔS versus S_o. The slope of the linear relationship, therefore, provides a very useful tool to couple the sophisticated kinetic model with simple and practical process analysis.

The dimensionless form of equation (12) has reduced the number of independent parameters to be considered in the process analysis from eleven to four $(X^*, S_o^*, L^*/D^*$ and $S_{min}^*)$. The following process analysis focuses on the relationship between the slope of the ΔS^* vs S_o^* (the approximate percentage removal) and the four dimensionless parameters.

Dimensionless detention time is the determining factor for the value of the slope. Plotting the slope of Figure 2-6 vs X^* in Figure 2-7 (a), we see that the slope of ΔS^* vs S_o^* increases with increasing X^* for given S_o^*, L^*/D^* and S_{min}^*. For a given pilot/full scale, packed-bed, it may be assumed that the kinetics (τ), the substrate diffusivity (D_f) and the specific surface area (α) are given and constant. Because $X^* = \theta\frac{\alpha D_f}{\tau}$, X^* is determined by θ. In other words, the average percentage removal is determined by the average detention time. As long as the average detention time remains the same, different combinations of hydraulic loading rate and column depth would achieve the same removal of BOM. This is strongly supported by the results of a pilot study reported by Servais et al. (1992).

However, what is more important is the convex shape of the slope versus X^* curve: the slope increases steeply at low X^* and then more gradually. Beyond a certain value of X^*, further increases in X^* will not help much to increase the slope and the slope approaches unity. In practical terms, this means that, above a certain EBCT, further increases in the detention time will result in only a minimal increase in percentage removal. A slope of unity implies removal down to S_{min}. An economical design should avoid trying to achieve an unrealistically high percentage BOM removal, i.e. a depth of packed bed beyond the convex part of the curve should not be employed. The end of the convex part of the curve occurs at a value of X^* of about 3 in Figure 2-7. By comparison, calculated values of X^* in Table 2-3 range from 0.55 to 2.3 and the approximate percentage removal rates range from 57% to 81%, as plotted in Figure 2-8. The middle curve in Figure 2-7(a), which corresponds to the situation of $S_{min}^* = 0.001$, $L^*/D^* = 0.025$ and $S_o^* < 0.036$, is also presented in Figure 2-8 for comparison. The actual data points in Figure 2-8 are seen to agree generally with the theoretical predictions. Figure 2-8 further shows that the biofilm columns used in Huck et al. (1991) do not appear to be too deep for the hydraulic loading rates used.

The extent of the convexity of the slope-versus-X^* curve is affected by the three independent parameters other than X^*: S_o^*, L^*/D^* and S_{min} *. In general, the convexity increases with a decrease in the range of S_o^*. As shown in Figure 2-7(a), increasing the range of S_o^* from 0 to 3.6×10^{-2} to 0 to 1.2×10^{-1} would only cause a limited decrease in the convexity whereas decreasing the range of S_o^* to one third of 0 to 3.6×10^{-2} substantially increases the convexity. This suggests that the biofilm reactors in the study by Huck et al. (1991) could tolerate three times higher influent AOC levels without significant loss in AOC removal and, of course, if the range of influent AOC concentrations was lower, the performance would be much better.

Figure 2-7 (b) indicates that decreasing S_{min}^* from 10^{-3} (which is equivalent to 10 mg acetate-C/m^3 because K_s was assigned as 10^4 mg acetate-C/m^3) to 2.0×10^{-4} would noticeably increase the convexity and therefore increase the amount removed for a given X^*. This is because a smaller S_{min}^* represents a higher potential for net biogrowth and thus more biomass in the packed bed (Heath et al., 1990), and implies that finding packing media with better surficial properties for biomass accumulation may substantially improve the performance of biological water treatment processes. An increase of S_{min}^* to 5.0×10^{-3} only results in a minimal decrease in convexity, which suggests that the bioreactors were quite stable. In other words, a bit less biomass would not have substantially impaired the performance.

L^*/D^* represents the relative importance of external mass transfer resistance. Consistent with the earlier discussion, Figure 2-7(c) confirms that the L^*/D^* value of 2.5×10^{-2} calculated in Table 2-3 represents the insignificance of external mass transport in the study by Huck et al. (1991) because a further decrease of L^*/D^* by one order of magnitude results in little increase in convexity. An increase of one order of magnitude in L^*/D^*, however, would measurably decrease the removal because of the increase in external mass transfer resistance.

Although the linear simplification is a very valuable tool in process analysis, the intrinsic nonlinearity around S_{min} should not be overlooked in process design. For one thing, S_{min} is the lower limit for sustaining a steady-state biofilm. In other words, a process design should not set an unrealistic treatment goal which is below S_{min}. Furthermore, the slope should not be oversimplified as the true percentage removal. A rather safe expectation for the effluent concentration (S_e) would be $S_e = Slope \times S_{min} +$

(1 - Slope) $\times S_o$, which is the relationship proposed by Mitton et al. (1994) on the basis of the empirical linear model.

CONCLUSIONS

This chapter presents, for the first time, a kinetic approach to interpret AOC removal in biological water treatment processes using the existing steady-state biofilm model. The steady state biofilm model, developed by Rittmann and McCarty (1980) and improved by Sáez and Rittmann (1988, 1992), appeared to be able to fit adequately to pilot scale AOC data from Huck et al. (1991). Although adequate data-fitting does not prove that the steady state biofilm model is the best model for describing AOC removal, it does suggest that it is feasible to use the model as a framework for analyzing biological drinking water treatment processes.

Because of the intrinsic scatter of AOC data, there could be a number of alternative models which may fit AOC data equally as well. One of the alternative models is the empirical linear relationship between AOC removal and influent AOC concentration presented initially by Huck and Anderson (1992) and developed further in a paper coauthored by the author (Huck et al., 1994). This model has the most practical importance in process analysis because the slope of such a linear relationship represents approximate percentage AOC removal, the key objective parameter for the analysis and design of biological drinking water treatment processes. It was found in the present research that such a linear relationship can also be expected from the steady state biofilm model. The slope of the linear relationship thus provides the link between empirical modeling and kinetic modeling.

The dimensionlessness of the slope allows us to use the dimenionless model derived for packed bed biofilm columns in this chapter to analyze the impact of operating conditions, biofilm kinetics and substrate concentration on the process performance in terms of percentage AOC removal. In the dimensionless domain, the number of factors involved in process analysis was reduced from ten to four. Among the four factors, dimensionless detention time (X^*), which is directly proportional to the average detention time, is the determining factor for the value of the slope. The

slope increases convexly with increasing X^*, and the extent of the convexity was found to be affected by three other factors, S_o^*, S_{min}^* and L^*/D^*.

The use of the steady state biofilm model requires that the substrate being modelled represents the primary substrate. AOC has long been suspected by some researchers to be only a small portion of the total BOM, even though there is no direct evidence to support such a perception. A recent survey by Kaplan et al. (1992) involving a large number of water facilities across North America has found that AOC represents a prime portion of the total BOM (as represented by BDOC), which lays the ground for using the steady state biofilm model to model AOC data.

This research provides, for the first time, values of AOC kinetic parameters. S_{min} values estimated through data fitting fell in a narrow range of 4.5 to 10 mg acetate-C/m^3, although this must be viewed in the context of the intrinsic scatter of AOC data and of the fact that many influent AOC values were close to S_{min}. Sensitivity analysis indicated that variations in other physical and kinetic parameters had almost no impact on S_{min} estimates. Such robust consistency in S_{min} estimates strongly suggests that S_{min} exists for AOC and provides additional support for modeling AOC as a primary sustrate.

The three other parameters estimated through the data fitting are D, kX_f and K_s. Among them, the estimates of D (3.1×10^{-5} to 4.2×10^{-5} m^{2}d^{-1}) and kX_f (290 to 450 g acetate C/m^3-d) were considered reasonable. The K_s value, ranging from 6.6 to 36 g acetate-C/m^3, is about three orders of magnitude higher than the results of two other reported investigations using acetate or oxalate as substrate. However, it is still low in comparison with typical values for wastewater and it generally agrees with the results of current research by others on drinking water biotreatment.

Since the pilot study was not originally designed for parameter estimation, the values estimated for the biofilm kinetic parameters should be considered as merely a semi-quantitative indication of the ranges of these parameters rather than precise estimates. Nevertheless, the parameter estimation does help identify certain areas of concern.

The first major concern is the variation in K_s estimates and seemingly higher-than-expected magnitude of K_s. The reasons for the variation might include (1) the lengthy plug-flow biofilm columns used in the pilot-study, which made the response of effluent AOC concentration rather insensitive to the change of influent AOC concentration, (2) the pseudo-steady state nature of the pilot study, and (3) the non-negligible error of the influent AOC data, which was not accounted for by the data fitting algorithm.

While it is unclear to what extent each of the above uncertainties may contribute to the variation in parameter estimates, a more fundamental reason for the uncertainties in the higher-than-expected estimates of K_s could be the high K_s itself. If K_s is indeed intrinsically high, much higher than the influent AOC concentration, it would be very difficult to obtain precise estimation for K_s in numerical computation, because of "ill-conditioning". In this situation, K_s along with kX_f can "drift" to higher magnitude with little impact on the prediction.

A well controlled study is presented in Chapter 3, which reduces the uncertainties attributable to the first three reasons. If the high range of K_s is further confirmed in Chapter 3, the intrinsic kinetics of AOC utilization should then be considered as first-order. For a first-order biodegradation kinetics, an analytical solution is available for packed-bed biofilm reactors (Skowlund and Kirmse, 1989). This solution would then provide a much simplified and yet analytical solution for process analysis and parameter estimation in drinking water biotreatment.

The second major concern was that, based on the definition of S_{min} used in this chapter (equation [4]), an unrealistic biofilm thickness was predicted for the estimated S_{min} values. The S_{min} definition in equation (4) assumed that biofilm detachment rate was a first order function of biofilm mass (Rittmann, 1982; Sáez and Rittmann, 1988). Chapter 4 will demonstrate that the relationship between S_{min} and the biofilm detachment mechanism and thus biofilm thickness can be very complex. Therefore, the artificially high prediction of biofilm thickness does not suggest that the S_{min} estimates are unrealistic; it rather reflects the fact that biofilm detachment is not a simple first order process (Chang and Rittmann, 1988).

However, it should be noted that the pseudoanalytical solution of Sáez and Rittmann (1988, 1992) (equation [1]) was derived on the basis of the first order assumption. It would appear that if the first order assumption could predict unrealistically high biofilm thickness, the pseudoanalytical solution derived using the first order assumption could also be problematic. Chapter 5 further demonstrates that the first order assumption has little impact on the relationship between substrate removal flux and substrate concentration so long as S_{min} is treated as an independent parameter measured *in-situ* or, as in this chapter, estimated through data fitting. The parameters estimated in this chapter using the pseudoanalytical solution of Sáez and Rittmann (1988, 1992), therefore, should not be impacted by the first order detachment assumption.

Table 2-1. Parameters measured, calculated or assigned for data-fitting.

Column	Measured		Calculated		Assigned	
	v (m/d)	X (m)	dp-60% (μm)	α (m^{-1})	ε	D$_f$/D
Dual-Media Filter 1	120	0.75	882	6161	0.425	0.5
Dual-Media Filter 2	240	0.75	882	6161	0.425	0.5
GAC Contactor 2	192	2.78	1206	5056	0.425	0.5
GAC Contactor 3	96	2.65	1206	5056	0.425	0.5
GAC Contactor 4	192	2.78	1206	5056	0.425	0.5

Table 2-2. Goodness-of-fit tests.

Column	n	T	t$_{0.05/2}$	n$_r$	n$_+$	n$_-$	P$_r$
Dual-Media Filter 1	15	0.268	2.15	10	7	6	0.966
Dual-Media Filter 2	17	0.233	2.12	10	7	9	0.806
GAC Contactor 2	17	0.167	2.12	9	7	8	0.704
GAC Contactor 3	17	0.026	2.12	12	8	8	0.968
GAC Contactor 4	19	0.024	2.10	12	9	9	0.891

Table 2-3. Parameters estimated through nonlinear optimization or calculated subsequently.

Column	Parameters Estimated				Parameters Calculated			
	K_s (gC/m3)	kX_f (gC/m^3-d)	D (m^2/d)	Smin (mgC/m^3)	X*	τ (μm)	L (μm)	L*/D*
Dual-Media Filter 1	6.6	290	3.5e-5	6.3	1.1	640	42	0.033
Dual-Media Filter 2	8.7	340	4.2e-5	10	0.55	740	33	0.023
GAC Contactor 2	28	360	3.1e-5	4.5	1.1	1100	40	0.018
GAC Contactor 3	36	310	3.6e-5	5.4	1.7	1400	56	0.020
GAC Contactor 4	9.0	440	4.0e-5	6.5	2.3	640	43	0.034

Table 2-4. Sensitivity analysis for Filter 2.

Scenario	Parameters Estimated				Parameters Calculated		
	K_s (gC/m^3)	kX_f (gC/m^3-d)	D (m^2/d)	S_{min} (mgC/m^3)	X*	τ (μm)	L (μm)
Dual-Media Filter 2 (from Table 2-2)	8.7	340	4.2e-5	10	0.55	740	33
0.5α	3.3	250	8.9e-5	10	0.56	770	41
1.5α	27	370	5.3e-5	10	0.55	1400	35
D$_f$/D=0.8	14	310	4.7e-5	10	0.56	1300	34

```
                            RAW WATER
                                |
                           COAGULATION
                      (Polyaluminum Chloride)
                                |
                   FLOCCULATION/SEDIMENTATION
          ┌─────────────────────────┴─────────────────────────┐
    OZONE CONTACTOR                              OZONE CONTACTOR
  Ozone/TOC = 0.5 mg/mg                        Ozone/TOC = 1.0 mg/mg
    ┌──────────┴──────────┐                    ┌──────────┴──────────┐
ANTHRACITE/SAND   ANTHRACITE/SAND        ANTHRACITE/SAND   ANTHRACITE/SAND
FILTER (0.75 m)   FILTER (0.75 m)        FILTER (0.75 m)   FILTER (0.75 m)
   (5 m/h)           (10 m/h)               (5 m/h)           (10 m/h)
      |                 |                      |                 |
GAC CONTACTOR     GAC CONTACTOR          GAC CONTACTOR     GAC CONTACTOR
   (2.65 m)          (2.78 m)              (2.65m)           (2.78 m)
   (4 m/h)           (8 m/h)               (4 m/h)           (8 m/h)

  Stream 1          Stream 2              Stream 3          Stream 4
```

Figure 2-1. Flow diagram of pilot plant.
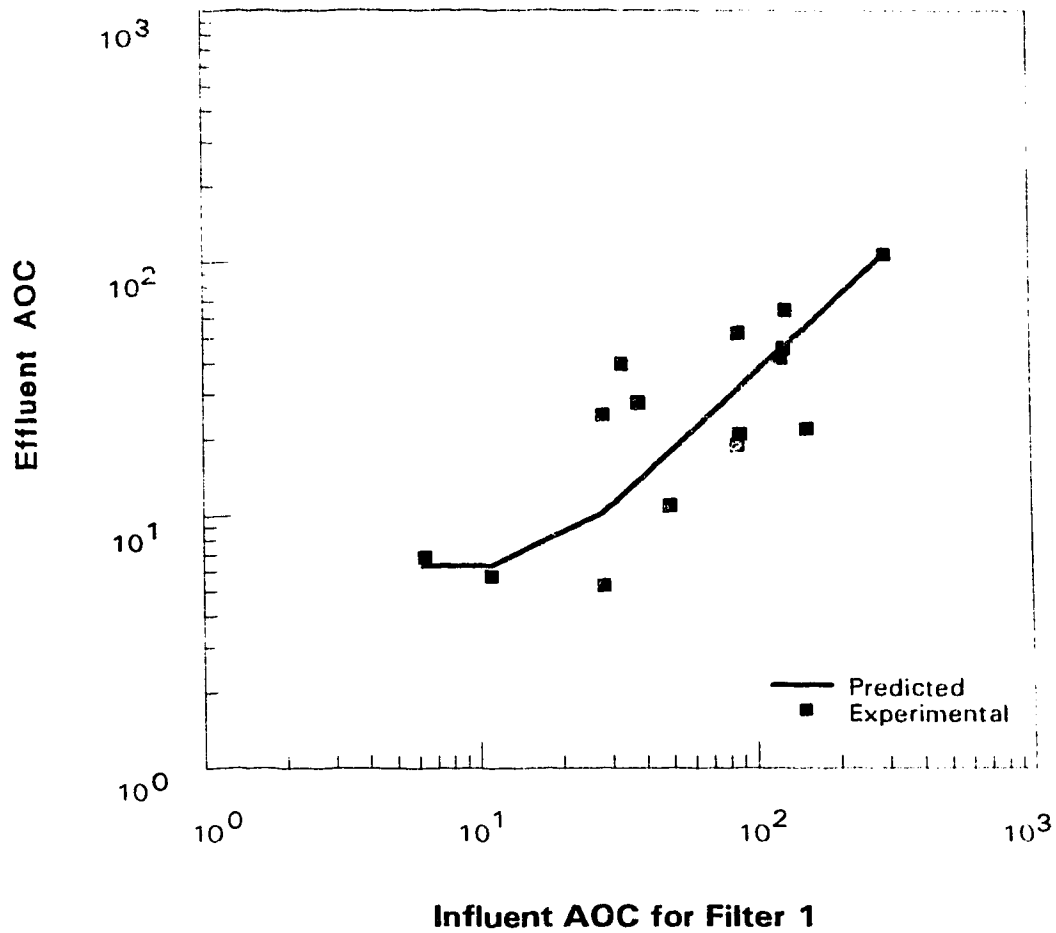
Figure 2-2(a). Prediction of effluent versus influent AOC concentration using the best estimates (AOC expressed as mg acetate C/m^3).
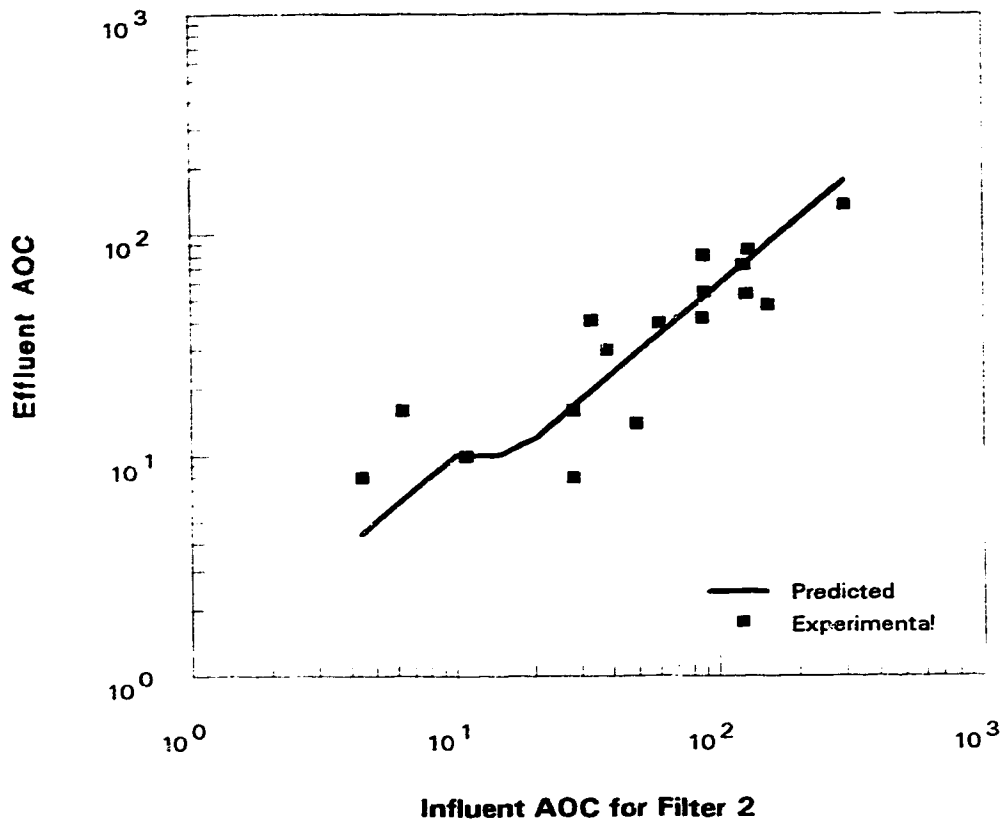
Figure 2-2(b). Prediction of effluent versus influent AOC concentration using the best estimates (AOC expressed as mg acetate C/m^3).
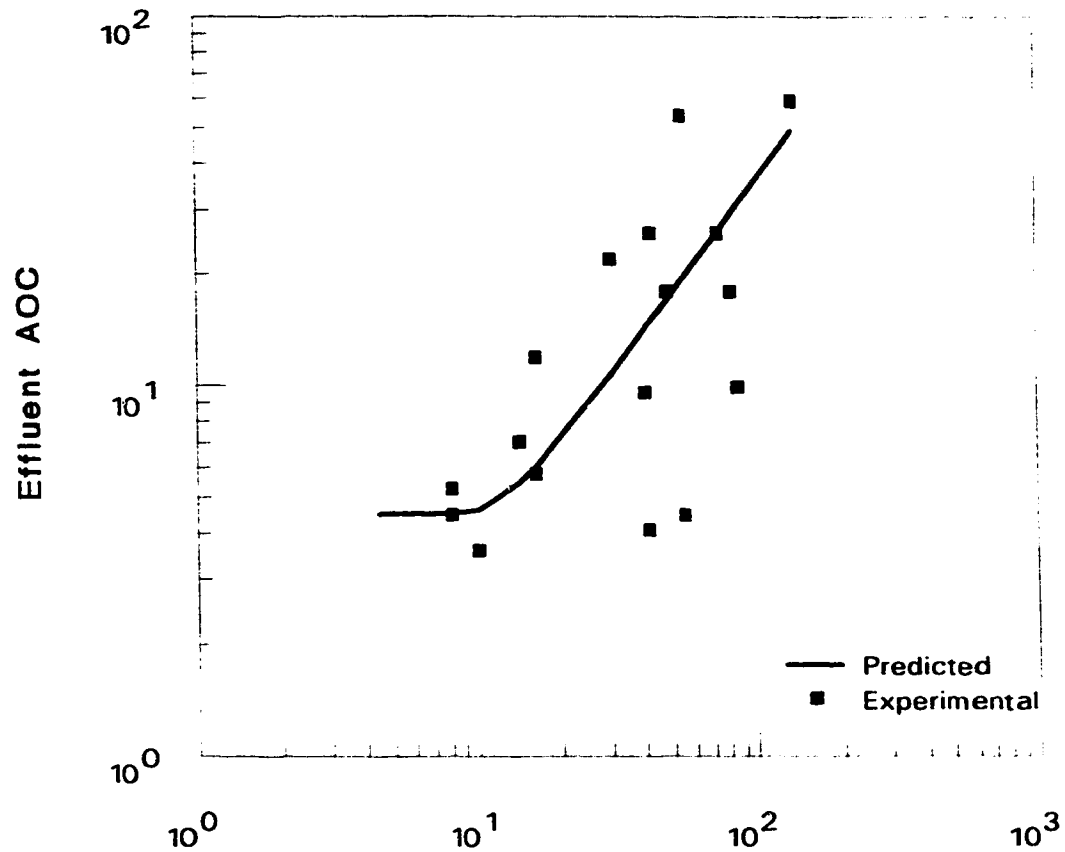
Figure 2-2(c). Prediction of effluent versus influent AOC concentration using the best estimates (AOC expressed as mg acetate C/m^3).

Figure 2-2(d). Prediction of effluent versus influent AOC concentration using the best estimates (AOC expressed as mg acetate C/m^3).
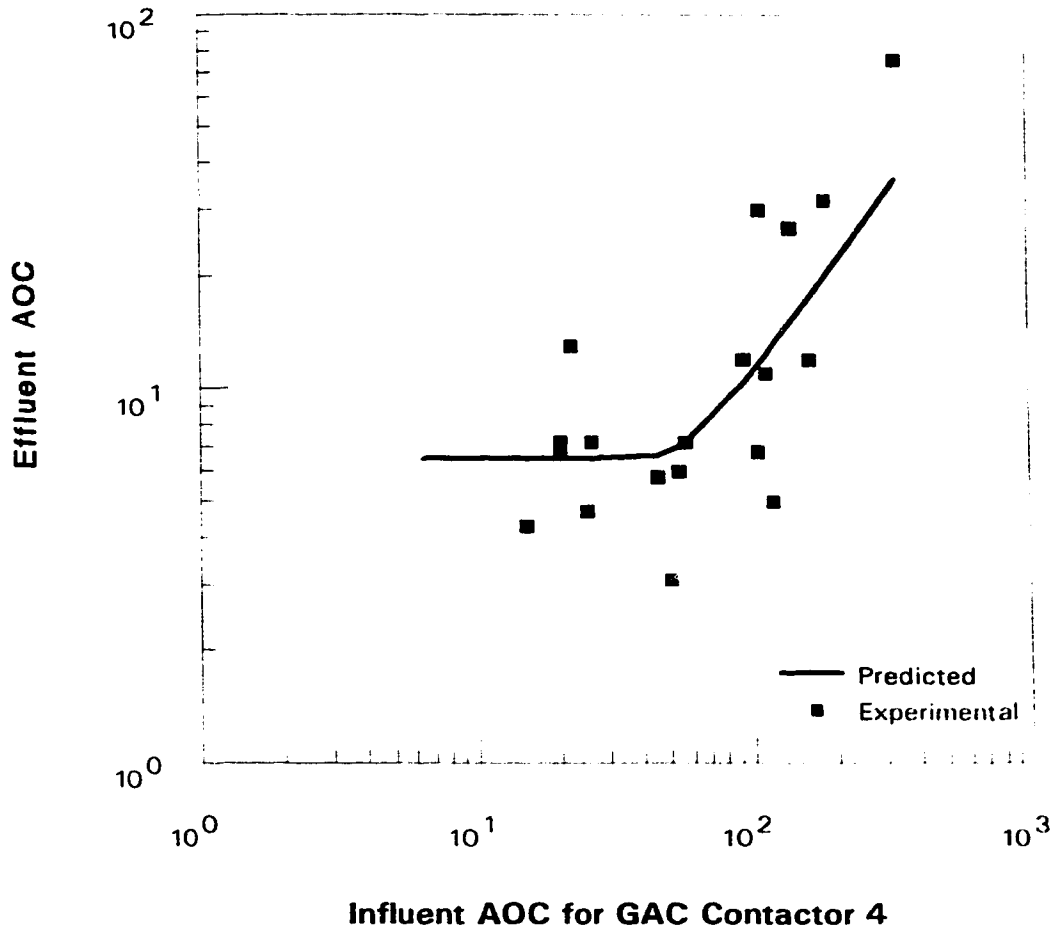
Figure 2-2(e). Prediction of effluent versus influent AOC concentration using the best estimates (AOC expressed as mg acetate C/m^3).
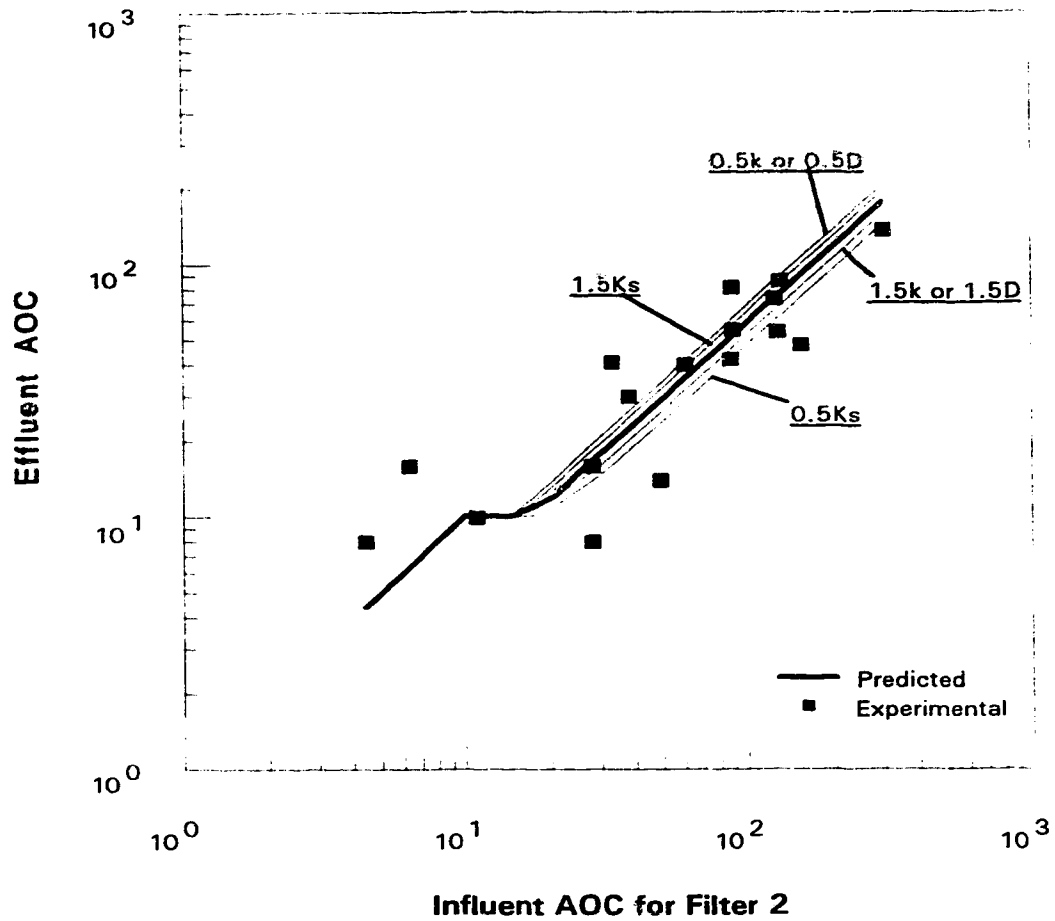
Figure 2-3(a). Sensitivity analysis for Filter 2 (AOC expressed as mg acetate C/m^3).
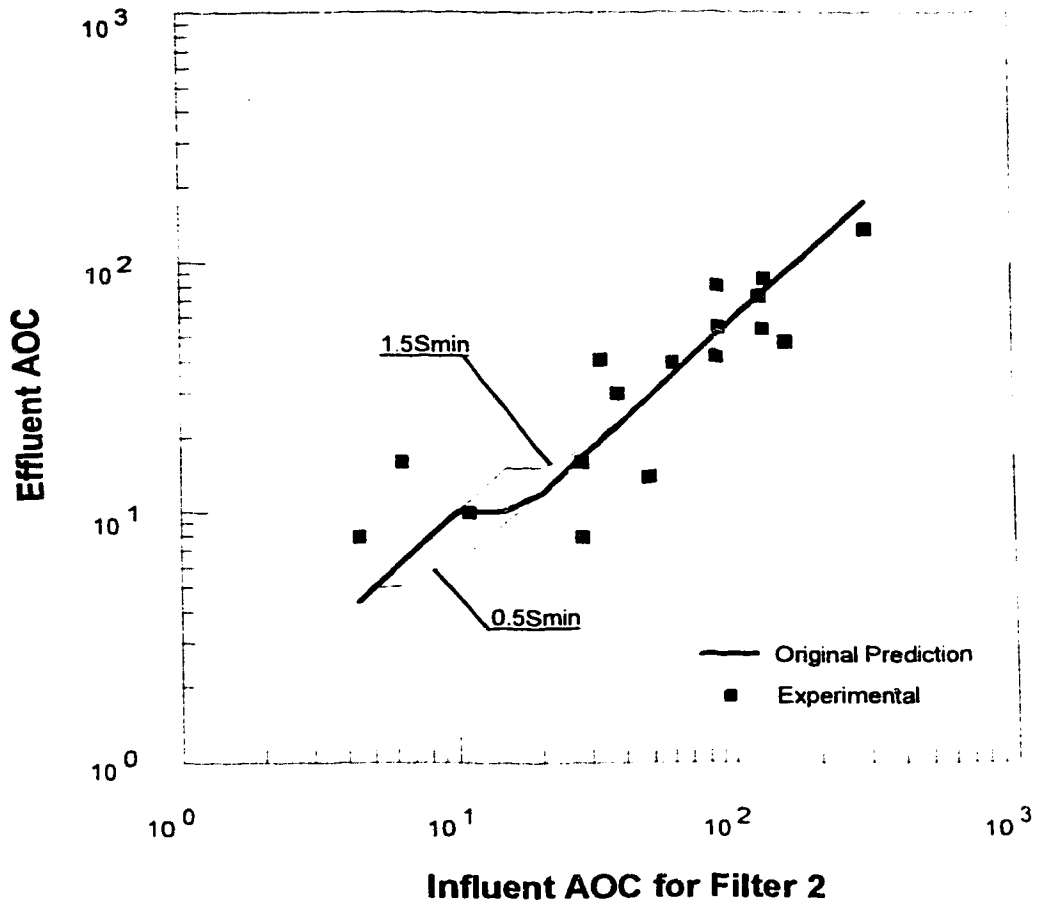
Figure 2-3(b). Sensitivity analysis for Filter 2 (AOC expressed as mg acetate C/m^3).
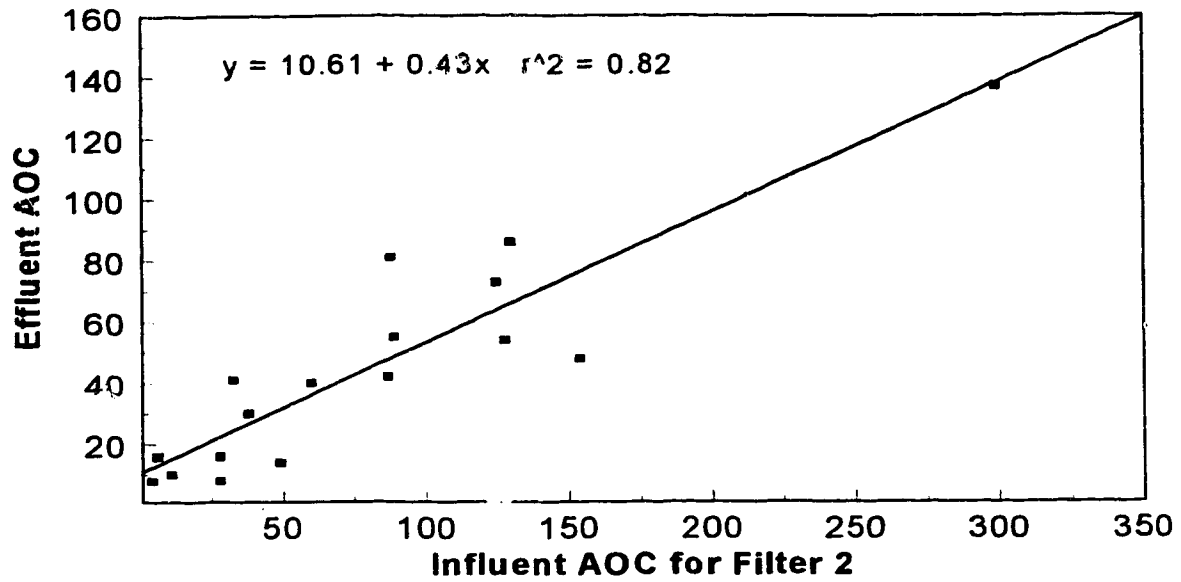
(a)
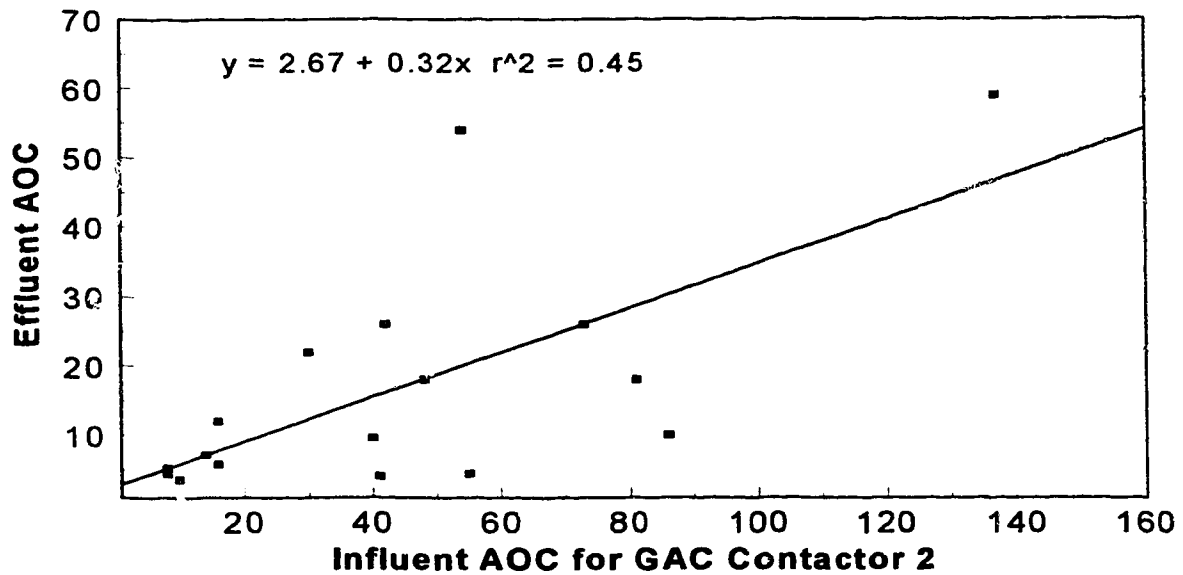
(b)

Figure 2-4. Weak linear relationship between effluent AOC and influent AOC concentration (AOC expressed as mg acetate C/m³).

(a)

(b)
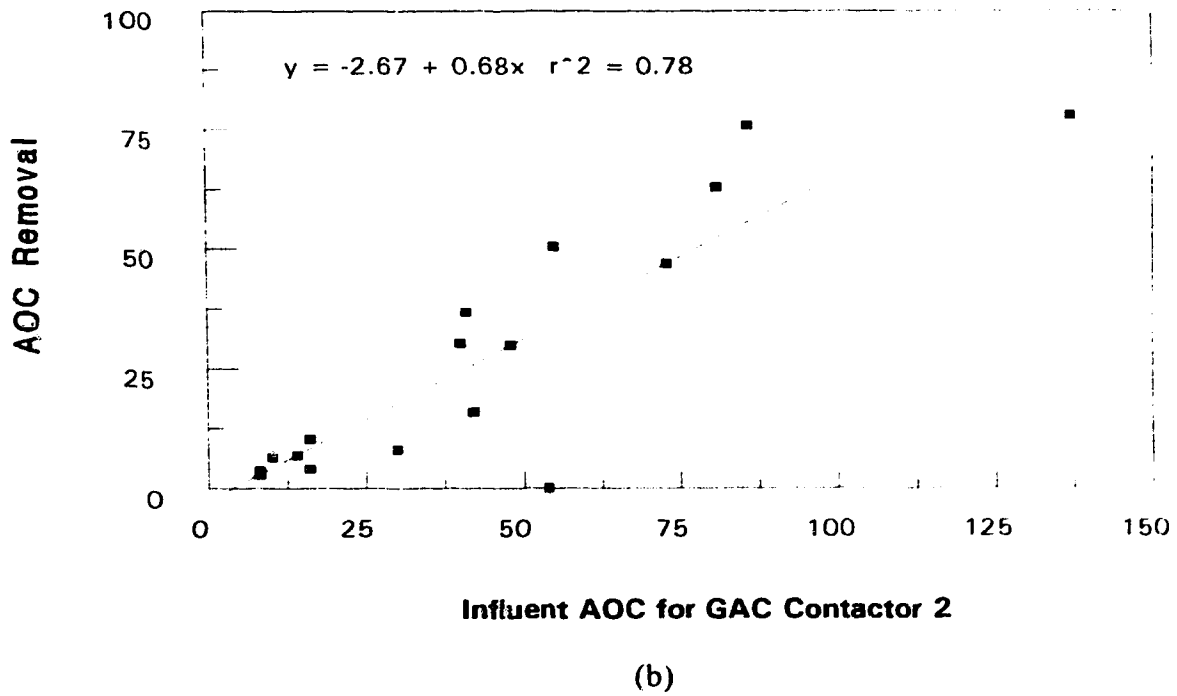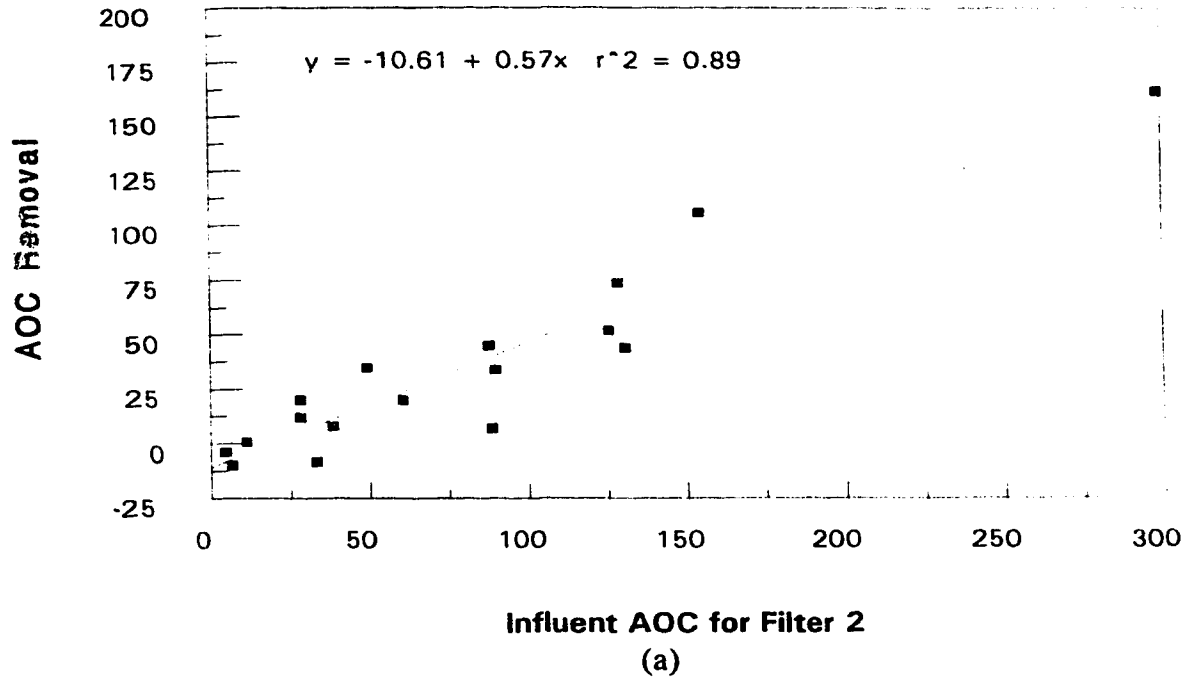
Figure 2-5. Enhanced linear relationship between AOC removal and influent AOC concentration (AOC expressed as mg acetate C/m^3).
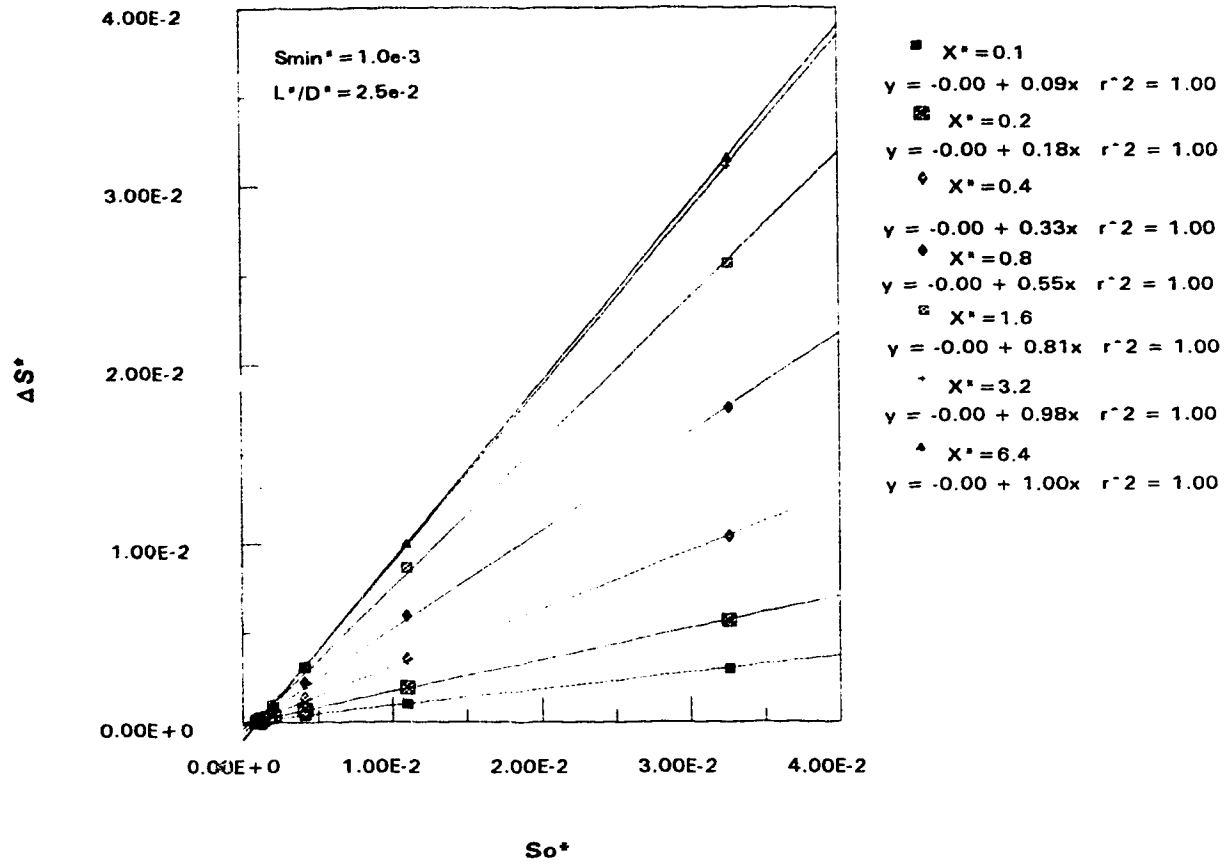
Figure 2-6. General linearity of substrate removal (ΔS^*) versus influent substrate concentration (S_0^*) for a variety of dimensionless detention times (X^*).
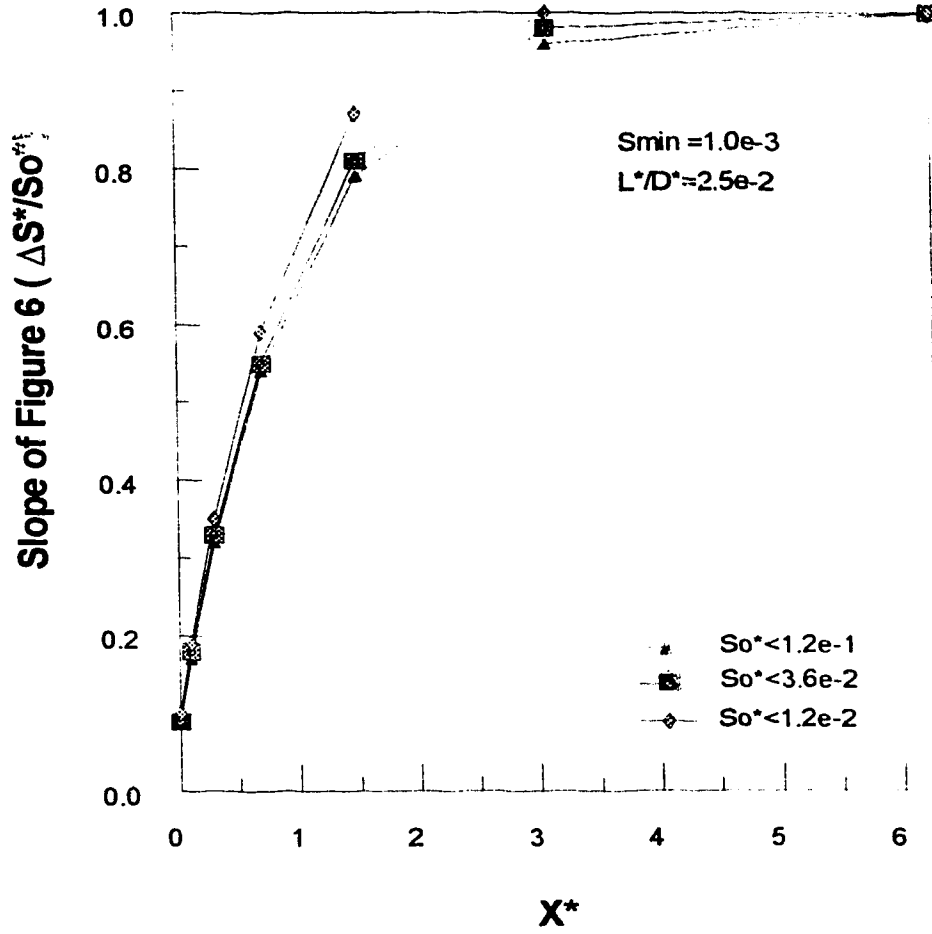
Figure 2-7(a). Factors affecting the convexity of the curve of the slope versus X*.
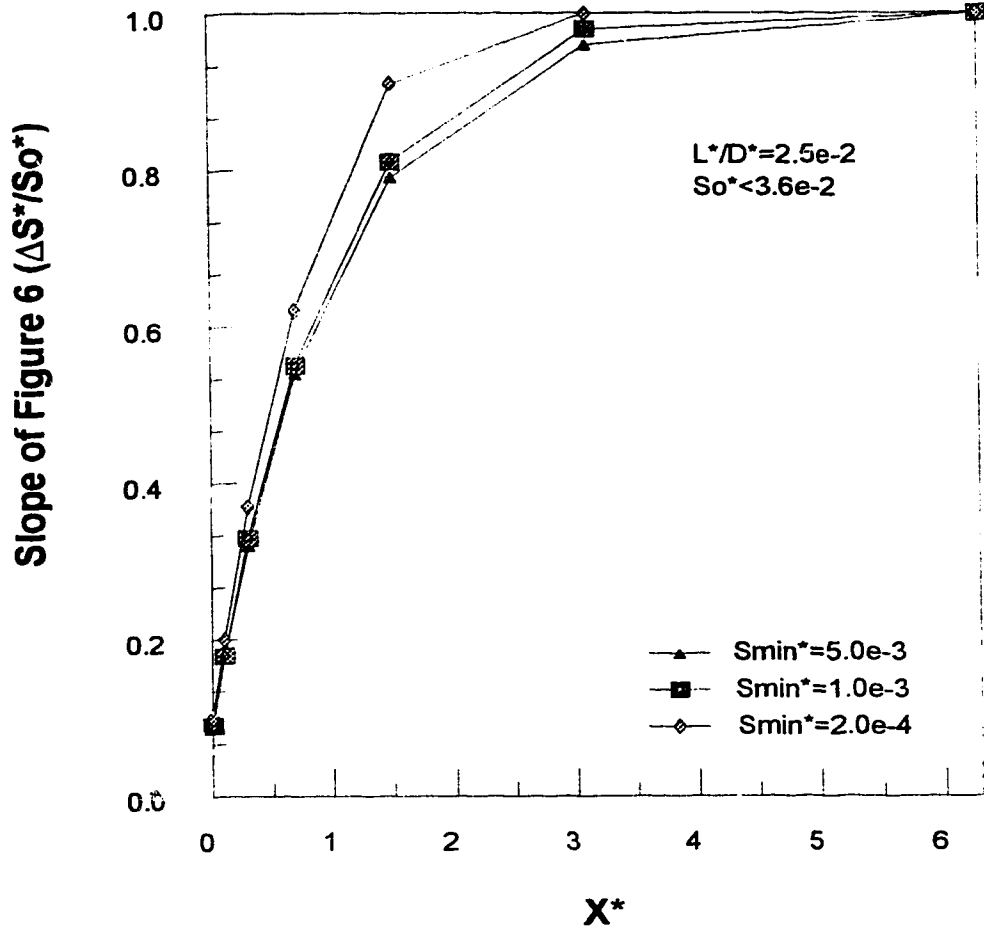
Figure 2-7(b). Factors affecting the convexity of the curve of the slope versus X*.
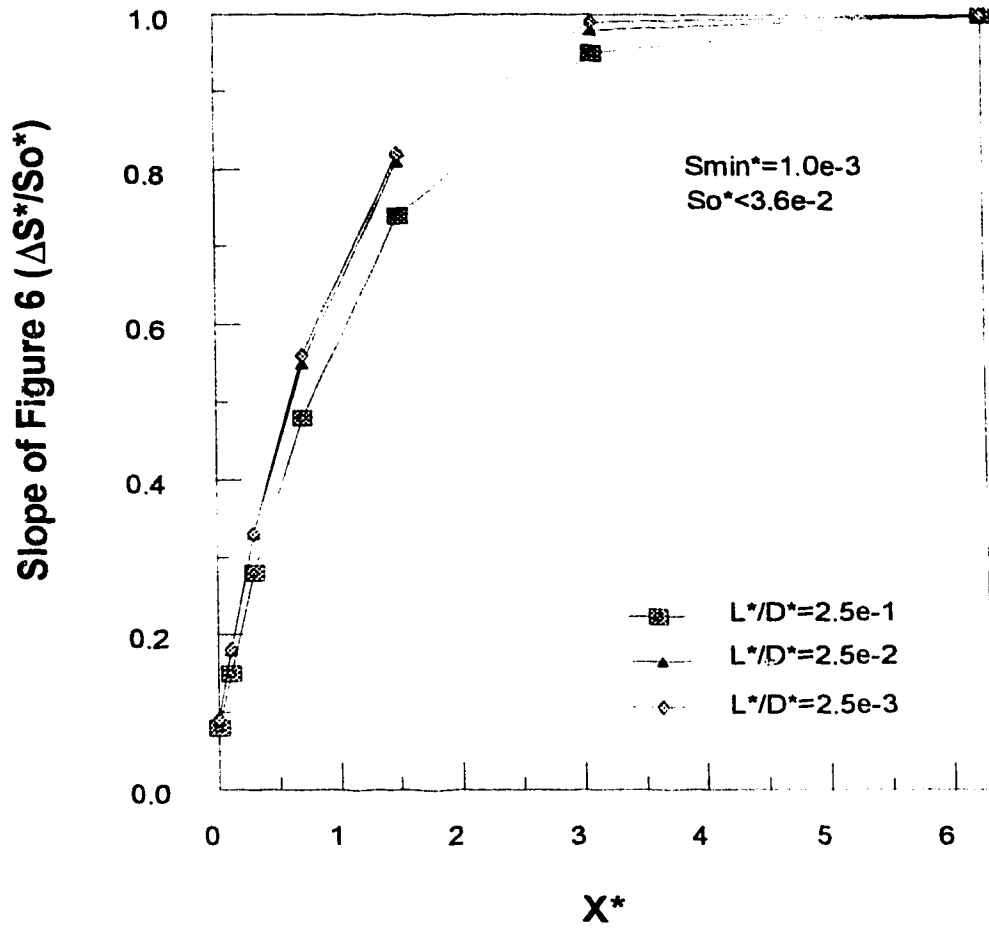
Figure 2-7(c). Factors affecting the convexity of the
curve of the slope versus X*.
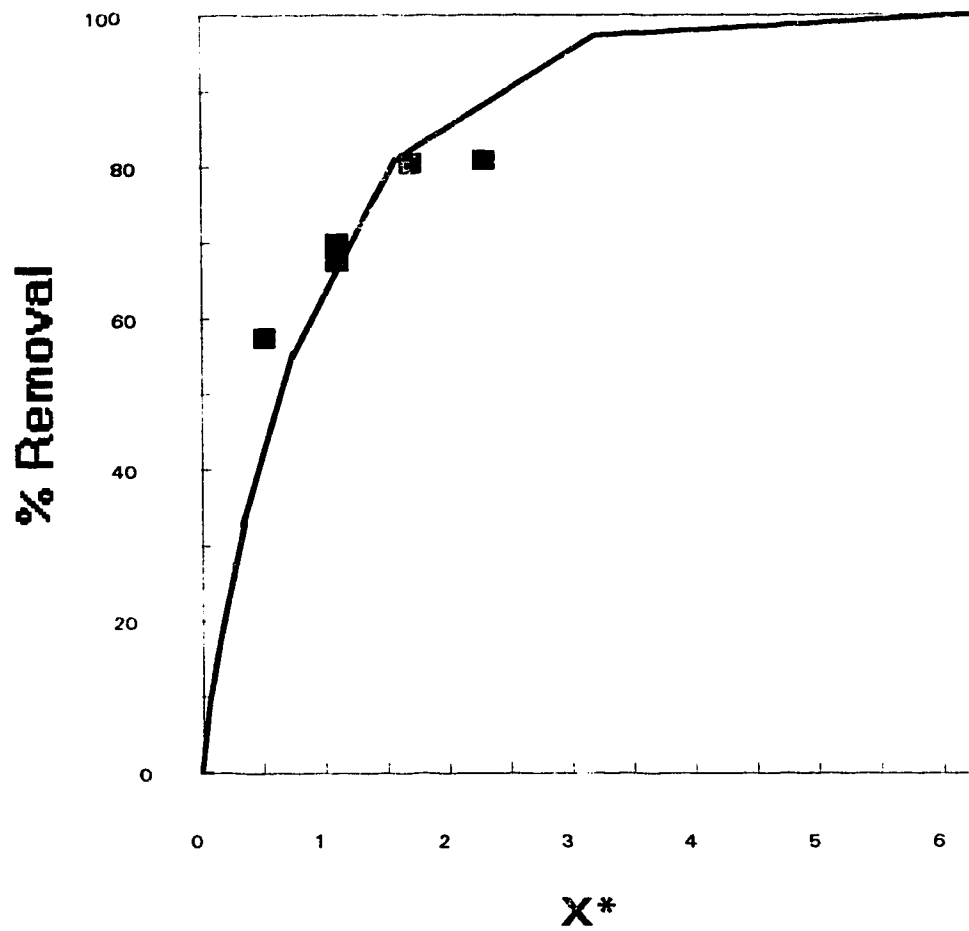
Figure 2-8. Actual percentage removal rate versus X*
for the five columns.

REFERENCES

Atkinson B. and Daoud I. S. (1968) The analogy between microbial "reaction" and heterogeneous catalysis. *Trans. Inst. Chem. Engrs.* **46**, T19-24.

Bailey J. E. and Ollis D. F. (1986) *Biochemical Engineering Fundamentals*, 2nd edition, McGraw-Hill, New York

Bard Y. (1974) *Nonlinear Parameter Estimation*. Academic Press, New York.

Bear J. (1988) *Dynamics of Fluids in Porous Media*, 2nd edition. Elsevier Publishing Company, Inc., New York.

Chang H. T. and Rittmann B. E. (1988) Comparative study of biofilm shear loss on different adsorptive media. *J. Wat. Pollut. Control Fed.*, **60**, 362-268.

Cornish-Bowden A. and Endreny L. (1981) Fitting of enzyme kinetic data without prior knowledge of weights. *Biochem. J.* **194**. 1005-1008.

Cussler E. L. (1976) *Multicomponent Diffusion*, Elsevier Scientific Publishing Company, New York.

Fan L. S. (1989) *Gas-Liquid-Solid Fluidization Engineering*, Butterworths, New York.

Heath M. S., Wirtel S. A. and Rittmann B. E. (1990) Simplified design of biofilm processes using normalized loading curves. *Res. J. Wat. Pollut. Control Fed.* **62**, 185-192.

Huck P. M. and Anderson W. B. (1992) Quantitative relationships between the removal of NVOC, chlorine demand and AOX formation potential in biological drinking water treatment. *Vom Wass.* **78**, 281-303.

Huck P. M., Fedorak P. M. and Anderson W. B. (1990) Methods for determining assimilable organic carbon and some factors affecting the van der Kooij method. *Ozone Sci. Engng.* **11**, 377-392.

Huck P. M., Fedorak P. M. and Anderson W. B. (1991) Formation and removal of assimilable organic carbon during biological treatment. *J. Am. Wat. Wks. Ass.* **83**(12), 69- 80.

Huck P. M., Zhang S. and Price M. L. (1994) BOM removal during biologial treatment: a first order model. *J. Am. Wat. Wks. Ass.* **86**(6), 61-71.

IMSL (1987) *IMSL User's Manual: MATH LIBRARY FORTRAN Subroutines for Mathematical Applications*, IMSL Inc, Chicago.

Kaplan L. A., Reasoner D. J., Rice E. W. and Bott T. L. (1992) A survey of assimilable organic carbon, biodegradable organic carbon and coliform growth response in US drinking water. *J. Wat. Sci.* **5** (special number), 207-224

Lu P. (1993) *Measurement of Biofilms in a Biological Drinking Water Treatment Plant.* M.Sc. Thesis, Department of Civil Engineering, University of Alberta, Edmonton Canada.

Metcalf and Eddy, Inc. (1991) *Wastewater Engineering: Treatment, Disposal and Reuse*, 3rd edition, McGraw-Hill, New York.

Mitton M. J., Huck P. M., Krasner S. W., Miltner R. J., Prévost M. and Reckhow D A. (1994) Using a First Order Relationship to Interpret and Predict Removals in Biological Drinking Water Treatment. *Submitted to J. Am. Wat. Wks. Ass.* for review, June 1994.

Montgomery J. M., Inc. (1985) *Water Treatment Principles and Design*, John Wiley and Sons, New York.

Nedler J. A. and Mead R. (1965) A Simplex method for function minimization. *Computer J.*, **7**, 308-317.

Perry R. H. and Green D. (Editors) (1984). *Perry's Chemical Engineers Handbook*, 6th edition, McGraw-Hill: New York.

Peyton B. M. and Characklis W. G. (1993). A statistical analysis of the effect of substrate utilization and shear stress on the kinetics of biofilm detachment. *Biotechnol. Bioengng.* **41**, 2343-2357.

Prévost M., Coallier J., Mailly J., Desjardins R. and Duchesne D. (1992). Comparison of biodegradable organic carbon (BOC) techniques for process control. *J. Wat. Supply Res. Technol.-Aqua*, **41**(3), 141-150.

Reilly P. M. and Patino-Leal H. (1981) A Bayesian study of error-in-variables model. *Technometrics*, **23**, 221-231.

Rittmann B. E. (1982) The effect of shear stress on biofilm loss rate. *Biotechnol. Bioengng.* **24**, 501-506.

Rittmann B. E. and McCarty P. L. (1980). Model of steady-state-biofilm kinetics. *Biotechnol. Bioenngg.* **22**, 2343-2357.

Rittmann B. E., Crawford L., Tuck C. K. and Namkung E. (1986). *In situ* determination of kinetic parameters for biofilms: isolation and characterization of oligotrophic biofilms, *Biotechnol. Bioengng.* **28**, 1753-1760.

Roberts P. V., Cornel, P. and Summers R.S . (1985). External mass-transfer rate in fixed-bed adsorption. *J. Environ. Eng. Div.* **111**, 891-905.

Robinson J. A. (1985) Determining microbial kinetic parameters using nonlinear regression analysis. In *Advances in Microbial Ecology* (Edited by Marshall K. C.), Plenum Press, Vol. 8, pp. 61-114.

Sáez P. B. and Rittmann B. E. (1988). Improved pseudo-analytical solution for steady-state biofilm kinetics. *Biotechnol. Bioengng.* **32**, 379-385.

Sáez P. B. and Rittmann B. E. (1992). Accurate pseudo-analytical solution for steady-state biofilms. *Biotechnol. Bioengng.* **39**, 790-793.

Servais P., Billen G. and Hascoët M. C. (1987). Determination of the biodegradable fraction of dissolved organic matter in waters. *Wat. Res.* **21**, 445-450.

Servais P., Billen G., Bouillot P. and Benezet M. (1992). A pilot study of biological GAC filtration in drinking water treatment. *J. Wat. Supply Res. Technol. - Aqua*, **41**, 163-168.

Skowlund C. T. and Kirmse D. W. (1989) Simplified models for packed-bed biofilm reactors. *Biotechnol. Bioengng.* **33**, 164-172.

Swed F. S. and Eisenhart C. (1943) Tables for testing randomness of grouping in a sequence of alternatives. *Ann. Math. Stat.* **14**, 66-78.

van der Kooij D. and Hijnen W. A. M. (1984). Substrate utilization by an oxalate consuming *Spirillum* species in relation to its growth in ozonated water. *Appl. Envir. Microbiol.* **47**, 551-559.

van der Kooij D., Hijnen W. A. M. and Kruithof J. C. (1989). The effects of ozonation, biological filtration and distribution on the concentration of easily assimilable organic carbon (AOC) in drinking water. *Ozone Sci. Engng.* **11**, 297-311.

Zhang S. L. and Huck P. M. (1996) Removal of AOC in biological water treatment processes: a kinetic approach. *Wat. Res.*, in press.

Chapter 3

PARAMETER ESTIMATION FOR BIOFILM PROCESSES IN BIOLOGICAL DRINKING WATER TREATMENT[2]

INTRODUCTION

In Chapter 2, a framework was presented for applying a steady-state biofilm model to analyze pilot scale biological drinking water treatment data. The model was used to estimate the necessary parameters for process design: the parameters of Monod-type biodegradation kinetics (k and K_s), the average diffusivity of Assimilable Organic Carbon (AOC), and the minimum substrate concentration required to sustain a steady-state biofilm (S_{min}). Such parameters were not available in the literature.

One major concern raised in the previous chapter was that the K_s estimates seemed to be much higher than expected and that kX_f and K_s estimates vary substantially. Simply from a modeling perspective, a high K_s value could be beneficial to process analysis because if K_s is much higher than the typical AOC level in biological drinking water treatment processes, AOC biodegradation kinetics can be considered as first-order. For first-order biodegradation kinetics, an analytical solution is available for a packed-bed biofilm reactor (Skowlund and Kirmse, 1989). Further process analysis and parameter estimation are then much simplified.

However, estimation of parameters from pilot scale data suffers from several limitations, which might have artificially led to the high estimates. For example, the influent concentrations at pilot or full scale are normally not controllable, and the experimental design and physical conditions such as contact times selected to meet other objectives may not be optimal for parameter estimation. In addition, parameter estimation using plug-flow type biofilm reactors is mathematically complex, which

---

[2]A version of this chapter has been published. *Zhang and Huck 1996. Water Research. 30: 456-464.*

prevents us from taking the non-negligible error of influent AOC measurement into account in the data fitting algorithm.

These problems can be addressed in a bench scale study where the experimental conditions can be well controlled and a nearly CSTR biofilm reactor can considerably simplify the mathematical model. This chapter describes such a study Important features of the investigation are the use of steady-state as opposed to nonsteady-state bioreactors (e.g. Rittmann et al., 1986), the use of the Error-in-Variables Model for parameter estimation, and the use of the jackknife technique to estimate confidence intervals.

STEADY-STATE BIOFILM MODEL

According to Sáez and Rittmann (1992), the flux $(J, M_x L^{-2} T^{-1})$ of biodegradable substrate into a steady-state biofilm can be expressed as a function of the substrate concentration at the biofilm outer surface $(S_s, M_x L^{-3})$ and the minimum substrate concentration for sustaining the steady-state biofilm $(S_{min}, M_x L^{-3})$. In dimensionless form,

$$J^* = \{2[S_s^* - \ln(1+S_s^*)]\}^{1/2} \times \tanh[\gamma(S_s^*/S_{min}^* - 1)^\beta] \tag{1}$$

where

$$\gamma = 1.557 - 0.4117 \tanh(\log S_{min}^*)$$
$$\beta = 0.5035 - 0.0257 \tanh(\log S_{min}^*) \tag{2}$$

This is the continuous pseudo-analytical solution to the nonlinear differential equation of diffusion-with-bioreaction (Eq. [1] in Chapter 1) in the so-called "steady-state biofilm model", which also includes the following three equations proposed by Rittmann and McCarty (1980):

$$S_s^* = S_b^* - J^* L^*/D^* \tag{3}$$

$$S_{min}^* = b/(Yk - b) \tag{4}$$

-84-

$$L_f^* = \frac{1 + S_{min}^*}{S_{min}^*} \quad J^* = J^*kY/b \tag{5}$$

The parameters in the above equations are all in the dimensionless domain. They relate to actual dimensional parameters through the following relationships:

where $\quad S_b^* = S_b/K_s \qquad\qquad S_s^* = S_s/K_s \qquad\qquad S_{min}^* = S_{min}/K_s$

$\qquad\qquad J^* = J\tau/K_sD_f \qquad\qquad L_f^* = L_f/\tau \qquad\qquad L^* = L/\tau$

$\qquad\qquad D^* = D/D_f \qquad\qquad (\tau = [K_sD_f/kX_f]^{1/2}, \; L)$

where S_b is the bulk liquid concentration of the substrate (M_sL^{-3}); D is the free liquid diffusivity (L^2T^{-1}); D_f is the diffusivity in the biofilm (L^2T^{-1}); K_s is the half-velocity constant in the Monod expression (M_sL^{-3}); k is the maximum specific rate of substrate utilization (T^{-1}); Y is the yield coefficient, M_x/M_s; b denotes the overall biofilm decay rate coefficient (T^{-1}); X_f is the biofilm density (M_xL^{-3}); L_f is the biofilm thickness (L) and L denotes the thickness of the effective diffusion layer (L).

Of the above parameters, only S_b is directly measurable. In a CSTR biofilm system (Figure 3-1), S_b equals S_e, the effluent substrate concentration (M_sL^{-3}). For a CSTR biofilm reactor, J can be calculated through the following formula:

$$J = Q(S_i - S_e)/\alpha V \tag{6}$$

where Q denotes the flowrate in and out of the CSTR system; S_i is the influent concentration (M_sL^{-3}); V is the volume of biofilm reactor (L^3); and α is the specific surface area of the solid support medium (e.g. glass beads) (L^{-1}). L can be calculated through hydrodynamic equations for a given superficial velocit (Rittmann and McCarty 1980).

PARAMETER ESTIMATION

Previous Investigations

Using a nonsteady-state recycle biofilm column with a nearly CSTR feature, similar to that shown in Figure 1, Rittmann et al. (1986) developed an approach to determine k and K_S through manual curve-fitting. Their nonsteady-state approach was based on the assumption that the biofilm thickness of an established biofilm would not change during a short period (4 hours) of sudden change of the feed solution. Such an experimental approach requires prompt detection of the response of the effluent concentration to ensure a pseudo-steady condition for sampling. It also requires a small sample volume so that the sampling can be finished in a short time. Rittmann et al. (1986) were able to use radioactively-labeled compounds as substrate. However, AOC measurements usually require more than 1 week of incubation and 600-mL sample volume. Also, AOC consists of a number of unknown substrates, and therefore radioactive-labeling cannot be used. These factors would make the nonsteady-state technique unfeasible for parameter estimation for biological drinking water treatment.

Even without the above experimental difficulties, Rittmann's technique was not applicable for biological drinking water treatment because it required a value for substrate diffusivity which is an unknown for BOM in natural water. Even if we can assign a value for the diffusivity (Zhang and Huck, 1995), the estimation obtained from Rittmann's approach would still be subject to considerable error because of the need to choose visually among a series of very similar curves. When BOM is measured as AOC, the error could become very large because AOC data can be subject to high variability. For a data set discussed later in this paper, duplicate measurements led to a coefficient of variation of 12%. Individual determinations can vary by a greater amount. For high variability, the fitting procedure becomes somewhat arbitrary.

Theoretically, the model parameters could be estimated through nonlinear regression. By substituting equation (3) into equation (1), the flux (J) can be expressed as a function of the bulk concentration (S_b):

-86-

$$J^* = \{2[(S_b^*-J^*L^*/D^*)-\ln(1+S_b^*-J^*L^*/D^*)]\}^{1/2}$$
$$\times \tanh\{\gamma([S_b^* - J^*L^*/D^*]/S_{min}^*-1)^\beta\} \qquad (7)$$

If each of the dimensionless quantities in equation (7) is replaced by the appropriate dimensional values, the resulting expression contains two measurable variables, J and S_b, and four model parameters, D, S_{min}, K_s and kX_f (k and X_f are mathematically combined as a single parameter). Theoretically, by providing at least four sets of J and S_b data, the four model parameters could be estimated.

However, conventional nonlinear regression techniques are not feasible in this case, for two reasons. First, conventional regression requires dependent variables to be explicit functions of independent variables. However, equation (7) is an implicit function because J appears on both sides. Second, conventional regression assumes that independent variables are error-free or, at least, have negligible error. However, because the error associated with AOC measurements may be more than 10%, as will be shown later, neither the flux (J) nor the substrate concentration (S_b) can be regarded as error-free.

Error-in-Variables Method

When both dependent and independent variables are subject to error, parameters can be estimated using the "Error-in-Variables Model (EVM)". In an EVM, there is no distinction between dependent and independent variables. Instead, all observations are considered as coming from some unknown true values. Therefore, the EVM technique should be able to estimate not only the model parameters but the "true" values of the observations as well. In a milestone article, Reilly and Patino-Leal (1981) presented an algorithm which permitted solution of error-in-variables problems through iterative use of conventional nonlinear optimization approaches.

Without the distinction between dependent and independent variables, equation (7) can be expressed as the following implicit function:

$$g(z, \theta) = 0 \qquad (8)$$

where column vector $z=(J, S_e)^T$, and vector $\theta=(D, S_{min}, K_s, kX_f)^T$. For each observation z_i there is assumed to be a column vector of true values $\hat{z}_i = (\hat{J}_i, \hat{S}_{ei})^T$.

-87-

The maximum likelihood estimation of the vector of model constants ($\hat{\theta}$) is obtained by minimizing the error (Q) between the observed values and the "true" values while keeping the constraint equation (8) satisfied:

$$Q = \min \sum_{i=1}^{n} (z_i - \hat{z}_i) V_i^{-1} (z_i - \hat{z}_i) \qquad i = 1,2,\ldots n \qquad (9)$$

$$g_i = g(\hat{z}_i, \hat{\theta}) = 0 \qquad i = 1,2,\ldots n \qquad (10)$$

where n is the number of observations and V_i is the covariance matrix. Because J (a function of S_i) is independent of S_e, we can assume that the errors of J and S_e are uncorrelated. Therefore,

$$V_i = \begin{bmatrix} \sigma^2_{Ji} & 0 \\ 0 & \sigma^2_{Sei} \end{bmatrix} \qquad (11)$$

where σ_{Ji} is the standard deviation of J_i, and σ_{Sei} is the standard deviation of S_{ei}. In practice, the standard deviations can be replaced by the standard errors.

Reilly and Patino-Leal (1981) have shown that minimization of Q is equivalent to minimizing

$$S(\hat{\theta}) = \min \sum_{i=1}^{n} [g_i + B_i(z_i - \hat{z}_i)]^2 (B_i V B_i^T)^{-1} \qquad i = 1,2,\ldots n \qquad (12)$$

where $B_i = \dfrac{\partial g(\hat{z}_i, \hat{\theta})}{\partial \hat{J}_i}, \dfrac{\partial g(\hat{z}_i, \hat{\theta})}{\partial \hat{S}_{ei}}]$.

$\hat{z}_i$ in equation (12) is an unknown vector which has to be determined through an iterative procedure. Initially we can assign $\hat{z}_i = z_i$. A function minimization subroutine is used to find the value of $\hat{\theta}$ which minimizes $S(\hat{\theta})$. The second step is to renew $\hat{z}_i$ by substituting the $\hat{\theta}$ estimated in the first step into equation (13):

$$\hat{z}_i^{new} = z_i - V B_i^T (B_i V B_i^T)^{-1} [g_i + B_i(z_i - \hat{z}_i)] \qquad (13)$$

Then the third step is to replace $\hat{z}_i$ in equation (12) with $\hat{z}_i^{new}$ calculated in the second step. The iteration carries on until the values of vector $\hat{\theta}$ are stabilized.

A FORTRAN77 program was developed to handle the enormous amount of calculation involved in the parameter optimization. The Simplex algorithm (Nedler and Mead, 1965) was used to minimize the function $S(\hat{\theta})$. This algorithm does not require the gradient (derivative) of the objective function and, therefore, can avoid ill-conditioning (which may occur in any gradient-based optimization algorithm) when K_S is too high (Zhang and Huck, 1995). The principle of the Simplex algorithm is described by Zhang and Huck (1995). A printout of the FORTRAN77 program and a sample output from the program are included in Appendix 3.

The evaluation of model adequacy for an EVM has been extensively discussed in Bard (1974). Briefly, to assess whether the mean residuals between the observed and the "true" values (e) differ from zero, the mean residuals ought to be compared with the variance of the residuals (V') using the statistic

$$\chi^2 = (\frac{n}{1 - p/n})e^T V'^{-1} e \tag{14}$$

$$e = \frac{1}{n-1}\sum_{i=1}^{n}(z_i - \hat{z}_i) \qquad i = 1,2,...n \tag{15}$$

$$V' = \frac{r}{n-p}\sum_{i=1}^{n}(z_i - \hat{z}_i)^T(z_i-\hat{z}_i) \qquad i = 1,2,...n \tag{16}$$

where r is the number of observed variables for each observation (in this case, 2) and p is the number of parameters estimated (in this case, 4). χ^2 in equation (14) has a chi-square distribution with r degrees of freedom (Bard, 1974).

Jackknife Technique for Precision Estimation

The jackknife procedure was first introduced by Quenouille (1956) as a technique for eliminating bias in parameter estimation and has been widely used in the analysis of enzyme kinetics (Oppenheimer et al., 1981). The procedure can be used for confidence interval estimation in nonlinear models when confidence intervals cannot be estimated using the variance-covariance matrix because of severe ill-conditioning (Cornish-Bowden and Wong, 1978; Oppenheimer et al., 1981). In the model being considered, ill-conditioning occurs when K_s is much higher than S_e, which is indeed the situation encountered. Therefore, the jackknife technique was chosen to estimate the confidence intervals for the parameters estimated by the EVM method.

For a sample with n observations, the jackknife procedure requires one estimate of θ with all n observations ($\hat{\theta}$) and n estimates with the ith observation deleted ($\hat{\theta}_{-i}$). Then the pseudo-values are the vectors

$$P_i = n\hat{\theta} - (n-1)\hat{\theta}_{-i} \qquad\qquad i = 1,2,...n \qquad (17)$$

The maximum likelihood estimate $\hat{\theta}$ is not necessarily unbiased. The jackknife estimate then provides an unbiased estimate, which is the mean of the pseudo-values

$$\bar{P} = \hat{\theta}_J = \frac{1}{n}\sum_{i=1}^{n} P_i \qquad\qquad i = 1,2,...n \qquad (18)$$

with the estimated variances:

$$S^2[\hat{\theta}_J] = \frac{1}{n(n-1)}\sum_{i=1}^{n}[P_i - \hat{\theta}_J]^2 \qquad\qquad i = 1,2,...n \qquad (19)$$

Then the confidence intervals for the pseudo-values can be determined by using Student's t test with (n-1) degrees of freedom.

METHODS AND MATERIALS

Bioreactor

Figure 3-1 is a schematic diagram of the bench scale biofilm reactors used in this research. The design was adapted from Rittmann et al. (1986). To prevent contamination caused by leaching of organics from the reactor system, all wetted parts were made of Teflon or glass except that the pump tubing was high quality Pharmed® tubing. The size and the operating conditions of the biofilm reactors are summarized in Table 3-1. The recycle flowrate (Q_r) of about 40 to 50 mL/min was chosen to produce a superficial velocity similar to the hydraulic loading rate normally used in pilot or full scale drinking water treatment plants. A low feed rate (Q) was used to guarantee a high ratio of Q_r/Q. With the ratio of Q_r/Q greater than 25, the biofilm columns can be regarded as CSTR bioreactors (Rittmann et al., 1986). The feed solution was contained in a 12-L glass jar and autoclaved before use to reduce biogrowth in the jar. The feedstock concentrations were chosen to attempt to produce effluent AOC concentrations which would be evenly distributed over the range of AOC values usually experienced in pilot scale studies. To ensure a steady state had been reached before sampling, the bioreactor was usually allowed at least two weeks to stabilize after a change of feed stock concentration. A time period of several days was found in other studies to be sufficient for an existing biofilm to adjust to a new steady-state (Wanner and Gujer, 1986; Skowlund, 1990). In a parallel pilot study operated by the author, it was also found that the response time of the biofilm to an increase in influent substrate concentration was in the order of several days (Lu, 1993). However, much longer time may be required to develop a biofilm on a fresh surface. During inoculation it was observed that the biofilm column took about 2-3 months to develop biomass and reach a visual steady state as evidenced by no visual change in the amount of biofilm present.

Synthetic Medium

Synthetic medium was used as the feed solution in the first stage of this study to establish the biofilm and to assess the feasibility of the apparatus and the

experimental design. After the experimental approach had been fully tested, ozonated natural water was used as the feedstock.

The synthetic water was prepared from laboratory deionized water to which were added four common AOC components and inorganic nutrients. In choosing a carboxylic acid as a primary AOC component, acetate is reasonable because from the beginning AOC has been expressed as acetate equivalents (e.g. van der Kooij et al., 1982). One reason for this choice is that there was good linearity between acetate addition to water samples and biomass growth. van Hoof et al. (1986) found that acetate could represent 20% of the total AOC after ozonation of filtered water. Indeed, acetate is one of the most common ozonation end-products. Another important carboxylic acid in ozonated water is oxalate. Total AOC includes AOC-P17 and AOC-NOX. van der Kooij and Hijnen (1984) indicated that AOC-NOX, which is likely largely oxalate, made up one third of the total AOC in ozonated water.

Recent evidence (Xie and Reckhow, 1992) has indicated that ketoacids could be a group of significant ozonation products in ozonated water. Among them glyoxylate was the most significant species at low ozone dose. In fact, the importance of glyoxylate was recognized by Jarret et al. (1986), and the biodegradation of glyoxylate in a BAC process has been investigated at pilot scale.

Aldehydes are also common ozonation by-products from humic substances. Van Hoof et al. (1986) found that low molecular weight (C_1-C_3) aldehydes were a significant portion of the overall AOC (about 30%) after ozonation of filtered water.

Consequently, in this research, acetate and oxalate were chosen to represent carboxylic acids, acetaldehyde was chosen to represent aldehydes and glyoxylate was selected to represent ketoacids. The organic content of the synthetic water was 30% acetate, 30% oxalate, 15% glyoxylic acid and 25% acetaldehyde, based on their theoretical oxygen demand (ThOD). On a weight oasis, the percentages were 11.1% of sodium acetate (CH_3COONa), 72.5% of sodium oxalate ($[COONa]_2$), 12.4% of glyoxylic acid ($C_2H_2O_3 \cdot H_2O$), and 4.0% of acetaldehyde (C_2H_4O). A concentrated stock solution with expected AOC concentration of 1.2 g/L acetate carbon was prepared by dissolving into one liter Milli-Q water with approximately 1.2 g of sodium acetate, 8 g of sodium oxalate, 1.4 g of glyoxylic acid, and 0.5 ml of acetaldehyde.

When diluted to 12 liters, each 10 ml of the concentrated stock solution could be expected to result in an actual AOC concentration of 1000 μg acetate C/L.

The inorganic nutrients consisted of 8.5 mg KH_2PO_4, 21.8 mg K_2HPO_4, 17.7 mg Na_2HPO_4, 1.0 mg $NaHCO_3$, 15.0 g KNO_3, 27.5 mg $CaCl_2$, 11.0 mg $MgSO_4$ and 0.15 mg $FeCl_3$ per liter Milli-Q water. These concentrations ensured that organic carbon was limiting. Other micronutrients were provided as impurities in the inorganic salts.

Ozonated Water

High TOC water (75 mg/L) was obtained from the raw water source of a small village in northern Alberta, Canada. The organic carbon is believed to be largely of algal origin because the water was light green-yellow in color. The major raw water quality parameters are summarized in Table 3-2. Analyses were performed by a laboratory at Gold Bar Wastewater Treatment Plant, the City of Edmonton, based on Standard Methods (APHA-AWWA-WEF, 1992).

The raw water was ozonated by bubbling ozone into a glass jar containing 20 L of the raw water for 60 min. The gas stream had an ozone concentration of 4% (w/w) and a pressure of 6897 N/m^2. The flow rate was 2 L/min. An indigo solution, prepared for detecting an ozone residual up to 0.1 mg O_3/L, was used to monitor qualitatively the ozone residual in the glass jar. Every 3 min, while the ozone gas was bubbling, a sample was taken from the glass jar to fill a 40 mL vial containing 4 mL of the indigo solution. At the beginning, the mixture of the ozonated water and the indigo solution resulted in a blue color which was not different from the blank, indicating that all the ozone was consumed by the high TOC water. After 30 min of ozonation, the blue color became almost invisible, indicating that the ozone residual in the glass jar was about 0.1 mg O_3/L. The high TOC water continued to be bubbled for another 30 min, resulting in an applied ozone dose of approximately 2 mg O_3/mg TOC. The ozonated high TOC water was stored at 4°C until use.

In order to spread the effluent concentration in a wide range, the AOC concentration of the feed solution was varied in a wide range. Feed solution AOC concentrations are presented in Table 3-3 for the ozonated water and in Table 3-4 for

the synthetic water. For the ozonated water, the AOC concentration in the feed solution was adjusted by adding varied volume (0.5 to 12 liters) of the ozonated high TOC water into the 12-L jar. Then the feed solution jar was filled with distilled water to 12 liters, if required. For the synthetic water, the AOC concentration in the feed solution was controlled by adding varied amount (6 to 1000 ml) of the concentrated stock solution into the 12-L jar containing 12 liters of Milli-Q water enriched with the inorganic nutrients. It is worth noting that the actual AOC concentrations for the synthetic medium in Table 3-4 varied less than 20% from the concentration calculated from the amount of the concentrated stock added.

Inoculation

The inoculum was water from biologically active pilot scale dual media filters to which were added the four major AOC components discussed above, in the proportion indicated. The total concentration of these components was 2000 µg acetate C eq/L. The inoculum was recycled through the glass-bead columns for about 3 days. The biofilm systems took about 3 months to reach steady state as evidenced by no visual change in the amount of biofilm present.

Assimilable Organic Carbon (AOC)

AOC was used as the surrogate for influent and effluent substrate concentrations. The method utilized was as described by van der Kooij et al. (1982) with the inclusion of *Spirillum* strain NOX in addition to *Pseudomonas fluorescens* strain P17 (van der Kooij, 1987), with minor modifications (Huck et al., 1991). The two strains were added simultaneously at the beginning of the test. The yields established in our laboratory were 2.2×10^6 CFU/mg acetate C for P17 and 1.1×10^7 CFU/mg acetate C for NOX respectively. The results for each strain were expressed as µg acetate C equivalents/L, and denoted as AOC-P17 and AOC-NOX, respectively. These two values were added to give a total AOC value.

RESULTS AND DISCUSSION

Experimental results for the ozonated water and the synthetic water are tabulated in Tables 3-3 and 3-4 respectively. There were nine sets of influent/effluent data generated for the ozonated water and six sets for the synthetic water. The results for the ozonated natural water are considered first and given more weight than those for the synthetic water because more data are available and because they were obtained with an actual water.

Although there was no replication of the AOC measurements in this bench scale experiment, there were about a dozen duplicates performed for AOC measurements at various concentrations in the pilot scale investigations conducted in parallel. Coefficients of variation were derived from these duplicates for AOC-P17 and AOC-NOX respectively. Coincidentally, the two coefficients of variation were both 0.117. The standard errors for total influent and effluent AOC concentrations were then calculated using these coefficients. The flux of AOC into the biofilm (J) was calculated through equation (6) and its standard deviation was calculated accordingly.

From the influent AOC data in Table 3-3, it appears that for the ozonated natural water AOC-NOX is the dominant portion when total AOC is relatively low while AOC-P17 becomes dominant when total AOC is relatively high. It is known that strains P17 and NOX can both use some of the same substrates (van der Kooij et al., 1982; van der Kooij and Hijnen, 1984). When substrate is plentiful, the competition may not be significant, but could become substantial when substrate is scarce. In this situation, NOX tends to be the winner because it is the more robust strain, as has been observed in AOC measurements in the parallel pilot plant study. However, for synthetic water, the influent AOC data in Table 3-4 consistently show a pattern of AOC-NOX domination. This may be because the synthetic water only contains four simple organic compounds. In this situation, there may be little (if any) substrate commonly assimilable by both strains and thus available for competition.

What is really important, however, is that without exception, AOC-P17 is the dominant portion of the AOC in the effluent for both the ozonated and synthetic waters (see Tables 3-3 and 3-4). Such domination is especially substantial for the synthetic water effluent, where AOC-NOX is almost negligible. This implies that AOC-NOX is much more easily biodegradable than AOC-P17 and/or that the

biodegradation by-products of AOC-NOX can act as substrate for strain P17. Such a diauxic pattern of substrate utilization is not uncommon for a mixture of two or more substrates (Harder and Dijkhuizen, 1982).

The data in Tables 3-3 and 3-4 therefore show that in both AOC measurement and AOC biodegradation, the relationship between AOC-NOX and AOC-P17 is complicated. The implication of this is that AOC- 'OX and AOC-P17 cannot be considered separately. Total AOC should be used as the surrogate for the whole substrate.

The EVM estimates for the four model parameters are summarized in Tables 3-5 and 3-6 for the ozonated and synthetic waters respectively. A sample computer output for the parameter estimation is included as Appendix 1. The estimated kX_i values of 71.8 kg acetate C/m^3-d for the ozonated water and 24.3 kg acetate C/m^3-d for the synthetic water are two orders of magnitude higher than those estimated from a previous pilot-scale study (0.29 to 0.44 kg acetate C/m^3-d) (Zhang and Huck, 1994) and one order of magnitude higher that the result of Rittmann et al. (1986) for acetate of about 3.5 kg acetate C/m^3-d (5.7 kg COD/m^3-d).

The EVM estimates for K_s of 54.7 g acetate C/m^3 for the ozonated water and 16.8 g acetate C/m^3 for the synthetic water are much higher than K_s values in the literature. For instance, in an oligotrophic biofilm system, the K_s value for acetate was 18 mg sodium acetate/m^3 (Rittmann et al., 1986), which is equivalent to 5.27 mg acetate C/m^3. However, as indicated earlier, the parameter estimation approach used in Rittmann et al. (1986) was potentially subject to considerable uncertainty. On the other hand, the high K_s estimates are consistent with the estimates from the pilot-scale study in Chapter 2 (Zhang and Huck, 1994). This consistency suggests that the high K_s values estimated in Chapter 2 are not attributable to the possible pseudosteady-state events occurred during the pilot study because the bench scale experiments were undertaken under well controlled steady-state conditions.

The EVM estimates of diffusivity (D) can be compared to those for major AOC components. Oxalic acid is probably the AOC component with the highest diffusivity, which is 1.40×10^{-4} m^2/d at $22°C$ (Perry and Green, 1984). In comparison with the diffusivity of oxalic acid, the estimated average AOC diffusivity of 1.27×10^{-4}

-96-

m^2/d (in Table 3-5) can be considered generally acceptable for the ozonated water, although perhaps a bit high, as discussed below with reference to the jackknife estimates.

The diffusivities of the four AOC components in the synthetic water can either be found in Perry and Green (1984) or be calculated using the information provided in Perry and Green (1984). The average diffusivity for the AOC in the synthetic water was calculated as 1.20×10^{-4} m^2/d at 22°C. The estimated average diffusivity of 1.44×10^{-4} m^2/d for the synthetic water (in Table 3-6) should therefore be considered fairly accurate, given the error of AOC measurements.

S_{min} estimates for the pilot scale data in Zhang and Huck (1994) ranged from 4.5 to 10 mg acetate C/m^3. The EVM estimates of S_{min} in this study (14.3 mg acetate C/m^3 for the ozonated water and 20.2 mg acetate C/m^3 for the synthetic water) are higher than the estimates from the pilot study, which should be considered reasonable because the surface of the glass beads used in this study is basically smooth in comparison with the highly irregular surface of the filter media and GAC particles used in the pilot study. In general, supporting media with irregular surface tend to retain biomass better and result in lower S_{min} than supporting media with smooth surface.

The jackknife technique was applied only to the ozonated water to estimate confidence intervals for the parameters (Table 3-5). It also gave a set of unbiased parameter estimates. These agreed reasonably well with those from the EVM, except for the average AOC diffusivity. For this parameter, the EVM estimate was considerably higher. The average AOC diffusivity for the ozonated water should be substantially lower than the diffusivity of oxalic acid (1.40×10^{-4} m^2/d) because a large portion of the AOC components in ozonated natural water are unlikely to be nearly as simple as oxalic acid. Therefore, the lower value of the jackknife estimate (8.05×10^{-5} m^2/d) seems to be more reasonable than the EVM estimate.

On the basis of the confidence intervals, only S_{min} is estimated with reasonable certainty. This is, however, not surprising. As Robinson (1985) indicated, a nonlinear model with two to three parameters generally requires eight to ten observations to obtain reasonably precise parameter estimates. For a model with four parameters, nine observations of AOC data with substantial scatter are not enough to produce good

estimates. For this reason, an estimate of confidence intervals was not attempted for the synthetic water with only six observations available.

However, as discussed in Chapter 2, a more fundamental reason for the uncertainties in the estimates of K_s, along with kX_f, for both pilot and bench scale data is probably the high K_s value itself. When K_s in the Monod expression is intrinsically high, it is mathematically very difficult to have precise estimates for both K_s and kX_f simultaneously. In the situation of "ill-conditioning", K_s along with kX_f can "drift" to higher magnitude with little impact on the prediction.

In the EVM technique, the "true" values based on the data available for the effluent AOC concentration and the flux were estimated simultaneously with the best-fit values for the four parameters. These "true" values are tabulated in Tables 3-7 and 3-8. The "true values" can also be calculated using the best-fit parameter estimates and equation (1). This equation was used to generate the best-fit curves plotted in Figures 3-2 and 3-3 for the ozonated and synthetic waters respectively, in comparison with the experimental values. To test the adequacy of the EVM estimates, χ^2 values in equation (14) were calculated for both ozonated and synthetic waters. The calculated χ^2 values were 0.86 for ozonated water and 0.087 for synthetic medium. Neither of these values are statistically significant at the 5% level (χ^2 [2, 0.05]=5.991). Therefore, the EVM estimates can be considered adequate.

CONCLUSIONS

This chapter presents an approach for estimating kinetic parameters for biofilm processes in biological drinking water treatment through bench-scale experiments and appropriate data analysis. The results presented in this chapter are significant because a method for estimating the parameters essential for kinetic modeling of biofilm processes for removal of AOC in natural waters has not been available in the literature.

Both synthetic medium and ozonated natural water were used in this study. AOC was used as a surrogate measure of substrate concentration. It was found not only that strains NOX and P17 competed for substrate in the AOC measurement but also that AOC-NOX was much more easily biodegradable than AOC-P17 in the

biofilm reactor. The diauxic pattern of the utilization of two AOC components suggests that AOC-P17 and AOC-NOX should not be modeled separately.

Kinetic parameters (k, K_s and S_{min}) and the average AOC diffusivity (D) were estimated for both the ozonated and synthetic waters using the error-in-variables technique. The estimated K_s values fell in a high range similar to the values estimated in Chapter 2. This suggests that the high K_s values estimated in Chapter 2 are not attributed to the uncertain conditions occurring in the pilot scale study or to the error in influent AOC measurement which was not able to be taken into account for pilot scale biofilm columns.

The estimates for k, D and S_{min} were reasonable. For the synthetic water, the estimated D value was close to the average diffusivity of the four AOC components which it contained.

The jackknife technique was employed to estimate the confidence intervals for the parameters for the ozonated water. Except for S_{min}, the confidence intervals were very wide, indicating that estimates in this paper for parameters other than S_{min} are subject to substantial uncertainty. In addition to the intrinsic scatter of AOC data and the limited number of data points, the uncertainties in the kX_f and K_s estimates may be mathematically attributed to the high K_s value.

Further efforts in confirming the high K_s value observed would be especially valuable. Should K_s indeed be much higher than BOM concentrations normally experienced in drinking water treatment, the intrinsic biodegradation kinetics could be simplified as first-order. Biofilm modeling for packed-bed biofilm columns in biological water treatment could be substantially simplified by using the analytical solution for first order transformation kinetics developed by Skowlund and Kirmse (1989). Precise estimates should then be obtainable for kX_f/K_s as a single first-order kinetic coefficient.

Table 3-1. Operating conditions of biofilm reactors.

Diameter of reactor (mm)	26.3
Length of the reactor (mm)	103
Number of glass beads	2540
Diameter of glass beads, d_p (mm)	3
Area of one glass bead (mm^2)	28.2
Total glass bead surface (mm^2)	71600
Volume of the reactor (mL)	56.0
Volume of voids (mL)	20.09
Porosity, ε	0.36
Temperature (°C)	22
Feed flow rate, Q (mL/min)	0.58 to 0.75
Recycle flowrate, Q_r (mL/min)	42 to 49
Recycle ratio Q_r/Q	82.6 to 65.5
Superficial velocity, v (m/h)	4.6 to 5.4
Detention time (min)	27.1 to 34.2
Time of one pass through column (min)	0.41

Table 3-2. Raw water quality of high TOC water from Northern Alberta.

TOC (mg/L)	75
pH	7.4
TKN (mg/L)	7.4
NH_3-N (mg/L)	2.0
Total Phosphate (mg/L)	0.03
Conductivity (μmho/cm at 25°C)	0.918
Hardness (mg $CaCO_3$/L)	155
Alkalinity (mg $CaCO_3$/L)	347
UV absorbance at 254 nm (m^{-1})	1.08

Table 3-3. Experimental results for ozonated water.

Observation number	Influent AOC S_i (mg acetate C/m^3)				Effluent AOC S_e (mg acetate C/m^3)				Flux (mg acetate C/m^2-d)	
	P17	NOX	Total	σ_{Si}	P17	NOX	Total	σ_{Sc}	J	σ_J
1	346	606	952	81.7	52.4	20.7	73.1	6.59	11.5	1.09
2	3260	1590	4850	424	179	62.2	241	22.2	55.6	5.18
3	5000	1250	6250	603	164	112	276	23.3	78.5	8.02
4	718	476	1190	101	37.2	7.40	44.6	4.44	13.5	1.19
5	3000	835	3830	364	104	88.2	192	16.0	50.6	5.12
6	3780	2420	6200	525	209	110	318	27.6	86.6	7.82
7	105	130	235	19.5	17.3	2.30	19.4	2.04	2.78	0.256
8	793	1170	1960	165	93.6	17.0	111	11.1	22.3	2.01
9	632	1530	2160	194	139	26.1	165	16.6	25.6	2.52

Table 3-4. Experimental results for synthetic medium.

Observation number	Influent AOC, S_i (mg acetate C/m^3)				Effluent AOC, S_e (mg acetate C/m^3)				Flux (mg acetate C/m^2-d)	
	P17	NOX	Total	σ_{Si}	P17	NOX	Total	σ_{Se}	J	σ_J
1	318	660	978	85.8	46.8	0.50	47.3	5.48	21.0	1.85
2	4860	6790	11700	978	382	4.30	386	44.7	168	14.6
3	235	566	801	71.7	34.5	0.44	34.9	4.04	9.73	0.922
4	3110	4350	7460	626	139	5.15	144	16.3	97.3	8.41
5	559	1450	2000	181	34.0	2.52	36.5	3.99	22.3	2.07
6	1590	3970	5560	501	119	1.46	121	14.0	58.4	5.43

Table 3-5. Estimated parameters for ozonated water.

	Parameter			
	kX_f (kg acetate C/m^3-d)	K_s (mg acetate C/m^3)	D (m^2/d)	S_{min} (mg acetate C/m^3)
EVM estimates	71.8	5.47e+4	1.27e-4	14.3
Jackknife estimates	94.5	4.27e+4	8.08e-5	13.3
Jackknife variances	33.0	1.60e+9	1.33e-9	3.43
Confidence intervals*	167	1.35e+5	1.65e-4	17.6
	21.9	-4.94e+4	-3.30e-6	9.05

* At 5% level with 8 degrees of freedom (t=2.306).

Table 3-6. Estimated parameters for synthetic water.

Parameters	Parameter			
	kX_f (kg acetate C/m^3-d)	K_s (mg acetate C/m^3)	D (m^2/d)	S_{min} (mg acetate C/m^3)
EVM estimates	24.3	1.68e+4	1.44e-4	20.2

Table 3-7. Comparison of experimental and predicted "real" values of J and S_e for ozonated water.

Observation number	Effluent AOC, S_e (mg acetate C/m^3)		Flux, J (mg acetate C/m^2-d)	
	Observed	Predicted	Observed	Predicted
1	73.1	58.5	11.5	13.2
2	241	240	55.6	55.9
3	276	295	78.5	68.8
4	44.6	51.7	13.5	11.5
5	192	201	50.6	46.8
6	318	340	86.6	79.2
7	19.4	19.5	2.78	2.77
8	111	102	22.3	23.5
9	165	127	25.6	29.4

Table 3-8. Comparison of experimental and predicted "real" values of J and S_e for synthetic water.

Observation number	Effluent AOC, S_e (mg acetate C/m^3)		Flux, J (mg acetate C/m^2-d)	
	Observed	Predicted	Observed	Predicted
1	47.3	46.3	21.0	21.2
2	386	325	168	180
3	34.9	30.5	9.73	10.0
4	144	161	97.3	89.4
5	36.5	42.6	22.3	19.9
6	121	109	58.4	61.4
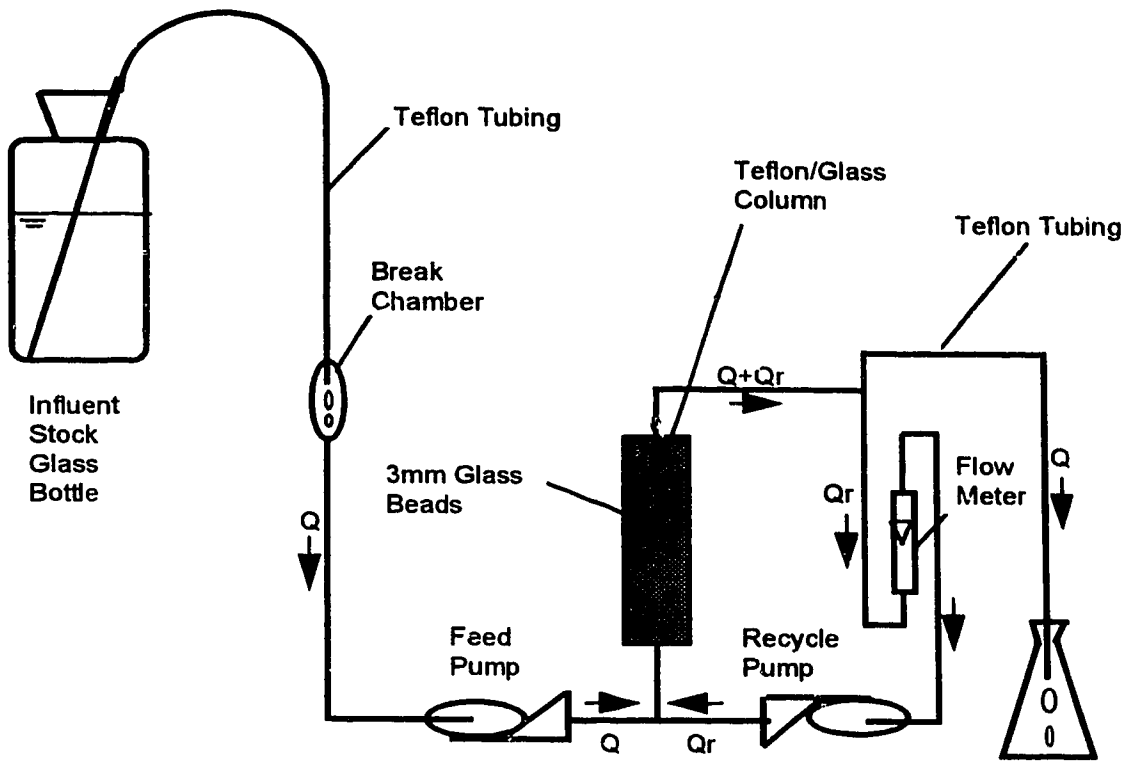
Figure 3-1. A schematic of CMBR biofilm-reactor system (after Rittmann et al., 1986).
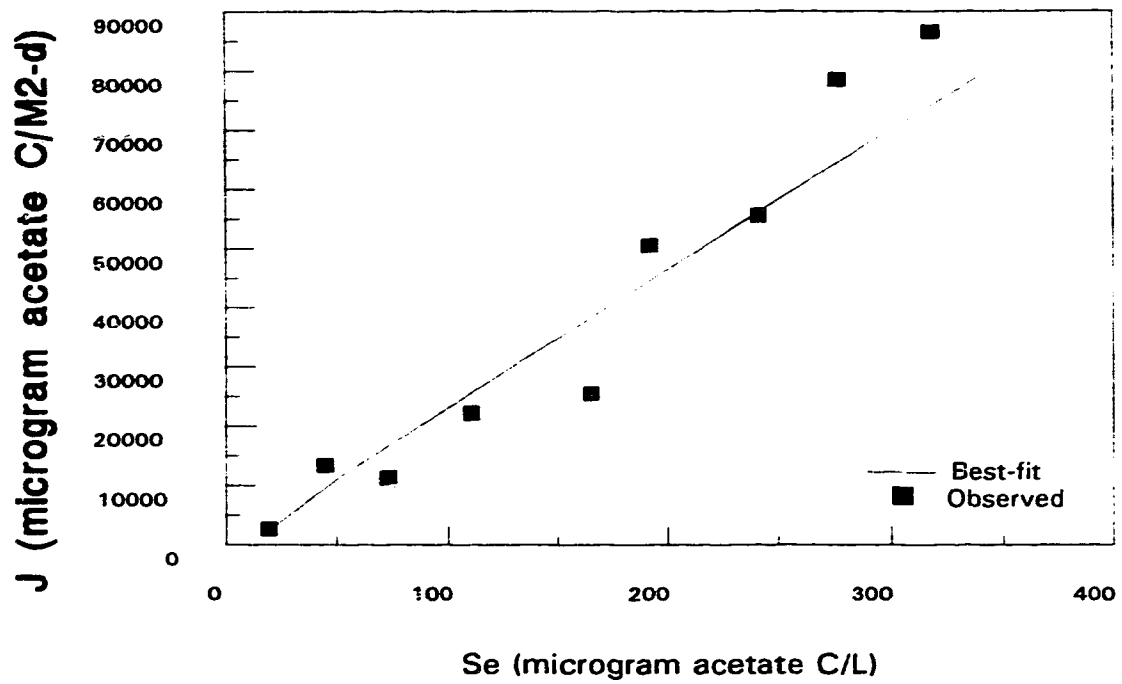
Figure 3-2.   Comparison of observed values and best-fit curve of J versus S_e for ozonated water.

J (microgram acetate C/M2-d)

200000

160000

120000

80000

40000

0

- - - - Best-fit
■ Observed

Se (microgram acetate C/L)

0   100   200   300   400
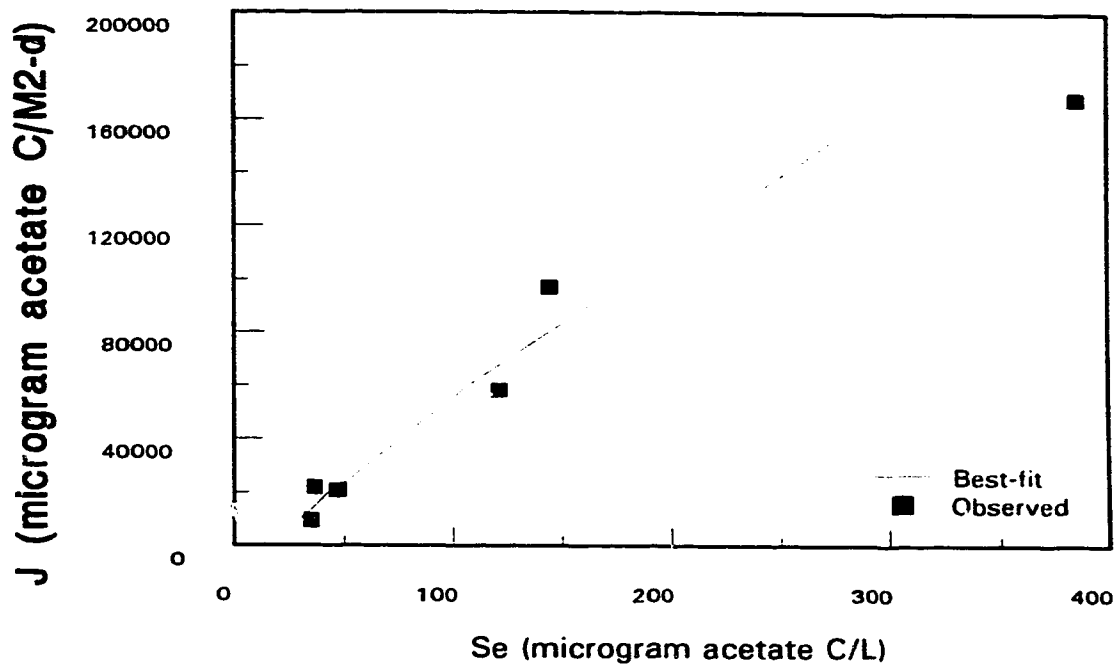
Figure 3-3.   Comparison of observed values and best-fit curve of J versus S_e for synthetic medium.

REFERENCES

APHA-AWWA-WEF (1992) *Standard Methods for the Examination of Water and Wastewater*, 18th edition. Washington.

Bard Y. (1974) *Nonlinear Parameter Estimation*. Academic Press, New York.

Cornish-Bowden A. and Wong J. T. F. (1978) Evaluation of rate constants for enzyme-catalysed reactions by the jackknife technique. *Biochem. J.* 175, 969-976.

Harder W. and Dijkhuizen L. (1982) Strategies of mixed substrate utilization in microorganisms. *Phil. Trans. R. Soc. Lond.* B 297, 459-480.

Huck P. M., Zhang S. and Price M. L. (1994) BOM removal during biological treatment: a first order model. *J. Am. Wat. Wks Ass.* 86(6), 61-71.

Huck P. M., Fedorak P. M. and Anderson W. B. (1991) Formation and removal of assimilable organic carbon during biological treatment. *J. Am. Wat. Wks Ass.* 83(12), 69-80.

Jarret M., Bermond A. and Ducauze C. J. (1986) Elimination du glyoxyal et de l'acide glyoxyique par filtration sur charbon actif en grains - mécanismes mis en jeu. *Sci. Eau.* 5, 377-400.

Lu P. (1993) *Measurement of Biofilms in a Biological Drinking Water Treatment Plant*. M.Sc. Thesis, Department of Civil Engineering, University of Alberta, Edmonton Canada.

Nedler J. A. and Mead R. (1965) A Simplex method for function minimization. *Comp. J.* 7, 308-345.

Oppenheimer L., Capizzi P. and Miwa G. T. (1981) Application of jackknife procedures to inter-experiment comparisons of parameter estimates for the Michaelis-Menten equation. *Biochem. J.* 197, 721-729.

Perry R. H. and Green D. W. (1984) *Perry's Chemical Engineers' Handbook*, 6th edition. McGraw-Hill, New York.

Quenouille M. H. (1956) Notes on bias in estimation. *Biometrika* **43**, 353-360.

Reilly P. M. and Patino-Leal H. (1981) A Bayesian study of error-in-variables model. *Technometrics*, **23**, 221-231.

Rittmann B. E., Crawford L., Tuck C. K. and Namkung E. (1986) *In-situ* determination of kinetic parameters for biofilms: isolation and characterization of oligotrophic biofilms, *Biotechnol. Bioengng.* **28**, 1753-1760.

Rittmann B. E. and McCarty P. L. (1980) Model of steady-state-biofilm kinetics. *Biotechnol. Bioengng.* **22**, 2343-2357.

Robinson J. A. (1985) Determining microbial kinetic parameters using nonlinear regression analysis. In *Advances in Microbial Ecology* (Edited by Marshall K.C.) Vol. 8, pp. 61-114. Plenum Press.

Sáez P. B. and Rittmann B. C. (1992) Accurate pseudo-analytical solution for steady-state biofilms. *Biotechnol. Bioengng* **39**, 790-793.

Skowlund C. T. (1990) Effect of biofilm growth on steady-state biofilm models. *Biotechnol. Bioengng.* **35**, 502-510.

Skowlund C. T. and Kirmse D. W. (1989) Simplified models for packed-bed biofilm reactors. *Biotechnol. Bioengng.* **33**, 164-172.

van der Kooij D. (1987) The effect of treatment on assimilable organic carbon in drinking water. In *Proceedings of the Second National Conference on Drinking Water* (Edited by Huck P.M. and Toft P.), pp. 317-328. Pergamon Press, Oxford, UK.

van der Kooij D. and Hijnen W. A. M. (1984) Substrate utilization by an oxalate consuming *Spirillum* species in relation to its growth in ozonated water. *Appl. Envir. Microbiol.* **47**, 551-559.

van der Kooij D., Visser, A. and Hijnen W. A. M. (1982) Determining the concentration of easily assimilable organic carbon in drinking water, *J. Am. Wat. Wks Ass.* **74**(10), 540-545.

van Hoof F., Janssens J. G. and van Dyck H. (1986) Formation of oxidation byproducts in surface water ozonation and their behaviour in water treatment. *Wat. Supply*, **4**, 93-102.

Wanner O. and Gujer W. (1986) A multispecies biofilm model. *Biotechnol. Bioengng.* **28**, 314-328.

Xie Y. and Reckhow D. A. (1992) Formation of ketoacids in ozonated drinking water. *Ozone Sci. Engng.* **14**, 269-275.

Zhang S. L. and Huck P. M. (1996) Parameter estimation for biofilm processes in biological water treatment. *Wat. Res.* **30**, 456-464.

Chapter 4

BIOFILM DETACHMENT AND A
GENERALIZED S_{min} DEFINITION

INTRODUCTION

In Chapter 2, the biofilm thickness calculated from estimated S_{min} was found unrealistically high, based on the assumption that biofilm detachment rate is a first order function of biofilm mass. This chapter reviews various biofilm detachment kinetics proposed in the literature and demonstrates that the relationship among S_{min}, biofilm detachment kinetics and biofilm thickness can be very complex. A generalized definition of S_{min} is proposed to present the complex relationship.

An idealized biofilm is a layer-like matrix of bacterial cells and extracellular polymeric substances (EPS) attached to a solid surface or substratum bathing in the bulk liquid. At the substratum, bacteria grow, reproduce and produce EPS. A biofilm can not grow infinitely. Its growth is limited by the endogenous decay of the cells and the net detachment of biomass from the biofilm to the bulk liquid. A steady state biofilm is a state of delicate balance between the gain in biofilm mass due to biogrowth and the loss in biofilm mass due to endogenous decay and net biomass detachment.

Figure 1-1 illustrates an idealized planar biofilm system (Rittmann and McCarty, 1980; Sáez and Rittmann, 1988). For the convenience of mathematical description, it is assumed (Rittmann and McCarty, 1980) that

(1)   there is a sole limiting substrate which is both diffusion and bioreaction limiting in the biofilm system;

(2)   the biofilm is homogeneous and continuous throughout and, thereby, has a uniform density of X_f ($M_x L^{-3}$);

(3)   the biofilm has a uniform thickness of L_f (L^{-1}); and

(4)   the substratum is impermeable.

In the biofilm system, the substrate with a concentration of S_b (M_sL^{-3}) is transported from the bulk liquid to the biofilm surface through an effective diffusion layer (an equivalent depth of liquid film through which the actual mass transport can be described by molecular diffusion alone) with a thickness of L (L). The substrate concentration on the outer surface of the biofilm is S_S (M_sL^{-3}), within the biofilm is S_f (M_sL^{-3}), and at the inner surface of the biofilm is S_w (M_sL^{-3}).

Rittmann and McCarty (1980) found that there is a threshold value for a biofilm, at a bulk substrate concentration lower than which no biofilm can be developed, and even an existing biofilm would decay and disappear if the low concentration lasts too long. At this threshold concentration, a steady state biofilm with a monolayer of bacteria would be able to be sustained. Rittmann and McCarty (1980) termed this threshold concentration S_{min}.

When biofilm detachment is negligible, S_{min} can be determined from given kinetic parameters. Rittmann and McCarty (1980) assumed that in the monolayer there is essentially no diffusion limitation, in other words, $S_w \cong S_f \cong S_{s-min}$. For a unit area of biofilm, the biomass growth rate of the monolayer is

$$R_g = \mu X_f L_f = YL_f k X_f S_s/(K_s + S_s)$$ (1)

where μ is the specific biogrowth rate (T^{-1}); K_s is the half velocity constant in the Monod expression (M_sL^{-3}); k is the maximum specific rate of substrate utilization (T^{-1}); Y is the yield coefficient.

For a unit area of biofilm, the endogenous decay rate for a biofilm with a thickness of L_f is

$$R_d = b_d X_f L_f$$ (2)

where b_d is the first-order endogenous decay rate coefficient (T^{-1}).

The steady state is a balance between R_g and R_d. Therefore, the minimum surface concentration for the steady-state biofilm, S_{s-min} (M_sL^{-3}), is

$$S_{s-min} = K_s b_d/(kY - b_d)$$ (3)

The minimum bulk substrate concentration, S_{min}, is approximately equal to the minimum surface concentration, S_{s-min}, because the substrate flux from the bulk liquid into the monolayer biofilm is very low. In other words,

$$S_{min} \cong S_{s-min} = K_s b_d / (kY - b_d) \tag{4}$$

However, as a primary mechanism that counter-balances microbial growth (Peyton and Characklis, 1993), biofilm detachment is not negligible in many situations (Peyton and Characklis, 1993). Therefore, S_{min} should account for both endogenous decay and biomass detachment.

CURRENT S_{MIN} DEFINITION

Rittmann (1982) proposed that, analogous to the endogenous biofilm decay rate (R_d), the biofilm detachment rate for a unit area of biofilm (R_{det}) can also be related to $X_f L_f$ through a coefficient (b_{det}, T^{-1}):

$$R_{det} = b_{det} X_f L_f \tag{5}$$

where b_{det} can be termed the biofilm detachment rate coefficient.

The total biomass loss rate for a unit area of biofilm (R, $M_x L^{-1} T^{-1}$) is then the sum of R_d and R_{det},

$$R = R_d + R_{det} \tag{6}$$

Analagously, a total biofilm loss rate coefficient, b', can be defined as

$$b' = b_d + b_{det} \tag{7}$$

Rittmann (1982) found that for a biofilm with $L_f < 30$ μm, R_{det} is a first order function of biofilm mass ($X_f L_f$). In other words, b_{det} is a first order rate constant. In this case, it is possible to have a total first order rate constant for the total biofilm loss rate which can be termed b (T^{-1}), and b' = b. By simply substituting b_d in equation (4)

with b' = b, S_{min} can now account for biofilm detachment and is computed as (Rittmann and McCarty, 1980; Rittmann, 1982; Sáez and Rittmann, 1988):

$$S_{min} \cong S_{s-min} = K_s b'/(kY-b') = K_s b/(kY-b) \tag{8}$$

This definition of S_{min} has been widely used in the current literature (e.g. Sáez and Rittmann, 1988; Heath et al., 1990; Rittmann, 1990; Wirtel et al., 1992). However, the use of equation (8) should be cautiously limited to situations where biofilm detachment rate can be considered as a first order function of L_f. Although b_{det} can always be considered in parallel with b_d to calculate the overall biofilm loss rate coefficient (b'), such parallel should not be automatically extended to the computation of S_{s-min}. For example, in Rittmann (1982), b_{det} was found to be a function of L_f when $L_f>30$ μm. In that case, a simple parallel between b_d and b_{det} would no longer be applicable because S_{min} in equation (8) would otherwise become a function of L_f.

Furthermore, recent experimental results have shown that, in addition to biofilm thickness, biofilm detachment rate is also controlled by a number of other factors, such as biogrowth rate and substratum surface characteristics (Trulear and Characklis, 1982; Chang and Rittmann 1987, 1988; Speitel and Digiano, 1987; Peyton, 1992; Peyton and Characklis, 1993; Stewart, 1993). There is therefore a need for a generalized definition for S_{min}, which reflects the complex nature of biofilm detachment processes.

BIOFILM DETACHMENT

Probably because of the complex nature of biofilm detachment processes, besides the first order kinetics, there are many other biofilm detachment rate expressions being currently used in the literature. Stewart (1993) summarized all mechanisms of biofilm detachment in common use. In these expressions, the dependence of the detachment rate on the biofilm thickness (L_f) ranges from zero order to second order. Some recently proposed mechanisms relate the detachment to biogrowth. For instance, Speitel and DiGiano (1987) assumed that the biofilm detachment rate coefficient was a variable proportional to the specific growth rate. The most recent experimental evidence (Peyton and Characklis, 1993; Peyton, 1992)

has shown that the biofilm detachment rate was dependent on biomass production and proportional to the average biomass growth rate of the whole biofilm.

Based on mechanistic deductions, Stewart (1993) proposed a generalized expression for the biofilm detachment rate, which includes two terms. The first term enables growth-associated detachment to be accommodated. Because the biofilm detachment may not be purely related to biogrowth, the formula also includes a nongrowth-related term which leads to a second order dependence of detachment rate on biofilm thickness. The expression thus includes a detachment coefficient related to the specific growth rate (b_g, L^{-1}) and another detachment rate coefficient related to biofilm thickness (b_2, $L^{-1}T^{-1}$):

$$R_{det} = 2b_g X_f \int_0^{L_f} \mu(r_f)(L_f - r_f)dr_f + b_2 X_f L_f^2 \qquad (9)$$

where r_f denotes the depth ordinate in the biofilm (L).

The first order detachment mechanism is not considered in equation (9). However, from a modeling point of view if the total detachment rate contains a first order component, a first-order detachment mechanism can be taken into account by simply adjusting the endogenous decay rate coefficient (b_d) (Speitel and DiGiano 1987). After all, as discussed later, when the impact of biofilm detachment is significant S_{min} would have to be determined independently anyway. For the convenience of further discussion, the first order detachment rate coefficient is assigned as b_1. For all mathematical deductions, b_d and b_1 can be combined as a single parameter $b=b_d+b_1$, which can be termed the first order biofilm loss rate coefficient (T^{-1}).

For a biofilm with a complex detachment mechanism, such as that described in equation (9), the overall loss rate coefficient (b') can still be defined through equation (7),

$$b' = b + b_2 L_f + \frac{b_g}{L_f} \int_0^{L_f} \mu(r_f)(L_f - r_f)dr_f \qquad (10)$$

In equation (10), b' is not only a function of L_f but a function of the substrate concentration profile as well, because $\mu(r_f)$ is defined by the profile of S_f versus r_f. The

implication of this is two-fold: (1) The simple formula of equation (8) is no longer appropriate for defining $S_{s\text{-min}}$ (and thus S_{min}) because S_{min} would become a function of L_f and S_f. (2) b_{det} experimentally determined through equation (5), i.e. $b_{det} = R_{det}/X_f L_f$ can no longer be used to compute $S_{s\text{-min}}$ because b_{det} itself could be a function of L_f. As discussed in the following section, for a biofilm with complex detachment mechanisms, it may be too impractical to compute $S_{s\text{-min}}$ from various detachment coefficients.

GENERALIZED S_{MIN} DEFINITION

In a monolayer biofilm, $S_w \cong S_f \cong S_{s\text{-min}}$ (Rittmann and McCarty, 1980). $\mu(r_f)$ is thus a constant equal to $YX_f L_{fmin} k S_{s\text{-min}}/(1+S_{s\text{-min}})$ with L_{fmin} representing the thickness of the monolayer biofilm (L). At steady state, biogrowth is just balanced by endogenous decay and biofilm detachment. For a unit area of biofilm:

$$\frac{YkS_{s\text{-min}}}{K_s + S_{s\text{-min}}} X_f L_{f\,min} = bX_f L_{f\,min} + (b_g \frac{YkS_{s\text{-min}}}{K_s + S_{s\text{-min}}} X_f L^2_{f\,min} + b_2 X_f L^2_{f\,min}) \qquad (11)$$

For a given biofilm system and a given population of bacteria, L_{fmin} should be a constant approximately equal to the average size of bacteria (say $1\mu m$). By eliminating $X_f L_{fmin}$ from both sides of equation (11), a new definition of S_{min} can be extracted from equation (11):

$$S_{min} \cong S_{s\text{-min}} = \frac{K_s(b + b_2 L_{f\,min})}{(1 - b_g L_{f\,min})Yk - (b + b_2 L_{f\,min})} \qquad (12)$$

Equation (12) is analogous to the original S_{min} defined in equation (4). In this generalized definition, b_d is replaced by $b+b_2L_{fmin}$ while Yk is offset by the portion of biofilm detachment associated with the biogrowth and becomes $(1-b_gL_{fmin})Yk$. Therefore, b_2 and b_g reflect the impacts of non-first-order biofilm detachment processes on S_{min} whereas b_1, as a portion of b, reflects the effect of the first order biofilm detachment process on S_{min}. L_{fmin}, on the other hand, relates S_{min} to the physiological characteristics of the microbial population.

-117-

When the impact of biofilm detachment is insignificant, $b_g L_{fmin}$ can be very small in comparison with unity and becomes negligible. Similarly, $b_2 L_{fmin}$ and b_1 may be negligible in comparison with b_d. In that case, equation (12) will be reduced to equation (4). Rittmann and McCarty's (1980) original S_{min} definition is thus a limiting case for the general formula of equation (12). Where the impact of biofilm detachment is insignificant, S_{min} defined by equation (4) may well represent the real S_{min}.

When the impact of biofilm detachment is significant, S_{min} would be independent of the intrinsic kinetic parameters: k, Y and b_d. Because of the complex nature of biofilm detachment and the limit of current experimental techniques, b_g, b_1, b_2 and L_{fmin} in equation (12) are not measurable in practice. Therefore, it is not realistic to expect to compute S_{min} from equation (12) by experimentally determining each of the detachment kinetic coefficients.

However, if we treat S_{min} itself as a characteristic parameter for a given biofilm system, it would be much easier to determine S_{min} experimentally as a single independent parameter. In suspended-culture experiments, kinetic parameters, such as k, K_s and b_d, have long been estimated through data fitting. As a "biofilm kinetic parameter", S_{min} can similarly be estimated through data fitting (recognizing, of course, that a biofilm kinetic model is a bit more complicated than a suspended-culture kinetic model). The S_{min} value is specific to a given biofilm system and, therefore, should be measured or estimated *in-situ*.

The generalized definition of equation (12) has illustrated how the concept of S_{min} can be related to most of the biofilm kinetics proposed in current literature. With the advancement of our understanding of biofilm mechanisms, further modification or generalization of the S_{min} definition would almost certainly be required to accommodate alternative biofilm detachment kinetics. Treating S_{min} as an additional independent biofilm kinetic parameter would allow us to incorporate the alternative detachment kinetics into the concept of S_{min} without requiring a new approach to determine S_{min}.

It is worth noting that Stewart's (1993) mechanistic model considers the detachment of a biomass particle as a random event which has a certain frequency or probability per unit area of biofilm for given conditions. When the particle size is small

the detachment is considered erosion whereas when the particle size is comparable or larger than the thickness of the biofilm itself the detachment is considered sloughing. Therefore, Stewart's modeling concept allows the existing biofilm detachment models, which have largely been considered only applicable to the continuous biofilm detachment process (i.e. erosion), to elucidate discrete detachment processes, such as sloughing. For example, under Stewart's modeling concept, the first order biofilm detachment kinetics can represent the biofilm sloughing process (Stewart, 1993).

Although Rittmann and McCarty (1980) did not clearly state it, the existence and the definition of S_{min} do not require the monolayer biofilm to be continuous, because the biofilm density (X_f) and biofilm area are automatically canceled out in deriving S_{min}. In other words, at a bulk substrate concentration lower than S_{min}, not even "patchy" biofilm would be able to survive if the low substrate concentration lasts too long.

CONCLUSIONS

Biofilm detachment is a complex phenomenon. The overall biofilm detachment rate of a biofilm may be attributed to a combination of many possible mechanisms. The current definition of S_{min} only allows accommodation of one of the existing biofilm detachment kinetics, first order detachment. This chapter presents a generalized definition of S_{min} that allows incorporation of most biofilm detachment mechanisms in common use, including the first order mechanism. The generalized definition of S_{min} illustrates how the concept of S_{min} can be formulated against the complex background of biofilm detachment.

When biofilm detachment is insignificant, the generalized S_{min} definition is reduced to Rittmann and McCarty's original S_{min}, which can be determined by intrinsic microbial kinetic parameters. When the detachment is significant, S_{min} would become independent of intrinsic microbial kinetic parameters. In that case, S_{min} would be determined by a combination of several biofilm detachment rate coefficients which are not measurable in practice. Rather than computing S_{min} from those coefficients, it would be necessary to treat S_{min} itself as an additional "biofilm kinetic parameter". Treating S_{min} as an independent biofilm kinetic parameter would also allow us to

incorporate alternative detachment kinetics into the concept of S_{min} without requiring a new approach to determine S_{min}. Because this biofilm kinetic parameter characterizes each specific biofilm system, it should be determined *in-situ*. Techniques for *in-situ* determination of S_{min} will be discussed further in Chapter 5.

Usually the primary purpose of biofilm modeling is to describe the relationship between substrate transformation rate and substrate concentration rather than biomass accumulation although biomass accumulation is apparently essential for substrate biotransformation. As will be shown in Chapter 5, the relationship of substrate removal rate and bulk substrate concentration does not require the knowledge of biofilm thickness. For a steady state biofilm system, S_{min} is the only parameter required to reflect the effect of different biofilm detachment mechanisms on biomass accumulation or biofilm thickness, and thus on substrate biotransformation rate. Therefore, in engineering scale-up, S_{min} would be the key parameter to be determined *in-situ*.

REFERENCES

Chang H. T. and Rittmann B. E. (1987) Verification of the model of biofilm on activated carbon. *Biotechnol. Bioengng.* **21**, 280-288.

Chang H. T. and Rittmann B. E. (1988) Comparative study of biofilm shear loss on different adsorptive media. *J. Wat. Pollut. Control Fed.*, **60**, 362-268.

Heath M. S., Wirtel S. A. and Rittmann B. E. (1990) Simplified design of biofilm processes using normalized loading curves. *Res. J. Wat Pollut. Control Fed.* **62**(2), 185-192.

Peyton B.M. (1992) *Kinetics of Biofilm Detachment.* Ph.D. Thesis, Department of Chemical Engineering, Montana State University, Bozeman, USA.

Peyton B.M. and Characklis W.G. (1993) A statistical analysis of the effect of substrate utilization and shear stress on the kinetics of biofilm detachment. *Biotechnol. Bioengng.* **41**, 728-735.

Rittmann, B.E. (1982) The effect of shear stress on biofilm loss rate. *Biotechnol. and Bioengng.* **24**, 501-506.

Rittmann B. E. and McCarty P. L. (1980) Model of steady-state-biofilm kinetics. *Biotechnol. Bioengng.* **22**, 2343-2357.

Rittmann B. E. (1990) Analyzing biofilm processes in biofilm processes used in biological filtration. *J. Am. Wat. Wks. Ass.* **82**(12), 62-66.

Sáez, P. B. and Rittmann B. E. (1988) Improved pseudo-analytical solution for steady-state biofilm kinetics. *Biotechnol. Bioengng.* **32**, 379-385.

Speitel G. E. Jr. and DiGiano F. A. (1987) Biofilm shearing under dynamic conditions. *J. Envir. Engng. Div.* **113**, 464-475.

Stewart P. S. (1993) A model of biofilm detachment. *Biotechnol.Bioengng.* **41**, 111-117.

Trulear M. G. and Characklis W. G. (1982) Dynamics of biofilm processes. *J. Wat. Pollut. Control Fed.*, **54**, 1288-1301.

Wirtel S. A., Noguera D. R., Kampmeier D. T., Heath M. S. and Rittimann B. E. (1992) Explaining widely varying biofilm-process performance with normalized loading curves. *Wat. Envir. Res.*, **64**, 706-711.

Chapter 5

A NEW APPROACH TO SOLVING THE
STEADY-STATE BIOFILM MODELING

INTRODUCTION

Mathematical models for describing the mechanisms of a steady-state biofilm system are well established. The pioneers in this area are Atkinson and Daoud (1968) and Atkinson and Davies (1974) who combined substrate bio-utilization (using the Monod expression) with mass transport processes (Fick's Second Law) in the biofilm. Rittmann and McCarty (1980a) then defined the important concept of the "steady-state biofilm", the special and important case for which the growth in biofilm mass is just balanced by the net loss, and included external mass transport resistance in the considerations.

One primary difficulty in using the steady-state biofilm models is that the second-order differential equation for simultaneous substrate utilization and diffusion in the biofilm has not been able to be analytically integrated because of the nonlinearity of the Monod-type reaction term. In more than two decades, a variety of numerical solutions and pseudoanalytical solutions have been developed (Atkinson and Davies, 1974; Rittmann and McCarty 1981; Suidan and Wang 1985; Sáez and Rittmann 1988). Sáez and Rittmann (1988) indicated the previous pseudoanalytical solutions could suffer serious errors. However, the pseudoanalytical solutions of Sáez and Rittmann (1988, 1992) are based on the numerical solution which was computed by assuming that the biofilm detachment rate coefficient is a constant (i.e. biofilm detachment rate is a fisrt order function of biofilm mass). As discussed in Chapter 4, however, recent work has shown that in many cases the detachment rate coefficient could be a function of biofilm thickness and/or local biogrowth rate. A new solution is therefore required to accommodate the biofilm processes with more complex detachment mechanisms.

This chapter will demonstrate that, under steady-state conditions, the differential equation for simultaneous substrate utilization and diffusion mathematically

requires that the substrate concentration at the surface of an impermeable substratum (S_w) be a constant independent of biofilm thickness (L_f), the substrate flux into the biofilm (J) and the substrate concentration at the surface of the biofilm (S_s). For a given biofilm process, S_w approximately equals S_{s-min}. A new solution is thus devised to express J as a function of S_s and S_{s-min}, in which the impact of different biofilm detachment mechanisms on J is solely reflected through S_{s-min}. When S_{s-min} is treated as an independent biofilm kinetic parameter and determined through in-situ measurement or data fitting, instead of calculated using biofilm detachment kinetics, biofilm detachment mechanisms would be "detached" from and thus have little impact on the function of J versus S_s and S_{s-min}. This provides the justification for the use of the pseudoanalytical solution of Sáez and Rittmann (1992) in Chapter 2 despite the fact that the first order assumption predicted unrealistic biofilm thickness from the S_{min} estimate.

STEADY-STATE BIOFILM MODEL

Physical concept of an idealized biofilm system has been discussed in Chapter 1 and illustrated in Figure 1-1. In a idealized biofilm system (Rittmann and McCarty, 1980), it is assumed that

(1)   there is a sole limiting substrate which is both diffusion and bioreaction limiting in the biofilm system;

(2)   the biofilm is homogeneous and continuous throughout and, thereby, has a uniform density of X_f (M_xL^{-3});

(3)   the biofilm has a uniform thickness of L_f (L); and

(4)   the substratum is impermeable.

The substrate is transported from the bulk liquid with a concentration of S_b (M_sL^{-3}) perpendicularly to the biofilm surface through an effective diffusion layer (an equivalent depth of liquid film through which the actual mass transport can be described by molecular diffusion alone) with a thickness of L (L). The substrate concentration on the outer surface of the biofilm is S_s (M_sL^{-3}), within the biofilm is S_f (M_sL^{-3}), and at the inner surface of the biofilm is S_w (M_sL^{-3}).

In reality, a biofilm may not be completely continuous, in other words, it could be patchy. Nevertheless the biofilm can be treated as continuous as long as the dominant direction of substrate flux into the biofilm (J, $M_sL^{-2}T^{-1}$) is perpendicular to the substratum surface, i.e. the flux through the edges of the biofilm is negligible. In engineering design, the substratum surface area not covered by the biofilm should be deducted as was done in Chapter 2.

A steady state biofilm is a special case which satisfies two conditions (1) the substrate concentration profile in the biofilm would not change with time and (2) the gain in biofilm mass (due to new cell growth) is just balanced by the net loss in biofilm mass (Rittmann and McCarty, 1980a).

For a biofilm which satisfies the first condition, a second-order ordinary differential equation, which describes the substrate mass balance between molecular diffusion and bioreaction within a differential segment of biofilm, is presented in equation (1) in Chapter 1. Expressed in dimensionless form, the diffusion-with-bioreaction equation becomes

$$\frac{1}{L_f^{*2}} \cdot \frac{d^2 S_f^*}{dr_f^{*2}} - \frac{S_f^*}{1+S_f^*} = 0 \qquad\qquad 0 \leq r_f^* \leq 1 \qquad\qquad (1)$$

with $r_f^* = r_f/L_f$ $L_f^* = L_f/\tau$ $S_f^* = S_f/K_s$ $(\tau = [K_s D_f/kX_f]^{1/2}, L)$

where D_f (L^2T^{-1}) is the diffusivity in the biofilm; K_s is the half velocity constant in the Monod expression (M_sL^{-3}); k is the maximum specific rate of substrate utilization (T^{-1}); Y is the yield coefficient, M_x/M_s; r_f is the depth ordinate in the biofilm (L).

Based on Fick's First Law, $J_f = D_f\dfrac{dS_f}{dr_f}$, where J_f ($M_sL^{-2}T^{-1}$) is the substrate flux passing through r_f into the inner layer of the biofilm. In dimensionless form, J_f can be transformed as

$$\text{Definition 1: } \quad J_f^* = \frac{1}{L_f^*}\frac{dS_f^*}{dr_f^*} \qquad\qquad\qquad (2)$$

with $J_f^* = J_f\tau/K_sD_f$.

By substituting equation (2) into equation (1), equation (1) can be reduced to a first order differential equation of J_f^* vs S_f^*:

$$J_f^* \frac{dJ_f^*}{dS_f^*} = \frac{S_f^*}{1+S_f^*} \qquad S_w^* \le S_f^* \le S_s^* \qquad (3)$$

with $S_s^* = S_s/K_s$ and $S_w^* = S_w/K_s$

The substrate flux into the whole biofilm, J ($M_sL^{-2}T^{-1}$), can then be defined as:

$$\text{Definition 2:} \quad J^* = \frac{1}{L_f^*} \frac{dS_f^*}{dr_f^*}\bigg|_{r_f^*=1} \qquad (4)$$

with $J^* = J\tau/K_sD_f$.

Because the substratum is impermeable, equation (1) or (3) is subject to the following boundary condition:

$$\text{BC1:} \quad \frac{dS_f^*}{dr_f^*}\bigg|_{r_f^*=0} = 0 \quad \text{or} \quad J_f^* = 0 \text{ at } r_f^* = 0 \qquad (5)$$

The second condition of the steady-state biofilm requires that the biogrowth is just balanced by net biofilm loss. For a unit area of biofilm, the total biofilm loss rate (R, $M_xL^{-1}T^{-1}$) can be related to the biomass of the entire biofilm (X_fL_f) through a detachment rate coefficient (b', T^{-1}), $R = b'X_fL_f$.

The balance between biogrowth and biofilm loss can be expressed as (Rittmann and McCarty, 1980a):

$$JY = b'X_fL_f \qquad (6)$$

or

$$kYJ^* = b'L_f^* \qquad (7)$$

This second condition further leads to an important concept in the steady-state biofilm model, the minimum bulk substrate concentration, S_{min} (M_sL^{-3}) (Rittmann and

McCarty, 1980a). At a bulk substrate concentration lower than S_{min} no steady state biofilm can be sustained, and even an existing biofilm would decay and disappear if the low concentration lasts too long. When $S_b = S_{min}$, a steady state biofilm with a monolayer of bacteria would be able to be sustained (Rittmann and McCarty, 1980a).

Because a steady-state biofilm is subject to both equations (1) and (7), L_f is not an independent variable. L_f is determined through equation (7) provided that the overall biofilm loss rate coefficient, b', representing both endogenous-respiration and net shearing to the bulk liquid (Sáez and Rittmann, 1988), is defined for a given biofilm system.

There now appear to be two different approaches to provide the solution to the steady-state biofilm model. The first approach requires b' to be explicitly defined so that L_f, the substrate concentration profile within the biofilm and thus the substrate flux into the biofilm can be obtained through numerical integration. An example of such numerical integration has been presented in Sáez and Rittmann (1988). The second approach is to take advantage of equation (3), the transformed form of equation (1), where L_f happens to have been eliminated. This will provide the opportunity to obtain the relationship between J_f and S_f without determining L_f. A disadvantage of the later approach is that it does not provide the substrate concentration profile within the biofilm. However, the primary goal of biofilm modeling is to determine the relationship between J and S_s.

CURRENT SOLUTION FOR FIRST-ORDER DETACHMENT KINETICS

The current pseudoanalytical solution of Sáez and Rittmann (1992) is based on the numerical solution of Sáez and Rittmann (1988) which resulted from numerical integration, using the first approach discussed above. In Sáez and Rittmann (1988), b' in equation (6) was "assumed to be a constant". As discussed in Chapter 4, when b'=b is a constant independent of $X_f L_f$ and S_f,

$$S_{min}^* \cong S_{s-min}^* = b/(Yk - b) \qquad (8)$$

with $S_{min}^* = S_{min}/K_s$, $S_{s-min}^* = S_{s-min}/K_s$.

Suidan and Wang (1985) found that for the limiting case of a "deep" biofilm, where $S_w = 0$,

$$J_{deep}^* = \{2[S_s^* - \ln(1+S_s^*)]\}^{1/2} \tag{9}$$

For situations other than the limiting case, Sáez and Rittmann (1992) expressed the flux into a biofilm in the general situation as a fraction of J_{deep}:

$$J^* = f \times J_{deep}^* \tag{10}$$

where f is a pseudoanalytical dimensionless function of S_s/S_{min} (f ≤ 1) expressed as the following formula:

$$f = \tanh[\gamma(S_s^*/S_{min}^* - 1)^\beta] \tag{11}$$

where $\gamma = 1.5557 - 0.4117\tanh(\log S_{min}^*)$ and $\beta = 0.5035 - 0.0257\tanh(\log S_{min}^*)$. The expressions for γ and β were obtained by fitting linearly transformed equation (11) to the numerical solution of Sáez and Rittmann (1988) for various S_s^*/S_{min}^* values (Sáez and Rittmann, 1992).

However, as discussed in Chapter 4, b' cannot be treated as a constant in many cases because biofilm detachment has been found to be much more complicated than a first-order process. Therefore, a more general solution is required to accommodate biofilm processes with complex detachment mechanisms.

Although the pseudoanalytical solution (i.e. equations [10] and [11]) is applicable only when detachment is negligible or can be approximated as a first order process, it provides some significant insights into the steady-state biofilm model:

(1) J^* is only a function of S_s^* and S_{min}^*. The impact of b', in other words the biofilm detachment mechanisms, on the solution is reflected through S_{min}^*, which is related to b' though equation (8). It should be noted that, although L_f^* was used as a transient variable in the numerical integration, L_f^* does not appear in equations (10) and (11).

(2) In the numerical integration, which forms the basis of the pseudoanalytical solution, L_f^* and the steady-state substrate profile were obtained for given S_s^* and S_{min}^* (i.e. k,Y and b') without involving equation (7). The L_f^* computed through numerical integration was consistent with the L_f^* calculated from equation (7).

In short, for a given S_s^*, L_f^* is implicitly determined by S_{min}^* through numerical integration. S_{min}^* is the only parameter required in the final solution to reflect the balance between biofilm growth and loss.

The following section demonstrates an approach to obtain an expression of J* as a function of S_s^* and S_{min}^* without numerical integration. In this approach, no L_f^* is determined as a transient variable. However, L_f^* as the result of the balance between biofilm growth and loss is implied in S_{min}^*. Since different biofilm detachment mechanisms would impact only S_{min}^*, the solution would be generally applicable if S_{min}^* itself is considered to be an independent parameter. For a biofilm with complex detachment kinetics, b' in equation (7) could be a very complicated function of concentration profile and L_f^*. Calculating L_f^* from equation (7) would no longer be an easy task.

DEVELOPMENT OF A NEW SOLUTION

Integrating The Diffusion-with-Bioreaction Equation.

Although the second-order differential equation (1) is nonlinear and cannot be solved analytically as a function of S_f^* vs r_f^*, the most important goal of biofilm kinetic modeling is not to define an S_f^* vs r_f^* profile in a biofilm. Usually the goal of biofilm modeling is to find a function to describe the relationship between the substrate flux into the biofilm and the substrate concentration. Such a relationship can be obtained by integrating the reduced-order equation (3),

$$J_f^{*2}=2[S_f^*-\ln(1+S_f^*)+C] \tag{12}$$

where C is mathematically a constant of integration, which is mathematically a constant. By applying the boundary condition of equation (5) to equation (12),

$$C = -S_f^* \big|_{r_f=0} + \ln(1 + S_f^* \big|_{r_f=0}) \qquad (13)$$

$S_f^* \big|_{r_f=0}$ is S_w^*, which is also a constant because C is a constant. Mathematically, a constant is a value independent of any other variables in the function. In other words, the value of S_w^* is independent of J_f^* and S_f^*. Because $J_f^* = \dfrac{1}{L_f^*}\dfrac{dS_f^*}{dr_f^*}$, S_w^* is also independent of L_f^* and $\dfrac{dS_f^*}{dr_f^*}$. The independence of S_w^* with respect to S_f^*, L_f^* and $\dfrac{dS_f^*}{dr_f^*}$ is attributed to the fact that at and only at $r_f^*=0$, $\dfrac{dS_f^*}{dr_f^*}$ is a fixed value (zero) and r_f^* is independent of L_f^*. At anywhere other than $r_f^*=0$, $\dfrac{dS_f^*}{dr_f^*}$ would be a function of L_f^* and S_f^*. For $r_f^*>0$, even r_f^* is a function of L_f^* because $r_f^* = r_f/(L_f^*\tau)$.

Although equation (3) has been reduced to a first-order ordinary differential equation, solving this equation still requires that both J_f^* and S_f^* are given at one specific r_f^* (Martin and Reissner, 1964). Because S_w^* is a constant independent of J_f^* and S_f^*, for any biofilm subject to equations (1) and (5), we can assign a value to S_w^*. A given S_w^* value would lead to the following initial conditions:

$$r_f^*=0: \quad J_f^*=0, \quad S_f^*=S_w^* \qquad (14)$$

Mathematically the above initial conditions are sufficient to provide a solution for equation (1) or (3), which is

$$J_f^* = \{2[S_f^*-\ln(1+S_f^*) - S_w^*+\ln(1+S_w^*)]\}^{1/2} \qquad (15)$$

Suidan and Wang (1985) derived the same equation earlier but they failed to recognize that S_w^* is mathematically a constant for an impermeable substratum.

Equation (15) is applicable to the relationship between S_s^* and its corresponding flux, J^*, which leads to

$$J^* = \{2[S_s^*-\ln(1+S_s^*) - S_w^*+\ln(1+S_w^*)]\}^{1/2} \qquad (16)$$

It is important to note that $r_f=L_f$ is a moving boundary. Although dimensionless transformation has fixed the moving boundary at $r_f^*=1$, L_f^* as a variable

makes equation (1) actually represents a family of second-order differential equations. Therefore, for a given L_f^*, equation (15) defines one curve of J_f^* versus S_f^* within the biofilm and equation (16) defines a single data point, (J^*, S_s^*). If S_w^* is not independent of L_f^* or L_f^* somehow appears in equation (15), the equation can only be regarded as the solution for a specific L_f^*. The fact that L_f^* happens to be canceled out in the transformed differential equation (3) by taking advantage of Definition 1 (eq. [2]) and that S_w^* is independent of L_f^*, as discussed previously, means that equation (15) in fact represents a family of solutions and equation (16) is a function (rather than a single point) for J^* versus S_s^*. It is also interesting to note that equation (15) makes it possible to determine the substrate flux into a biofilm without the knowledge of the biofilm thickness because L_f^* has been embedded into the definition of J_f^*(eq. [2]).

In deriving equation (16), S_w^* has been mathematically regarded as a given value while it is physically unknown. For a specific biofilm system, S_w^* would be physically defined by factors other than J^*, S_s^* and L_f^*. Until this value is physically defined, equation (16) is still not a solution to the steady-state biofilm model. The following section will show how the value of S_w^* can be derived from a limiting case already **concealed** in the concept of S_{min}.

$S_w^* \cong S_{s\text{-}min}^*$

According to Rittmann and McCarty (1980a), when $S_b = S_{min}$ (or $S_s = S_{smin}$), only a monolayer of biofilm is sustainable. The thin monolayer biofilm can be regarded as one differential section. Applying the Euler-Cauchy integration method (Ceschino and Kuntzmann, 1966) to the differential section,

$$S_{smin} = S_w + L_{fmin}(\frac{dS_f}{dr_f}\Big|_{rf=Lfmin} + 0)/2 \tag{17}$$

which leads to

$$J_{min} = 2D_f(S_{smin} - S_w)/L_{fmin} \tag{18}$$

J_{min} can also be determined by an average substrate concentration within the monolayer biofilm,

$$S_{ave} = (S_{smin} + S_w)/2 \tag{19}$$

$$J_{min} = kX_fL_{fmin}S_{ave}/(K_s + S_{ave}) \tag{20}$$

Equations (18) and (20) can be transformed to dimensionless form:

$$J_{min}* = 2(S_{smin}* - S_w*)/L_{fmin}* \tag{21}$$

$$J_{min}* = (S_{smin}* + S_w*)L_{fmin}*/(2 + S_{smin}* + S_w*) \tag{22}$$

Equations (21) and (22) lead to

$$2S_w*^2 + (4 + L_{fmin}*^2)S_w* - 4S_{smin}* - 2S_{smin}*^2 + L_{fmin}*^2 S_{smin}* = 0 \tag{23}$$

The solution to equation (23) is

$$2S_w* = -(2 + L_{fmin}*^2/2) \pm SQRT\{(2 + L_{fmin}*^2/2)^2 - 4[(L_{fmin}*^2/2 - 2)S_{smin}* - S_{smin}*^2]\} \tag{24}$$

S_w* must be positive, therefore,

$$2S_w* = -(2 + L_{fmin}*^2/2) + \{(2 + L_{fmin}*^2/2)^2 - 4[(L_{fmin}*^2/2 - 2)S_{smin}* - S_{smin}*^2]\}^{1/2} \tag{25}$$

It should be noted that equations (18) and (20) are approximate in nature. Thus the solution of S_w* in equation (25) is approximate in a strictly mathematical sense. However, as will be shown in the following paragraphs, the error introduced by the approximation is negligible.

Although equation (25) is derived for the special case of $L_f* = L_{fmin}*$, it is generally applicable to any L_f* because, as discussed previously, S_w* is an integration constant independent of L_f*. Therefore, equation (25) can be substituted into equation (16) and leads to a new solution to the steady-state biofilm model. Because this solution is very complicated, one further minor approximation is made in the following paragraphs.

If we can further assume $L_{fmin}*^2 \ll 4$, or $L_{fmin}^2 \ll 4\tau^2$, which is true if L_{fmin} is in the order of 1 μm and τ is in the order of 10 μm (see the section on "Assessment" later in this chapter). Thus $L_{fmin}*^2$ is negligible and equation (25) becomes

$$2S_w^* \cong -2 + \{2^2 - 2[-4S_{smin}^* - 2S_{smin}^{*2}]\}^{1/2} \text{ or } S_w^* \cong S_{smin}^* \qquad (26)$$

Equation (26) further leads to equation (27), which is the new solution to the steady state biofilm model.

$$J^* \cong \{2[S_s^* - \ln(1+S_s^*) - S_{smin}^* + \ln(1+S_{smin}^*)]\}^{1/2} \qquad (27)$$

Although it is very likely that τ is much greater than 1 μm, as a precaution, τ (in μm) should be estimated to ensure that $4\tau^2 >> 1$ before using equation (27).

As the substrate concentration at the biofilm surface, $S_{s\text{-min}}$ is not actually measurable. However, $S_{min}^* \cong S_{s\text{-min}}^*$ (Rittmann and McCarty, 1980a) and S_{min}^* is measurable. For situations where S_{min}^* must be measured experimentally rather than determined by data-fitting, equation (27) can further be approximated as

$$J^* \cong \{2[S_s^* - \ln(1+S_s^*) - S_{min}^* + \ln(1+S_{min}^*)]\}^{1/2} \qquad (28)$$

The result that $S_w^* \cong S_{s\text{-min}}^*$ can also be derived through numerical integration. Using sophisticated numerical modeling, Skowlund (1990) found that under steady-state conditions S_w is a constant not affected by S_s and L_f, and more importantly, that S_w equals $S_{s\text{-min}}$ defined by Rittmann and McCarty (1980a). The consistency with the result shown herein is by no means a coincidence because $S_w^* \cong S_{s\text{-min}}^*$ is not an *ad hoc* boundary condition imposed on the steady-state biofilm model. It has always been embedded in the steady-state biofilm model: equations (1) and (5) require S_w^* to be a constant for all L_f^* while the concept of $S_{s\text{-min}}$ implies that $S_w^* \cong S_{s\text{-min}}^*$.

J^* and L_f^*

Because the new solution requires no details of the biofilm detachment mechanism(s), it is applicable to steady-state biofilms with various or even unknown detachment kinetics because the determination of S_{min}^* does not depend on knowing these kinetics. However, this seems hardly convincing because without the details of detachment kinetics L_f^* cannot be calculated. How could J^* be predicted without the knowledge of L_f^*? After all, it is the amount of biomass within the biofilm (X_fL_f) that consumes the substrate. In other words, the solution should not only satisfy the diffusion-with-bioreaction equation (1) or (3) but also satisfy the energy conservation

equation (6) or (7). In the following, it will be shown that indeed as long as the substrate concentration profile satisfies equation (1) or (3), equation (6) or (7) would be automatically satisfied no matter how thick the biofilm is.

For the convenience of demonstration, we use the general expression of the total biofilm loss coefficient described in Chapter 4:

$$b' = b + b_2 L_f + \frac{2b_g}{L_f} \int_0^{L_f} \mu(r_f)(L_f - r_f) dr_f \tag{29}$$

The above equation resulted from the integration of the local detachment rate coefficient, $b(r_f)$ (T^{-1}), proposed by Stewart (1993),

$$b(r_f) = 2b_2(L_f - r_f) + 2b_g \mu(r_f)(L_f - r_f) \tag{30}$$

The overall biofilm loss rate coefficient for the whole biofilm

$$b' = b + \frac{1}{L_f} \int_0^{L_f} b(r_f) dr_f.$$

For a differential section dr_f in a biofilm with a thickness of L_f, at position r_f,

$$\frac{\partial(X_f dr_f)}{\partial t} = \frac{Y k X_f S_f}{K_s + S_f} dr_f - (b + 2b_2[L_f - r_f] + 2b_g \mu(r_f)[L_f - r_f]) X_f dr_f \tag{31}$$

For the purposes of demonstration, we set $b_g=0$, therefore, $b'=(b+b_2 L_f)$. (The case where $b_g \neq 0$ is discussed on the next page.) For a steady-state biofilm with constant X_f, L_f is a constant independent of time (t, T),

$$\frac{X_f dL_f}{dt} = \int_0^{L_f} [\frac{\partial(X_f dr_f)}{\partial t}] dr_f = \int_0^{L_f} \{\frac{Y k S_f}{K_s + S_f} - [(b + 2b_2(L_f - r_f))]\} X_f dr_f = 0 \tag{32}$$

which leads to

$$\int_0^1 \frac{S_f^*}{1 + S_f^*} dr_f^* = \frac{\int_0^{L_f} [b + 2b_2(L_f - r_f)] dr_f}{Y k L_f} = \frac{b + b_2 L_f}{Y k} \tag{33}$$

As long as the concentration profile in the steady-state biofilm satisfies the diffusion-with-bioreaction equation (1) or the transformed equation (3), we have

$$\int_0^1 J_f^* \frac{dJ_f^*}{dS_f^*} dr_f^* = \frac{b + b_2 L_f}{Yk} = \frac{b'}{Yk}$$ (34)

Since $J_f^* = \frac{1}{L_f^*} \frac{dS_f^*}{dr_f^*}$, equation (34) can be transformed as

$$\int_0^{J^*} \frac{1}{L_f^*} dJ_f^* = \frac{b + b_2 L_f}{Yk} \quad \text{or} \quad \frac{1}{L_f^*} J^* = \frac{b'}{Yk}$$ (35)

We have now returned to the original energy conservation equation (7). In other words, when equation (1) is satisfied, the energy conservation equation (7) would be automatically balanced. This will remain true in spite of any change of the assumption of detachment mechanisms. For example, when $b_g \neq 0$, the same derivation is still applicable except that in the integration of equation (33), the integral $\int_0^{L_f} \mu(r_f)(L_f - r_f) dr_f$, which forms part of the definition of b', can be left unintegrated. For a first order biofilm detachment assumption (Sáez and Rittmann, 1988), which the current pseudoanalytical solution is based upon, one can simply replace $(b+b_2L_f)$ with b and go from equations (32) through (35). Therefore, the prediction of J* does not require the knowledge of biofilm thickness if S_{smin}^* is available.

On the other hand, with the solution of equation (27), biofilm thickness (L_f^*) can be calculated for a given S_s^* through equation (7), provided that b' can be expressed explicitly. When b' is expressed explicitly, both S_{smin}^* and L_f^* can be expressed explicitly as a function of b'. S_s^* and L_f^* can then be expressed explicitly as a function of each other.

For example, for the simplest case of b'=b being a constant, coupling equations (7) and (8) will lead to

$$L_f^* = \frac{1 + S_{min}^*}{S_{min}^*} J^* = J^* kY/b$$ (36)

which is equation (4) of Chapter 2.

However, for biofilms with complex detachment mechanisms, for example, if b' takes the form of equation (29), b' itself is in turn a function of the substrate concentration profile. In such cases simultaneous numerical computation of L_f^* and

the concentration profile within L_f^* is required. The relationship between L_f^* and S_{smin}^* is then implicit and a change in L_f^* may not have a significant impact on S_{smin}^*.

Although all biogrowth coefficients (Y, k) and loss coefficients (b_d and various detachment coefficients) are included in both L_f^* and S_{smin}^*, as will be demonstrated later the impact of detachment coefficients on L_f^* could be much more significant than on S_{smin}^* for biofilms with complex detachment mechanisms. In other words, an inappropriate assumption of biofilm detachment kinetics may have little impact on S_{smin}^* and thus J^* but result in a dramatic difference for L_f^*. In order to be able to calculate L_f^* explicitly, let us assume that in equation (29), $b_g=0$, therefore,

$$S_{smin}^* = (b+b_2L_{fmin})/(kY-[b+b_2L_{fmin}]) \qquad (37)$$

Let us assume that for a given biofilm system with S_{smin}^* determined by b and $b_2L_{fmin}=0.05b$, a given S_s^* supports a steady-state $L_f= 100$ μm. Assuming $L_{fmin}=0.5$μm, b'= $b+b_2L_f$ = $b+0.05b\times100\mu m/0.5\mu m=11b$. From equation (6), $J^*=100$ μm× $11bX_f/Y$. If the small increase in b' obtained by including the term $b_2L_{fmin}=0.05b$ is neglected in calculating S_{smin}^*, the S_{smin}^* value would not change much and this would have little impact on J^*. However, omitting b_2L_{fmin} implies that for the computation of S_{smin}^* biofilm detachment kinetics can be approximated as first order as assumed in Chapter 2. In this case, the (approximately) same flux, $J\cong100\mu m\times11bX_f/Y$, would be found to be able to support a biofilm thickness $L_f\cong Y(100 \mu m\times11bX_f/Y)/(bX_f)=1100$μm.

The impact of b_g would be even more profound than that of b_2 because the impact would be drastically "amplified" through not only L_f but also S_f. The above hypothetical case, however, has shown how a seemingly reasonable first order approximation of detachment kinetics, which does not have much impact on S_{smin}^* and thus J^*, could result in a very misleading result for biofilm thickness. In Chapter 2, biofilm detachment kinetics was assumed to be first order. This could partly explain the unrealistically high computed L_f values in the order of 10 mm.

As shown above, it appears that even a slightly different detachment kinetics can result in substantially different predicted biofilm thickness. This, on the other hand, suggests that two biofilms with substantially different thickness could be

sustained by the same amount of substrate flux into them. This seems hard to imagine because a thicker biofilm should require more substrate flux to sustain it. However, it should be noted that the substrate flux into a biofilm not only supports the biomass within the thickness but also provides the energy source to produce the biomass which continuously detaches away from the biofilm. Two biofilms of different thicknesses could exist at the same substrate concentration if the detachment rates were different.

Although Rittmann's later work has included detachment, when Rittmann and McCarty (1980a) first proposed the steady-state biofilm model, biomass detachment was not included. For a steady-state biofilm without biomass detachment, the model requires that the inner sections of the biofilm are in negative growth and the outer sections are in net positive growth so that the biofilm thickness can remain a constant. This requires $S_w^* < S_{smin}^*$ which appears to be in contradiction with the result derived in this chapter, which is that in steady-state $S_w^* \cong S_{smin}^*$. However, except in some natural systems, biofilm detachment is likely the primary process that balances cell growth in a biofilm (Wanner and Gujer, 1986; Peyton and Characklis, 1993). For biofilms with detachment as the primary process which balances the growth, it is understandable that $S_w^* \cong S_{smin}^*$ and the growth of outer sections is balanced by the detachment. This is especially so as more and more evidence has indicated that the detachment rate coefficient is related to growth rate and biofilm thickness. In other words, the faster the biofilm grows and the thicker it is, the more easily the produced biomass will be detached.

APPLICATION AND ASSESSMENT

Biofilm-Reactor Design

It is not practical to measure substrate concentration on the biofilm surface (S_s). To use the solution developed in this chapter for process design, the substrate flux into the biofilm should be related to the bulk liquid substrate concentration (S_b). The relationship between S_s and S_s is controlled by Fick's First Law,

$$S_s^* = S_b^* - J^* L^* / D^* \tag{38}$$

with $L^* = L/\tau$ $D^* = D/D_f$ $S_b^* = S_b/K_s$

where D (L^2T^{-1}) is the substrate diffusivity in the liquid.

In biofilm process design, we can also assume that the effect of suspended microorganisms in the bulk liquid is negligible.

A. Completely Mixed Biofilm Reactor

For a (nearly) completely mixed biofilm reactor (CMBR) such as a fluidized bed or a packed column with large enough recycle ratio (Bailey and Ollis, 1986),

$$Q(S_i-S_b)-J\alpha V=0 \tag{39}$$

where α denotes the specific surface area which is the biofilm surface area in each unit volume of the bioreactor (L^{-1}); V is the effective volume of the bioreactor (L^3); Q is the influent flow rate $(L^{-3}T^{-1})$; and S_i is influent substrate concentration, (M_sL^{-3}). With equations (27) and (38), for a desired effluent concentration S_b (i.e. given $S_b^*=S_b/K_s$) the two unknowns, S_s^* and J^*, can be determined by trial and error. Because $J=J^*K_sD_f/\tau$ while Q and S_i are usually given and α can be calculated, if kinetic parameters, k, and K_s, and $S_{s\text{-}min}$ are provided, the only unknown in equation (39) is V. Thus, the volume of the reactor can be determined.

B. Packed Column.

The solution developed in this chapter can also be directly applied to design biofilm columns of the plug-flow type. Under steady-state conditions, the mass balance in a small segment of a packed biofilm column, dx, can be described as (Bailey and Ollis, 1986, p. 519):

$$v\frac{dS_b}{dx} - D_H\frac{d^2S_b}{dx^2} + \alpha J = 0 \tag{40}$$

where v is the superficial flow velocity $(v=Q/A_c)$ (LT^{-1}); x is the longitudinal distance along the column (L) and D_H is the hydrodynamic dispersivity (L^2T^{-1}). Equation (40) is a nonlinear second-order differential equation which, again, has no analytical

solution. However, with proper approximation, it can be solved analytically, as described below.

By differentiating equation (40) with respect to x, we can obtain $v\frac{d^2S_b}{dx^2}$ - $D_H\frac{d^3S_b}{dx^3} + \alpha\frac{dJ}{dx} = 0$. Assuming the third-order derivative $\frac{d^3S_b}{dx^3} \cong 0$ (which is reasonable because the S_b vs. x curve would look like a curve of first-order kinetics, see Figure 4-1), we obtain $\frac{d^2S_b}{dx^2} = -\frac{\alpha}{v}\frac{dJ}{dx}$. Equation (40) then becomes

$$v\frac{dS_b}{dx} + D_H\frac{\alpha}{v}\frac{dJ}{dx} + \alpha J = 0 \tag{41}$$

Equation (41) can be solved by substituting S_b with S_s+JL/D,

$$x = \frac{v\tau}{\alpha D_f}\int_{S_{sx}^*}^{S_{so}^*}\frac{dS_s^*}{J^*} + (\frac{vL}{\alpha D} + \frac{D_H}{v})\ln\frac{J_o^*}{J_x^*} \tag{42}$$

where S_{so}^* is the dimensionless substrate concentration on the biofilm outer surface at the inlet end, (M_sL^{-3}); S_{sx}^* is the concentration at depth x, (M_sL^{-3}); J_o^* is the dimensionless substrate flux into the biofilm at the inlet end and J_x^* is the flux at depth x.

Thus, when influent and effluent concentrations are specified, equation (42) allows x, the required column length, to be calculated. In equation (42), $\frac{dS_s^*}{J^*} =$

$\frac{dS_s^*}{\{2[S_s^*-\ln(1+S_s^*)-S_{min}^*+\ln(1+S_{min}^*)]\}^{1/2}}$, which can not be integrated analytically. However, it can be integrated using a numerical integration algorithm, such as the Runge-Kutta method (Ceschino and Kuntzmann, 1966).

In engineering design, for a given influent concentration S_i, i.e. given $S_i^* = S_i/K_s$, S_{so}^* and J_o^* can be determined by equation (27) and (38). Then, the length of the column can be determined by equation (42) for a desired bulk effluent concentration S_{bx} $(=K_s[S_{sx}^*+L^*J_x^*/D^*])$.

In-Situ Determination of Kinetic Parameters

As discussed in Chapter 4, the value of $S_{s\text{-min}}$ relates to complicated biofilm detachment mechanisms. It is almost formidable to determine $S_{s\text{-min}}$ from biofilm detachment kinetics. On the other hand, if we treat $S_{s\text{-min}}$ itself as a biofilm kinetic parameter, the analytical solution can be used for *in-situ* determination of all three kinetic parameters, k, K_s and $S_{s\text{-min}}$, using completely mixed biofilm reactor devised by Rittmann et al. (1986).

Running different influent substrate concentrations (S_i) through the biofilm system will result in different effluent concentrations (S_b). The substrate flux J is determined by equation (39) and the corresponding S_S can be calculated using equation (38). Equation (27) is a nonlinear equation with three model parameters: kX_f, K_s and $S_{s\text{-min}}$. These parameters can be estimated simultaneously through nonlinear regression. Such an experimental approach has been used in Chapter 3 to estimate kinetic parameters for assimilable organic carbon in drinking water biological treatment processes. For a problem with three model constants, at least four sets of J steady-state and S_s are required for the nonlinear regression, to provide one extra degree of freedom for error estimation. Sometimes, the diffusivity of the substrate (D) is not available. In such cases, the diffusivity can be treated as an additional model parameter, requiring an additional experimental run.

In the design of full scale reactors, where kX_f and K_s may have been determined in the laboratory, $S_{s\text{-min}}$ would be the only parameter to be determined *in-situ*. A plug-flow type biofilm column with a certain detention time can be used to determine S_{min} and thus $S_{s\text{-min}}$. The influent concentration can be relatively high at the beginning. When a steady-state biofilm has been established, the influent concentration can be decreased gradually allowing the biofilm to reach a new steady state each time until it is barely higher than the effluent concentration. The effluent concentration would then be S_{min}. Under conditions where S_i is low (e.g. in biological drinking water treatment) and where the measured substrate concentration parameter has large inherent variability (e.g. AOC), it may be difficult to obtain precise estimate of S_{min}.

Alternatively, the amount of substrate removal can be plotted against the influent concentration for a range of influent concentrations. Extrapolating the curve to the x-axis, the influent concentration corresponding to zero removal would be

approximately S_{min}. The data-fitting approach described in Chapter 2 can also be used for S_{min} determination.

Assessment of the New Solution

Experimental verification of a reaction-with-diffusion model of immobilized cell metabolism has been a difficult proposition, owing to, among other factors, experimental uncertainties in assessing the activity of the cells, the effective diffusivity (Karel et al., 1985). Experimental data deliberately collected for verifying steady-state biofilm models are limited in the literature. In this section, the solution developed in this chapter is assessed using two examples of experimental data from the literature, one for a completely mixed biofilm reactor (CMBR) and another one for a packed-bed biofilm column. Kinetic parameters and experimental conditions are summarized in Tables 5-1 and 5-2 for the two examples respectively. Model predictions are also undertaken using the pseudoanalytical solution and compared with the prediction of the solution developed in this chapter to evaluate the agreement of the two solutions.

Experimental data used for assessing the solution developed in this chapter with the CMBR model are taken from Rittmann et al. (1986) where b was not given (see Table 5-1). Rittmann (1982) found that for a biofilm growing on the surface of glass beads, biofilm detachment can be approximated as a first-order process when $L_f<30$ μm. In this example, $L_f=18$ μm, therefore, the first-order biofilm loss coefficient, b, can be calculated as

$$b = J_{exp}Y/L_fX_f = (0.116 \times 0.134)/(18 \times 10^{-6} \times 33100) = 0.026 \text{ day}^{-1}$$

$$S_{s-min}* = b/(kY-b) = 0.026/(0.134 \times 1.6 - 0.026) = 0.138$$

$$\tau = (K_sD_f/kX_f)^{1/2} = [(8.6 \times 10^{-5} \times 0.018)/(1.6 \times 33100)]^{1/2} = 5.41 \times 10^{-6} \text{ m}$$

$$[4\tau(\mu m)^2 \cong 120 >> 1]$$

$$L* = L/\tau = 96/5.41 = 17.74.$$

By substituting the values of $S_{min}*$, S_b* and $L*$ into equations (27) and (38), Equations (43) and (44) can be obtained:

$$J^* = \{2[S_s^* \text{-} \ln(1\text{+}S_s^*)\text{-}0.00872]\}^{1/2} \qquad (43)$$

$$6.111 = S_s^* + 0.8 \times 17.74 J^* \qquad (44)$$

By trial-and-error, the solutions for equations (43) and (44) are: $J^* = 0.397$ and $S_s^* = 0.478$. Thus,

$$S_s = S_s^* \times K_s = 0.477 \times 0.018 = 0.0086 \text{ g/m}^3$$

$$J_{pred} = J^* K_s D_f / \tau = (0.397 \times 0.018 \times 8.6 \times 10^{-5}) / (5.41 \times 10^{-6}) = 0.114 \text{ g/m}^2\text{-day}$$

The relative error for the predicted flux then is,

$$E(\%) = (J_{exp} - J_{pred}) / J_{exp} = (0.116 - 0.114) / 0.116 = 2\%$$

The same calculation has been done using the pseudoanalytical solution instead of the new solution. The solutions are: $J^* = 0.398$ and $S_s^* = 0.457$. The difference in terms of predicted flux is only 0.3%.

To assess the new solution for the steady-state packed-bed biofilm model, data from the steady-state biofilm column experiments conducted by Rittmann and McCarty (1980b) will be used. All kinetic parameters and experimental specifications necessary for the assessment are listed in Table 5-2. Although S_{min} was given in Rittmann and McCarty (1980b), they had calculated it using equation (3) with $b=b_d$. As discussed previously, when the impact of biofilm detachment is insignificant, such an approximation is considered reasonable. Four columns had been used in the experiment. Only column BC1, with the lowest superficial velocity and thus the least of biofilm detachment, is selected for demonstration.

$$S_{min}^* = S_{min}/K_s = 0.66/3.9 = 0.169$$

$$S_i^* = S_i/K_s = 7.2/3.9 = 1.846$$

$$\tau = [K_s D_f / k X_f]^{1/2} = [(3.9 \times 8.7 \times 10^{-5})/(20 \times 2500)]^{1/2} = 8.24 \times 10^{-5} \text{ m}$$

$$[4\tau(\mu m)^2 \cong 250000 >> 1]$$

$$L^* = L/\tau = 2.26 \times 10^{-4}/8.24 \times 10^{-5} = 2.74$$

$$\frac{v\tau}{\alpha D_f} = (3.22 \times 8.24 \times 10^{-5})/(1320 \times 8.7 \times 10^{-5}) = 2.3 \times 10^{-3} \text{ m}$$

$$\frac{vL}{\alpha D} + \frac{D_H}{v} = (3.22 \times 2.26 \times 10^{-4}/1320 \times 1.09 \times 10^{-4}) + (1.19 \times 10^{-2}/3.22) = 8.76 \times 10^{-3} \text{ m}$$

By substituting the values of L^*, S_{min}^*, and S_b^* ($= S_i^*$) calculated above into equations (27) and (38), we obtain

$$J_o^* = \{2[S_{so}^* - \ln(1 + S_{so}^*) - 0.169 + \ln 1.169]\}^{1/2} \tag{45}$$

$$1.846 = S_{so}^* + 0.8 \times 2.74 J_o^* \tag{46}$$

By trial and error, the solution for equations (45) and (46) is $J_o^* = 0.536$ and $S_{so}^* = 0.669$. Substituting the values of J_o^*, S_{so}^*, $(\frac{v\tau}{\alpha D_f})$ and $(\frac{vL}{\alpha D} + \frac{D_H}{v})$ into equation (42), x can be determined corresponding to each S_{sx}^*. The steady-state concentration profile then can be predicted with $S_b(x) = K_s(S_{sx}^* + 0.8 \times 2.74 J_x^*)$.

The prediction of $S_b(x)$ vs x for column BC1 is plotted in Figure 5-1. Experimental data of Rittmann and McCarty (1980b) are also included for comparison. We see that the plug-flow model (i.e. equation [42]) predicts the concentration profile of S_b vs x very well.

The same curve of $S_b(x)$ vs x can also be predicted using the pseudoanalytical solution in place of the new solution. The two predicted curves were found to almost perfectly overlap each other.

CONCLUSIONS

The dimensionless flux of substrate into a steady-state biofilm (J^*) can be expressed as a function of substrate concentration on the biofilm surface (S_s^*) and the minimum substrate concentration on the biofilm surface (S_{s-min}^*), which is approximately equal to the minimum bulk substrate concentration (S_{min}^*). Sáez and Rittmann (1988, 1992) expressed such a relationship as pseudoanalytical solutions. The pseudoanalytical solutions were derived by assuming a first-order dependence of

biofilm detachment rate on biofilm thickness. Given the fact that biofilm detachment is much more complicated than a first order process, the pseudoanalytical solutions are not completely general.

This chapter presents a new expression for the relationship among J^*, S_* and S_{min^*}. Because it does not require any specific presumption of biofilm detachment kinetics, the solution developed in this chapter is applicable for biofilms with various detachment mechanisms. The effect of different biofilm detachment mechanisms on the flux is reflected in the new solution through the S_{s-min} value, which, in turn, is a constant for a specific biofilm system and is defined by biofilm kinetics and biofilm detachment mechanisms. Although in strictly mathematical sense the new solution involves an approximation, this approximation is considered to have little impact on the calculation of substrate removal in all practical situations.

Because of the complexity of the biofilm detachment mechanism, it would not be feasible to determine S_{min} by combining intrinsic kinetic parameters with a number of biofilm detachment rate coefficients, which may be impossible to measure in practice. S_{min} should instead be regarded as a biofilm kinetic parameter and be determined *in-situ* for a specific biofilm, using the *in-situ* techniques proposed in this chapter.

It is important to note that the knowledge of biofilm thickness is not necessary for predicting the substrate flux into a steady-state biofilm when S_{min} is treated an independent biofilm kinetic parameter and determined through *in-situ* measurement or data fitting. On the other hand, a different assumption of biofilm detachment kinetics, which may have little impact on S_{s-min} and thus J, could predict different and drastic biofilm thickness for independently determined S_{min}, as evident in Chapter 2.

Table 5-1. Parameters for CMBR biofilm column A2 (Rittmann et al., 1986)[a].

Parameter	Unit	Value
S_i	g/m^3	1.0
S_b	g/m^3	0.11
K_s	g/m^3	0.018
L_f	m	1.8×10^{-5}
L	m	9.6×10^{-5}
D_f	m^2/d	8.6×10^{-5}
X_f	g biomass/m^3	33,100
k	d^{-1}	1.6
Y'	g C/g acetate	0.071^b
Y	g biomass/g acetate	0.134^c
J_{exp}	g/m^2-d	0.116

a   The substrate was acetate and the substratum was 3 mm glass beads.
b   From Rittmann and McCarty (1980b).
c   Assuming a general formula for biomass of $C_5H_7NO_2$.

Table 5-2.   Parameters for plug flow biofilm column BC1 (from Rittmann and McCarty 1980b)[a].

Parameter	Unit	Value
k	g/g C-day	20
K_s	g/m^3	3.9
X_f (bacteria)	g C/ m^3	2,500
D	m^2/day	1.09×10^{-4}
D_f	m^2/day	8.7×10^{-5}
S_{min}	g/m^3	0.66
α	m^{-1}	1,320
v	m/day	3.22
L	m	2.26×10^{-4}
D_H	cm^2/day	1.19×10^{-2}
S_i	g/ m^3	7.2

a   The substrate was acetate and the substratum was 3 mm glass beads.
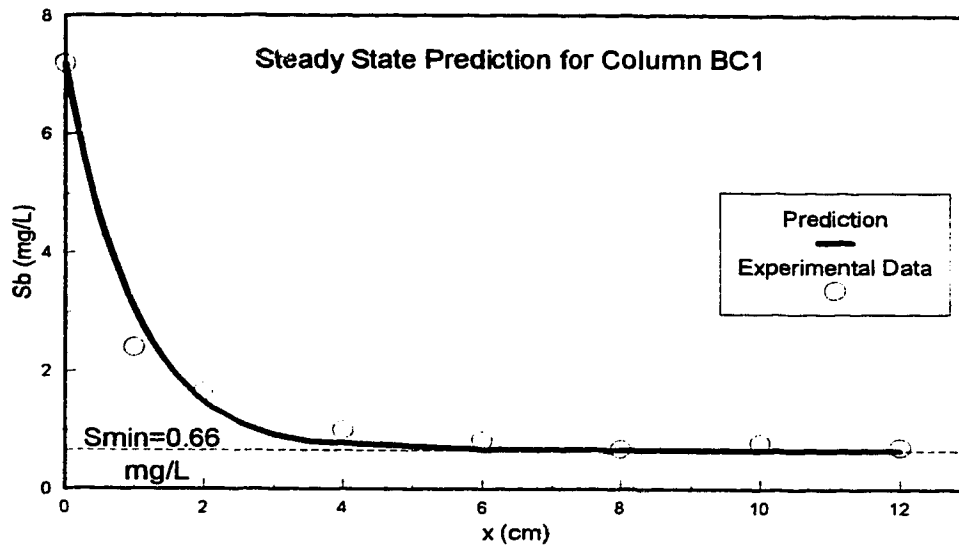
Figure 5-1. Prediction of concentration profile in plug-flow column BC1 (experimental data from Rittmann and McCarty, 1980b).

REFERENCES

Atkinson B. and Davies I. J. (1974) The overall rate of substrate uptake (reaction) by microbial films. *Trans. Inst. Chem. Engrs.* **52**, 248-59.

Atkinson B. and Daoud I. S. (1968) The analogy between microbial "reaction" and heterogeneous catalysis. *Trans. Inst. Chem. Engrs.* **46**, T19-24.

Bailey J. E. and Ollis D. F. (1986) *Biochemical Engineering Fundamentals*, 2nd Ed., McGraw-Hill, New York.

Chang H. T. and Rittmann B. E. (1987) Verification of the model of biofilm on activated carbon. *Biotechnol. Bioengng.* **21**, 280-288.

Chang H. T. and Rittmann B. E. (1988) Comparative study of biofilm shear loss on different adsorptive media. *J. Wat. Pollut. Control Fed.*, **60**, 362-268.

Ceschino F. and Kuntzmann J. (1966) *Numerical Solution of Initial Value Problems*, Prentice-Hall, Englewood Cliffs.

Huck P. M., Zhang S. and Price M. L. (1994) BOM removal during biologial treatment: a first order model. *J. Am. Wat. Wks. Ass.* **86**(6), 61-71.

Karel S. F., Libicki S. B. And Robertson C. R. (1985) The immobilization of whole cells: engineering principles. *Chem. Engng Sci.*, **40**, 1321-1354.

Martin W. T. and Reissner E. (1964) *Elementary Differential Equations*, Addison-Wesley, Reading.

Peyton B. M. (1992) *Kinetics of Biofilm Detachment.* Ph.D. Thesis, Department of Chemical Engineering, Montana State University, Bozeman, USA.

Rittmann B. E. (1982) The effect of shear stress on biofilm loss rate. *Biotechnol. Bioengng.* **24**, 501-506.

Rittmann B. E. and McCarty P. L. (1980a) Model of steady-state-biofilm kinetics. *Biotechnol. Bioengng.* **22**, 2343-2357.

Rittmann B. E. and McCarty P. L. (1980b) Evaluation of steady-state-biofilm kinetics. *Biotechnol. Bioengng.* **22**, 2359-2373.

Rittmann B. E. and McCarty P. L. (1981) Substrate flux into biofilm of any thickness. *J. Envir. Engng. Div.* **107**, 831-849.

Rittmann B. E., Crawford L. A., Tuck C. K. and Namkung E. (1986) *In situ* determination of kinetic parameters for biofilms: isolation and characterization of oligotrophic biofilms. *Biotechnol. Bioengng.* **28**, 1753-1760.

Sáez P. B. and Rittmann B. E. (1988) Improved pseudo-analytical solution for steady-state biofilm kinetics. *Biotechnol. and Bioengng.* **32**, 379-385.

Sáez P. B. and Rittmann B. E. (1992) Accurate pseudo-analytical solution for steady-state biofilms. *Biotechnol. Bioengng.* **39**, 790-793.

Skowlund C. T. (1990) Effect of biofilm growth on steady-state biofilm models. *Biotechnol. Bioengng.* **35**, 502-510.

Skowlund C. T. and Kirmse D. W. (1989) Simplified models for packed-bed biofilm reactors. *Biotechnol. Bioengng.* **33**, 164-172.

Stewart P. S. (1993) A model of biofilm detachment. *Biotechnol. Bioengng.* **41**, 111-117.

Suidan M. T., Rittmann B. E. and Traegner U. K. (1987) Criteria establishing biofilm-kinetic types. *Wat. Res.* **21**, 491-498.

Suidan, M. T. and Wang Y. T. (1985) Unified analysis of biofilm kinetics. *J. Envir. Engng.* **111**, 634-646.

Wanner O. and Gujer W. (1986) A multispecies biofilm model. *Biotechnol. Bioengng.* **28**, 314-321.

Chapter 6

GENERAL CONCLUSIONS AND
RECOMMENDATIONS

This thesis research represents a major effort towards rational process design and process analysis for biological drinking water treatment. Biological processes in drinking water treatment are basically of the biofilm type. The main objective of this research is to establish a framework based on the steady state biofilm model to enable mechanistic understanding and rational analysis of the performance of pilot or full scale biological drinking water treatment processes. The first phase of this research involved adapting the steady state biofilm model to plug flow biofilm reactors and then fitting it, using the pseudoanalytical solution of Sáez and Rittmann (1992), to AOC data from a pilot scale study. Three secondary objectives were derived from problems identified through the data fitting. The research was then extended to develop a more fundamental understanding of the steady state biofilm model.

PARAMETER ESTIMATION AND PROCESS ANALYSIS

It was found that the steady state biofilm model, with the pseudoanalytical solution of Sáez and Rittmann (1992) fitted AOC data from a pilot-scale biological drinking water treatment study, with adequate goodness-of-fit. Using the biofilm kinetic parameters estimated in the data fitting, it was found that the empirical linear relationship between AOC removal and influent AOC concentration observed in Huck et al. (1994) would be expected from the steady state biofilm model. The steady state biofilm model was then used as a framework to link process performance in terms of the slope of the linear relationship and process operating conditions and biodegradation kinetics.

Because the slope of the linear relationship (or approximate percentage AOC removal) is dimensionless, it enables the direct use of the dimensionless model derived for packed bed biofilm columns in Chapter 2 for process analysis. In the dimensionless domain, the number of factors involved in process analysis was reduced from ten to

four. Among the four factors, dimensionless detention time (X^*), which is directly proportional to the average detention time, is the determining factor for the value of the slope and therefore of the approximate percentage removal. The slope increases convexly with increasing X^*, and the extent of the convexity was found to be affected by three other factors: S_o^* (dimensionless influent substrate concentration), S_{min}^* (dimensionless minimum substrate concentration for sustaining a steady-state biofilm) and L^*/D^* (the ratio between dimentionless thickness of the effective diffusion layer and dimensionless substrate diffusivity).

The use of the steady state biofilm model requires that the substrate being modelled represents the primary substrate for growth. Although AOC has long been suspected by some researchers to be only a small portion of the total BOM, a recent survey involving a large number of water facilities across North America has found that AOC represents a substantial portion of the total BOM (as represented by BDOC). Although experimentally it is difficult to determine S_{min} precisely for a substrate parameter like AOC, it was found in this study that estimated S_{min} values were consistent and robust, despite the large variations of other parameters, which strongly suggests that S_{min} exists for AOC and that AOC can be regarded as a primary substrate.

Biofilm kinetic parameters for AOC are not available in the literature for comparison. K_s values estimated through the data fitting were found to be in the order of 10 mg acetate C equivalents/L. This is lower than the K_s value observed in wastewater treatment where the K_s value is typically in the order of 100 mg acetate C equivalents/L (Metcalf and Eddy, 1991). Bench scale experiments were further carried out under well controlled conditions (Chapter 3) to confirm the K_s values. K_s values estimated from the bench scale experiments were found to be generally consistent with those estimated from the pilot scale data. It appears that K_s is substantially higher than AOC concentrations normally experienced in biological drinking water treatment processes, therefore, the intrinsic AOC biodegradation kinetics can be approximated as first order.

The bench scale experiments also demonstrated the diauxic relationship between AOC-NOX and AOC-P17. It was found in the bench scale study that AOC-

NO^{-} is more easily biodegradable than AOC-P17 and that the intermediates of AOC-NOX degradation could be substrates for strain P17.

New Solution for the Steady-State Biofilm Model

Another major concern raised in the parameter estimation is that the biofilm thickness calculated from the estimated S_{min} (where S_{min} is based on the first order detachment assumption used to derive the pseudoanalytical solution of Sáez and Rittmann [1988, 1992]), was found to be unrealistically high. A review of various biofilm detachment kinetics present in the current literature demonstrated that the relationship between S_{min} and biofilm detachment kinetics and thus biofilm thickness can be very complex. Therefore, the unrealistically high prediction of biofilm thickness does not necessarily suggest that the S_{min} estimates are unrealistic; it may rather reflect the fact that biofilm detachment is not a simple first order process with respect to biomass in biological drinking water treatment processes.

In Chapter 4, a generalized definition of S_{min} was proposed to describe the complex relationships among biotransformation kinetics, biofilm detachment mechanisms and S_{min} and to provide flexibility to accommodate a variety of biofilm detachment mechanisms which may be simultaneously occurring in a biofilm. Because of the complexity of the biofilm detachment process phenomena, it may be impractical to calculate S_{min} from a complex combination of several biofilm detachment rate coefficients. It should rather be treated as an additional "biofilm kinetic parameter" and determined independently. Treating S_{min} as an independent biofilm kinetic parameter would allow the incorporation of alternative detachment kinetics into the concept of S_{min} without requiring a new approach to define S_{min}.

In an attempt to assess the impact of using the pseudoanalytical solution of Sáez and Rittmann (1992) in situations where biofilm detachment is not a simple first-order process, a new solution for J as a function of S_s and S_{min} was derived (Chapter 5), which requires no assumption concerning biofilm detachment kinetics. It was demonstrated that the impact of different biofilm detachment mechanisms on J is solely reflected through S_{min}. When S_{min} is treated as an independent biofilm kinetic parameter and determined through in-situ measurement or data fitting, instead of

calculated using biofilm detachment kinetics, biofilm detachment mechanisms would be "detached" from and thus have little impact on the function of J versus S_s and S_{min}. Therefore, it is reasonable to use the pseudoanalytical solution of Sáez and Rittmann (1992) so long as S_{min} is treated an independent parameter measured *in-situ* or otherwise estimated through data fitting, even though the first order detachment kinetics may predict unrealistic biofilm thicknesses from S_{min} values estimated from data-fitting.

The solution for the steady-state biofilm model devised in this thesis does not require any specific assumption with respect to biofilm detachment kinetics, and therefore can be used to replace the pseudoanalytical solution for biofilm with complex detachment kinetics. Although in strictly mathematical sense the new solution involves an approximation, this approximation is considered to have little impact on the calculation of substrate removal in all practical situations.

In the new solution, the effect of different biofilm detachment mechanisms on the flux is reflected through the S_{min} value, which, in turn, is a constant for a specific biofilm system and is defined by biofilm kinetics and biofilm detachment mechanisms. Because S_{min} is a biofilm parameter specific to each biofilm system, in engineering scale-up it would be the key parameter to be determined *in-situ*. A technique for *in-situ* determination of S_{min} is proposed in this thesis.

RECOMMENDATIONS FOR FUTURE RESEARCH

A critical problem remaining for the suitability of the steady-state biofilm model in modeling biological drinking water treatment processes is the large variation in the parameter estimates (other than S_{min}). Although the variation may be mainly attributable to the high K_s itself, other experimental untertainties may also have contributed to the variation. The long plug-flow biofilm columns used in the pilot-study made the response of effluent AOC concentration rather insensitive to the change of influent AOC concentration. For deep biofilm columns, substantially different kinetic parameters may predict little difference in effluent concentration. From a parameter estimation point of view, further investigations with plug flow biofilm reactors (at either bench or pilot scale) should use much shorter empty bed

-153-

contact time (probably 2 to 4 min) to achieve a more sensitive response of effluent substrate concentration to the change of influent substrate concentration. Such an experimental design should result in more precise estimates.

The intrinsic scatter of AOC data could be another experimental reason for the variation in parameter estimates. Further study of the error pattern of AOC data and further improvement in the precision of AOC measurement would help not only produce more precise parameter estimates but also enhance our understanding of and thus control over biological drinking water treatment processes.

Further efforts in confirming the high K_s values observed in this thesis would be especially valuable. Should K_s indeed be much higher than BOM concentrations normally experienced in drinking water treatment, the intrinsic biodegradation kinetics could be simplified as first-order. Biofilm modeling for packed-bed biofilm columns in biological water treatment could then be substantially simplified by using the analytical solution for first order transformation kinetics developed by Skowlund and Kirmse (1989). Precise estimates should then be obtainable for kX_f/K_s as a single first-order kinetic coefficient.

The bench scale technique developed in this thesis has the potential to allow determination of the kinetic parameters and AOC diffusivity prior to pilot/full scale studies. Parameters determined through bench scale experiments would help design focused and thus economical pilot/full scale studies by reducing the number of variables to be examined. Bench scale experiments also help to ensure that the biofilms are being examined under steady-state conditions versus the somewhat pseudosteady-state conditions occurring during pilot/full scale studies.

However, the bench scale technique requires a feedstock with high BOM concentration. In reality, high TOC water is rarely used as a drinking water source. To use the bench scale technique, raw water from the source under investigation should be concentrated to obtain the required level of TOC. Current natural water concentration techniques might result in a substantial loss of some portions of natural organics in the raw water and the concentrated water may not well represent the source water. An improved concentration technique is, therefore, required to obtain representative concentrated natural organic matter.

The generalized definition of S_{min} proposed in this thesis has yet to be verified experimentally. Experimental studies on *in-situ* determination of S_{min} would be required to further confirm the existence of S_{min} under different possible biofilm detachment mechanisms related to, for example, different bacterial species, substratum materials and/or hydrodynamic conditions. The relationship between S_{min} and biofilm detachment mechanisms would also be very valuable for better understanding of biofilm fundamentals and for controlling biofilm accumulation in drinking water distribution systems and other industrial aquatic systems.

In terms of practical application in the water industry, efforts should be made to establish a database which consolidates available pilot and full scale BOM data and to develop a (family of) typical curves(s) of percentage BOM removal versus the dimensionless detention time (X^*). From this information, it may be possible to develop a "rule of thumb" for the value of X^* required for a certain percent BOM removal. An example is presented in Appendix 4 to demonstrate how a typical curve of percentage BOM removal versus X^* can be used for designing a biofilm filter for a desired level of BOM removal.

REFERENCES

Huck P. M., Zhang S. and Price M. L. (1994) BOM removal during biologial treatment: a first order model. *J. Am. Wat. Wks. Ass.* **86**(6), 61-71.

Metcalf and Eddy, Inc. (1991) *Wastewater Engineering: Treatment, Disposal and Reuse*, 3rd edition, McGraw-Hill, New York.

Sáez P. B. and Rittmann B. E. (1988) Improved pseudo-analytical solution for steady-state biofilm kinetics. *Biotechnol. and Bioengng.* **32**, 379-385.

Sáez P. B. and Rittmann B. E. (1992) Accurate pseudo-analytical solution for steady-state biofilms. *Biotechnol. Bioengng.* **39**, 790-793.

Skowlund C. T. and Kirmse D. W. (1989) Simplified models for packed-bed biofilm reactors. *Biotechnol. Bioengng.* **33**, 164-172.

APPENDICES

APPENDIX 1: PILOT SCALE AOC DATA

Pilot Scale AOC Data (from Huck et al., 1991).

Summer / Fall - Winter

Sample Location	May 4* P17	NOX	Total	Jun.14 P17	NOX	Total	Jul.12 P17	NOX	Total	Aug.16 P17	NOX	Total	Aug.3 P17	NOX	Total	Sept.18 P17	NOX	Total	Oct.2 P17	NOX	Total	Oct.18 P17	NOX	Total
Post-Ozone Contactor 1	39	-	-	2	39	41	0.5	86	87	61	93	154	NG	6.3	6.3	NG	4.4	4.4	10	39	49	-	-	-
Post-Ozone Contactor 2	133	-	-	5	52	57	6	33	39	73	290	363	3.6	13	17	NG	9.3	9.3	16	30	46	4.2	26	30
Post-Filter 1	24	-	-	NG†	16	16	0.1	19	19	<0.1	22	22	0.04	6.9	6.9	-	-	-	0.01	11	11	-	-	-
Post-Filter 2	64	-	-	-	-	-	0.1	42	42	14	34	48	0.2	16	16	0.1	7.9	8.0	0.03	14	14	-	-	-
Post-Filter 3	124	-	-	-	-	-	1	33	34	<0.1	22	22	0.2	13	13	-	-	-	0.02	12	12	1.5	29	31
Post-Filter 4	182	-	-	-	-	-	12	100	112	<0.1	93	93	0.1	26	26	6.4	19	25	1.1	21	22.1	6.1	39	45
Post-GAC Contactor 1	26	-	-	-	-	-	8	3	11	13	3	16	5.5	0.3	5.8	-	-	-	-	-	-	-	-	-
Post-GAC contactor 2	18	-	-	-	-	-	20	6	26	14	4	18	4.8	1.0	5.8	0.2	4.3	4.5	0.02	7.1	7.12	-	-	-
Post-GAC contactor 3	33	-	-	-	-	-	11	5	16	9	2	11	5.2	0.2	5.4	-	-	-	1.2	2.9	4.1	0.05	2.2	2.3
Post-GAC contactor 4	21	-	-	-	-	-	3	8	11	8	4	12	5.8	1.4	7.2	0.1	4.6	4.7	4.5	8.6	13.1	0.04	5.8	5.8

(continued)

Fall - Winter (Continued)

Sample Location	Nov.1 P17	NOX	Total	Nov.15 P17	NOX	Total	Dec.12 P17	NOX	Total	Jan.03 P17	NOX	Total	Jan.17 P17	NOX	Total	Jan.31 P17	NOX	Total	Feb.14 P17	NOX	Total	Feb.28 P17	NOX	Total
Post-Ozone Contactor 1	5.2	23	28	2.8	25	28	1.0	37	38	0.02	11	11.0	3.3	30	33	25	35	60	36	53	89	21	66	87
Post-Ozone Contactor 2	5.8	19	25	1.4	39	40	1.2	37	38	0.01	11	11.0	3	24	27	27	56	83	35	91	126	-	-	-
Post-Filter 1	0.1	25	25	0.1	5.2	5.3	9.7	18	28	0.5	5.3	5.8	17	23	40	-	-	-	2.4	19	21	-	-	-
Post-Filter 2	0.3	16	16	0.2	7.8	8.0	12	18	30	0.4	10	10	17	24	41	21	19	40	32	23	55	21	25	46
Post-Filter 3	0.01	26	26	0.7	9.3	10	9.4	30	39	0.04	8.6	8.6	21	31	52	-	-	-	0.04	13	13	-	-	-
Post-Filter 4	5.5	14	20	3.9	16	20	13	44	57	0.2	15	15	1.5	48	50	5	49	54	32	86	118	27	77	104
Post-GAC Contactor 1	-	-	-	-	-	-	-	-	-	-	-	-	-	-	-	-	-	-	-	-	-	-	-	-
Post-GAC contactor 2	0.2	12	12	0.09	5.2	5.3	11	11	22	0.07	3.5	3.6	0.03	4.1	4.1	1.2	8.4	9.6	0.01	4.5	4.5	-	-	-
Post-GAC contactor 3	0.1	5.4	5.5	0.1	5.7	5.8	0.05	5.2	5.3	0.2	4.0	4.2	0.03	2.7	2.7	-	-	-	0.02	6.6	6.6	0.07	5.4	5.5
Post-GAC contactor 4	0.1	6.6	6.7	0.1	7.1	7.2	0.09	7.1	7.2	0.05	4.2	4.3	0.03	3.1	3.1	0.02	6.0	6.0	0.01	5	5.0	0.04	6.8	6.8

(continued)

Spring

Sample Location	Mar.8 P17	NOX	Total	Mar.14 P17	NOX	Total	Mar.21 P17	NOX	Total	Apr.4 P17	NOX	Total	Apr.11 P17	NOX	Total	Apr.25 P17	NOX	Total
Post-Ozone Contactor 1	279	260	539	39	91	130	109	190	299	30	95	125	17	71	88	35	93	128
Post-Ozone Contactor 2	242	298	540	44	146	190	99	269	368	57	105	162	28	93	121	32	119	151
Post-Filter 1	-	-	-	28	37	65	33	75	108	3.9	38	42	1.0	52	53	17	29	46
Post-Filter 2	-	-	-	37	49	86	46	91	137	14	59	73	31	50	81	20	34	54
Post-Filter 3	-	-	-	32	50	82	42	136	178	16	37	53	25	60	85	1.4	41	42
Post-Filter 4	-	-	-	36	124	160	88	245	333	36	148	184	19	119	138	20	86	106
Post-GAC Contactor 1	-	-	-	23	7.1	30	18	4.0	22	14	5.4	19	7.7	8.4	16	10	1.2	11
Post-GAC contactor 2	-	18	20	0.1	10	10	28	31	59	1.4	25	26	0.04	18	18	32	22	54
Post-GAC contactor 3	1.7	18	20	0.1	8.1	8.2	22	20	42	1.6	22	24	0.04	16	16	16	10	26
Post-GAC contactor 4	0.6	19	20	0.2	12	12	35	41	76	1.5	30	32	0.1	27	27	5.9	24	30

* Dates are 1989 - 1990; strains P17 and NOX added simultaneously except on May 4 when only strain P17 was used; all results expressed as µg acetate C eq/L.
† No growth.

APPENDIX 2: SYSTAT OUTPUT - PEARSON CORRELATION ANALYSIS

SYSTAT VERSION 5.0
COPYRIGHT, 1990-1992
SYSTAT, INC.

WELCOME TO SYSTAT!
WORKSPACE CLEAR FOR CREATING NEW DATASET
SYSTAT FILE VARIABLES AVAILABLE TO YOU ARE:

INFF1	EFFF1	INFF2	EFFF2	INFC2
EFFC2	INFC3	EFFC3	INFC4	EFFC4

SAT 3/25/95 3:16:41 PM   C:\THESIS\DEFENSE\AOC.SYS

PEARSON CORRELATION MATRIX

           INFF1   EFFF1

INFF1   1.000
EFFF1   0.837   1.000

BARTLETT CHI-SQUARE STATISTIC: 15.057 DF=   1 PROB= .000
NUMBER OF OBSERVATIONS: 15

PEARSON CORRELATION MATRIX

           INFF2   EFFF2

INFF2   1.000
EFFF2   0.906   1.000

BARTLETT CHI-SQUARE STATISTIC: 24.883 DF=   1 PROB= .000
NUMBER OF OBSERVATIONS: 17

PEARSON CORRELATION MATRIX

                INFC2   EFFC2

    INFC2   1.000
    EFFC2   0.668   1.000

BARTLETT CHI-SQUARE STATISTIC: 8.572 DF=   1 PROB= .003
NUMBER OF OBSERVATIONS: 17

PEARSON CORRELATION MATRIX

                INFC3   EFFC3

    INFC3   1.000
    EFFC3   0.761   1.000

BARTLETT CHI-SQUARE STATISTIC: 12.527 DF=   1 PROB= .000
NUMBER OF OBSERVATIONS: 17

PEARSON CORRELATION MATRIX

                INFC4   EFFC4

    INFC4   1.000
    EFFC4   0.870   1.000

BARTLETT CHI-SQUARE STATISTIC: 23.302 DF=   1 PROB= .000
NUMBER OF OBSERVATIONS: 19

APPENDIX 3: FORTRAN PROGRAMS AND OUTPUT SAMPLES

FORTRAN 77 Program for Plug Flow Biofilm Columns

```
C****************************************************************
            PROGRAM BOMSEARCH I
C         ~~~~~~~~~~~~~~~~~~~~~~~~~~~~~
C              EDITTED BY
C              SHULIN ZHANG
C       ENVIRONMENTAL ENGINEERING AND SCIENCE
C         DEPARTMENT OF CIVIL ENGINEERING
C             UNIVERSITY OF ALBERTA
C
C             OCTOBER, 1992
C
C****************************************************************
C    THIS IS A PROGRAM DESIGNED FOR SEARCHING OPTIMIZED
C    PARAMETERS, KXF, KS, DL AND SMIN, WITH GIVEN INFLUENT
C    AND EFFLUENT BOM (AOC/BDOC) CONCENTRATIONS FOR PLUG
C    FLOW TYPE BIOFILM COLUMNS USING SIMPLEX ALGORITHM
C    (IMSL MATH/LIBRARY:872-74).
C****************************************************************
C
C                   VARIABLE DECLARATION
      IMPLICIT  REAL*8  (A-H,L,O-Z)
      PARAMETER  (N=4,NT=17)
C           N = NUMBER OF PARAMETER TO BE OPTIMIZED
C              NT = NUMBER OF OBSERVATIONS
      DIMENSION  SB(NT), SE(NT), LF(NT), SEC(NT),
     &      X(N),XGUESS(N),XLB(N),XUB(N)
C
      COMMON  /IO/DP,E,H,V,A,L,HR,T,SB, SE, SEC, LF,SSR
      EXTERNAL DBCPOL, ROSBRK, UMACH
C
C                   INITIALIZATIONS
```

```
C                    SEARCHING DOMAIN IS SET AS:
C                    KXF (1.D3 - 7.D5)
C                    KS  (1.D0 - 1.D5)
C                    DL  (1.D-5 - 1.5D-4)
C                    SMIN(1.0D-2- 27.9)
      DATA XLB/1.0D3,1.,1.0D-5,1.0D-2/,XUB/5.0D5,5.0D4,1.0D-4,27.9/
C                         PROVIDE INITIAL GUESSES IN (KXF, KS, DL, SMIN)
      DATA XGUESS/4.0D5,1.0D3,4.0D-5,5.0/
C
C                         REPORT INITIALIZATION SETTINGS
      WRITE (6,3) XGUESS,XUB,XLB
3     FORMAT (/,' THE ININTIAL GUESS IS (',4(2X,D10.3),' )',/,
     &      ' THE UPPER BOUND IS   (',4(2X,D10.3),' )',/,
     &      ' THE LOWER BOUND IS   (',4(2X,D10.3),' )',/)
C
C                         PROVIDE PARAMETER INPUTS
C          PHYSICAL PARAMETERS: DP IN MM; E DIMENSIONLESS;
C                               H IN M; V IN M/DAY
      READ (5,*) DP, E, H, V
C          INPUT INFLUENT AND EFFLUENT AOC IN MICROGRAM/L
      READ (5,*) (SB(II),SE(II),II=1,NT)
C
C                         SET CONVERGENCE CRITERIA
      IBTYPE = 0
      FTOL = 1.0E-9
      MAXFCN =30000
C
C                         CALL IMSL "COMPLEX"-DBCPOL
C                         OPTIMIZATION SUBROUTINE
      CALL DBCPOL(ROSBRK,N,XGUESS,IBTYPE,XLB,XUB,FTOL,
     1       MAXFCN,X,F)
C
      CALL UMACH (2, NOUT)
C
```

```
C                         OUTPUT OPTIMIZED PARAMETERS
      WRITE (NOUT, 4) X,F
4     FORMAT (' THE SOLUTION IS (',4(2X,D10.3),' )',/,
     1' THE FUNCTION VALUE IS ',D15.8)
C
C             REFRESH CONC PROFILE WITH OPTIMIZED PARAMETERS
      CALL BOM (X(1), X(2), X(3), X(4))
C                 CHECK SUM OF SQUARED RESIDUALS
      WRITE (6,5) SSR
5     FORMAT (' THE SUM OF SQUARED RESIDUALS IS ',F10.3)
C
C             CALCULATE K FROM OPTIMIZED KXF FOR XF=30,000MG/L
      XF=30000.
      FK=X(1)/(XF*1000.)
      RKKS=FK/X(2)
C
C                         OUTPUT BEST-FIT PROFILE
      WRITE (6,6) A,T,L,HR,X(1),X(2),X(3),X(4),FK,RKKS
6     FORMAT (/,2X,'A=',F10.3,4X,'T=',D10.3,3X,'L=',D10.3,
     1     3X,'XR=',F10.3,/,2X,'KXF=',D10.3,
     2     2X,'KS=',D10.3,2X,'DL=',D10.3,2X,'SMIN=',F8.3,/,
     3     2X,'K= ',D10.3,2X,'K/KS=',D10.3,
     4     /,21(2X,'*'))
      WRITE (6,8)
8     FORMAT (/,10X, 'SB',9X,'SEC',10X,'SE',10X,'LF',/)
      WRITE (6,9) (SB(II),SEC(II),SE(II),LF(II),II=1,NT)
9     FORMAT (2X,F10.3,',',1X,F10.3,',',1X,F10.3,',',3X,D10.3,',')
C
      STOP
      END
C****************************************************************
C                 EXTERNAL FUNCTION TO BE MINIMIZED
C****************************************************************
      SUBROUTINE ROSBRK (N,X,F)
```

```fortran
      IMPLICIT REAL*8  (A-H,L,O-Z)
      DIMENSION      X(N)
      COMMON /OBJECTIVE/SUM
C
      CALL BOM (X(1), X(2), X(3), X(4))
      F=SUM
C    PRINT *, F
      RETURN
      END
C*********************************************************************
*
C        A SUBROUTINE TO CALCULATE THE SUM OF SQUARED
C        RESIDUALS FOR GIVEN PARAMETERS
C*********************************************************************
*
      SUBROUTINE BOM (XFK, SK, DL, SMIN)
C
      IMPLICIT REAL*8  (A-H,L,O-Z)
      PARAMETER (NT=17)
      DIMENSION SB(NT), SE(NT), LF(NT), SEC(NT)
      COMMON /IO/DP,E,H,V,A,L,HR,T,SB, SE, SEC, LF,SSR
      COMMON /OBJECTIVE/SUM
      COMMON SMINR, LR, DR
      COMMON /IR/ SSIR
      COMMON /ER/ CXR, CSSER
      EXTERNAL RJ
C
C                   RESET SUM OF RESIDUAL AS ZERO
      SUM=0.0
      SSR = 0.0
C                   CALCUALTE A IN M-1
      A=0.9*1.5*(1-E)*6000./(1.2*DP/1.4)
C
      DR=1/0.8
```

```fortran
      DF=DL/DR
      VIS=1.306E-6
C                 VIS IS THE KINETIC VISCOCITY OF WATER IN M2S-1
C                 THE VALUE IS BASED ON AN AVERAGE TEMP OF 8OC
      R=V*DP/(VIS*24*3600*1000)
      SC=VIS*24*3600/DL
      L=DP/(1000*(2.+0.644*R**0.5*SC**(1./3.))*(1+1.5*(1-E)))
      SMINR=SMIN/SK
      T=DSQRT(SK*DF/XFK)
C     PRINT *, 'T= ',T
      LR=L/T
      HR=(H*A*DF)/(V*T)
      CXR=HR
C                 TO START DO LOOP TO SEARCH SEC FOR
C                       EACH GIVEN SB
      DO 10 II=1,NT
      SBR=SB(II)/SK
      IF (SBR.LE.SMINR) THEN
      SEC(II) = SB(II)
      LF(II) = 0.0
      GOTO 13
      END IF
      CALL ROOT(SBR)
C                       TO CALCULATE LF(II)
      LF(II)=T*RJ(SSIR)/(SMINR/(1+SMINR))
C
      CALL INTE (SSIR)
C                       TO FIND OUT SEC(II)
      SEC(II)=(CSSER+(LR/DR)*RJ(CSSER))*SK
C                 CALCULATE CURRENT RESIDUAL
13    RES = DLOG(SE(II))-DLOG(SEC(II))
C13   RES = (SE(II)-SEC(II))/SE(II)
      RES2 = DABS(RES)
      SUM =SUM+RES2
```

```
      SSR =SSR+(SEC(II)-SE(II))**2
10    CONTINUE
      RETURN
      END
C***************************************************************
C    A SUBROUTINE TO FIND INFLUENT SS (SSIR) THROUGH ROOT
C    SEARCHING
C***************************************************************
      SUBROUTINE ROOT (SBIR)
C
      IMPLICIT REAL*8  (A-H,L,O-Z)
      COMMON SMINR, LR, DR
      COMMON /IR/ SSIR
      EXTERNAL RJ
C                    THE IMPLICIT FUNCTION SB=SS+J(SS)*L/D
      FS (SS) = SBIR-SS-(LR/DR)*RJ(SS)
C
C                    SET CONVERGENCE CRITERIA
      EPS3=1.J  7
      KMAX=10
C                    SET INITIAL VALUES
      SS1=SMINR
      SS3=SBIR
      K=0
      D=SBIR-SMINR
C
100   F3 = FS (SS3)
      SS2 = (SS1+SS3)/2
      F2 = FS (SS2)
C                    CONVERGENCE TEST
      IF (D.LT.(EPS3*SMINR)) THEN
      SSIR = SS2
      GOTO 200
C                    CHECK FOR CROSSING IN RIGHT HALF
```

-169-

```
      ELSE IF (F2*F3.LT.0.) THEN
      D=(SS3-SS2)
      F1=F2
      SS1=SS2
C                           OR IN THE LEFT HALF
      ELSE IF(F2*F3.GT.0.) THEN
      D=(SS2-SS1)
      F3=F2
      SS3=SS2
C                           OR F2=0.0 OR ERROR
      ELSE IF (F2.EQ.0.0) THEN
      PRINT *, 'FS(',SS2,') IS IDENTICALLY ZERO'
      PRINT *, 'K=', K
      STOP
      ELSE
      PRINT *, 'THE CURRENT INTERVAL', SS1, 'TO', SS3
      PRINT *, 'ERROR, NO ROOT'
      STOP
      END IF
C                           INCREMENT ITERATIONS
      K = K+1
      IF (K.GT.KMAX) THEN
      PRINT *, 'FAILURE TO CONVERGE AT K=1000'
      STOP
      ELSE
      GOTO 100
      END IF
C                           END OF ROOT SEARCHING
200   RETURN
      END
C***********************************************************************
C        AN INTEGRATOR TO CALCULATE SSER FOR A GIVEN CXR
C***********************************************************************
      SUBROUTINE INTE(SSI)
```

```
C
      IMPLICIT REAL*8  (A-H,L,O-Z)
      COMMON SMINR,LR, DR
      COMMON /ER/CXR,CSSER
      EXTERNAL FX, RJ, DQDAG, UMACH
C
C               SET ENDING CRITERIA
      EPS1 = 2.0D-7
      JMAX=50
C               SET INITIAL VALUES
      J=0
      S1 = SSI
      S3 = SMINR
C
1000  DSSR = DABS(S1-S3)
      IF (DSSR.LT.(SMINR*EPS1))THEN
      S2=(S1+S3)/2
      CSSER = S2
      GOTO 6000
      ELSE IF (J.GT.JMAX) THEN
      PRINT *, 'J SHOULD NOT EXCEED JMAX, TRY GREATER JMAX'
      STOP
      ELSE
      S2 = (S1+S3)/2
      END IF
C
      SSE = S2
      EPS2 = 5.D-7
C
C                    AN IMSL INTEGRATION SUBROUTINE-DQDAG
      ERRABS = 0.0
      ERRREL = 1.0D-6
      IRULE = 3
      CALL UMACH(2, NOUT)
```

```fortran
      CALL DQDAG (FX, SSE, SSI, ERRABS, ERRREL,IRULE,
     i       RESULT, ERREST)
      XR=RESULT+(LR/DR)*(DLOG(RJ(SSI))-DLOG(RJ(SSE)))
      ERROR = DABS(XR-CXR)
C
C                         CONVERGENCE TEST
      IF (ERROR.LE.(EPS2*CXR)) THEN
      CSSER = SSE
C     WRITE (NOUT, 9999) RESULT, EXACT, ERREST, ERROR
9999  FORMAT (25(2X,'*'),/,2X,'COMPUTED=',F8.3,13X,'EXACT=',F8.3,/,
     1     2X,'ERROR ESTIMATE =', D10.3, 6X, 'ERROR =', D10.3)
      GOTO 6000
      ELSE IF(XR.LT.CXR) THEN
      S1 = S2
      ELSE IF(XR.GT.CXR) THEN
      S3 = S2
      END IF
      J = J+1
      GOTO 1000
C
6000  RETURN
      END
C**********************************************************************
C                 DECLARE EXTERNAL FUNCTIONS
C**********************************************************************
C
C**********************************************************************
C                 FUNCTION2 - 1/J(SS) FOR INTEGRATION
C**********************************************************************
      FUNCTION FX (S)
      IMPLICIT REAL*8 (A-H,L,O-Z)
      COMMON SMINR
      EXTERNAL RJ
C
```

```fortran
      FX = 1/RJ(S)
      RETURN
      END
C*********************************************************************
C                    FUNCTION1 - J = F(SS)
C            THE PSEUDO-ANALYTICAL SOLUTION FOR STEADY-STATE
C            BIOFILM MODEL FROM SAEZ AND RITTMANN (1992).
C*********************************************************************
      FUNCTION RJ (S)
      IMPLICIT REAL*8 (A-H,L,O-Z)
      COMMON SMINR
C
      RJ =DSQRT(2.0*(S-DLOG(1.0+S)))*DTANH((1.5557-0.4117*
     1 DTANH(DLOG10(SMINR)))*(S/SMINR-1.0)**(0.5035-0.0257*
     2 DTANH(DLOG10(SMINR))))
      RETURN
      END
```

Output Sample for Plug Flow Biofilm Columns

<u>COMPUTATION OUTPUT FOR FILTER 2 WITH DF/D=0.8</u>

THE INITIAL GUESS IS (0.400E+06   0.100E+04   0.400E-04   0.500E+01)
THE UPPER BOUND IS   (0.500E+06   0.500E+05   0.100E-03   0.279E+02)
THE LOWER BOUND IS   (0.100E+04   0.100E+01   0.100E-04   0.100E-01)

THE SOLUTION IS   (0.312E+06   0.138E+05   0.467E-04   0.100E+02)
THE FUNCTION VALUE IS 0.62197675E+01
THE SUM OF SQUARED RESIDUALS IS   5468.501

A= 6160.711   T= 0.128E-02   L= 0.342E-04   XR=   0.560
KXF= 0.312E+06   KS= 0.138E+05   DL= 0.467E-04   SMIN= 10.000
K= 0.104E-01   K/KS= 0.754E-06

* *

SB	SEC	SE	LF
87.000,	50.336,	42.000,	0.109E-01,
154.000,	89.150,	48.000,	0.193E-01,
6.300,	6.300,	16.000,	0.000E+00,
4.400,	4.4	8.000,	0.000E+00,
49.000,	28..	14.000,	0.616E-02,
28.000,	16.520,	16.000,	0.349E-02,
28.000,	16.520,	8.000,	0.349E-02,
38.000,	22.102,	30.000,	00.477E-02
11.000,	10.000,	10.000,	0.695E-03,
33.000,	19.282,	41.000,	0.413E-02,
60.000,	34.727,	40.000,	0.754E-02,
89.000,	51.494,	55.000,	0.112E-01,
130.000,	75.239,	86.000,	0.163E-01,
299.000,	173.332,	137.000,	0.374E-01,
125.000,	72.342,	73.000,	0.157E-01,

88.000,   50.915,   81.000,   0.111E-01,
128.000,   74.080,   54.000,   0.161E-01,

FORTRAN77 Program for Dimensionless Process Analysis

```
C****************************************************************
            PROGRAM LINEARITY
C           ~~~~~~~~~~~~~~~~~~~
C               EDITTED BY
C               SHULIN ZHANG
C         ENVIRONMENTAL ENGINEERING AND SCIENCE
C           DEPARTMENT OF CIVIL ENGINEERING
C              UNIVERSITY OF ALBERTA
C
C               JANUARY 1993
C****************************************************************
C     THIS IS A PROGRAM  DESIGNED  FOR DIMENSIONLESS PROCESS
C         ANALYSIS FOR PLUG FLOW TYPE BIOFILM COLUMNS
C****************************************************************
*
C
      IMPLICIT REAL*8  (A-H,L,O-Z)
      PARAMETER (NS=11,NX=8)
      DIMENSION SBR(NS), XR(NX), SER(NS,NX), FLUX0(NS)
      COMMON SMINR, CSSER, CXR, LR, DR
C
C               FUNCTION SENTENCES
C          PSEUDO-ANALYTICAL SOLUTION FOR STEADY-STATE
C          BIOFILM MODEL FROM SAEZ AND RITTMANN (1992).
C
      FLUXR(SS) =DSQRT(2*(SS-DLOG(1+SS)))*DTANH((1.5557-0.4517*
     1 DTANH(DLOG10(SMINR)))*(SS/SMINR-1)**(0.5035-0.0257*
     2 DTANH(DLOG10(SMINR))))
C
      FS (SS) =SBR(II)-SS-(LR/DR)*FLUXR(SS)
C
      SMINR=1.0D-3
```

```fortran
      DR=2.00
      LR=5.D-2
C                    START TO FIND ROOT-SSIR
      EPS3=1.D-9
      KMAX=1000
C                TO START DO LOOP TO SEARCH SEC FOR
C                EACH GIVEN SB
      DO 2 II=1,NS
      SBR(II)=SMINR+10D-3*10**(0.5*(II-7))
      SS1=SMINR
      SS3=SBR(II)
      K=0
      D0=SBR(II)-SMINR
      D=1
C
100   F1 = FS (SS1)
      F3 = FS (SS3)
      SS2 = (SS1+SS3)/2
      F2 = FS (SS2)
C                    CONVERGENCE TEST
      IF (D.LT.EPS3) THEN
      DO 3 JJ=1,NX
      XR(JJ)=0.2*2**(JJ-2.)
      CXR = XR(JJ)
      CALL INTE (SS2)
C                    TO FIND OUT SEC(II)
      IF (JJ.EQ.1) THEN
C
C
      FLUX0(II) = FLUXR(CSSER)
      END IF
      SER(II,JJ)=CSSER+(LR/DR)*FLUXR(CSSER)
3     CONTINUE
      GOTO 2
```

```
C
      ELSE IF (K.GT.KMAX) THEN
      PRINT *, 'FAILURE TO CONVERGE AT K=100'
      STOP
      END IF
C              CHECK FOR CROSSING IN LEFT HAND
      IF (F1*F2.LT.0.) THEN
      D=(SS2-SS1)/D0
      F3=F2
      SS3=SS2

C              OR IN THE RIGHT HALF
      ELSE IF(F2*F3.LT.0.) THEN
      D=(SS3-SS2)/D0
      F1=F2
      SS1=SS2
C              OR F2=0.0 OR ERROR
      ELSE IF (F2.EQ.0.0) THEN
      PRINT *, 'FS(',SS2,') IS IDENTICALLY ZERO'
      PRINT *, 'K=', K
      STOP
      ELSE
      PRINT *, 'THE CURRENT INTERVAL', SS1, 'TO', SS3
      PRINT *, 'ERROR, NO ROOT'
      STOP
      END IF
C              INCREMENT ITERATIONS
      K=K+1
      GO TO 100
C              THE END OF ROOT SEARCHING
2     CONTINUE
C
      WRITE (6,6) (XR(JJ), JJ=1,NX)
6     FORMAT (18X, 8(E8.3,','))
```

```fortran
      DO 5 II=1,NS
      WRITE (6,4) SBR(II),FLUX0(II), (SER(II,JJ), JJ=1,NX)
4     FORMAT (10(E8.3,','))
5     CONTINUE
      STOP
      END
C*******************************************************************
C          AN INTEGRATOR TO CALCULATE SSER FOR A GIVEN CXR
C*******************************************************************
      SUBROUTINE INTE(SSIR)
C
      IMPLICIT REAL*8 (A-H,L,O-Z)
      COMMON SMINR, CSSER, CXR, LR, DR
      EXTERNAL  FX, DQDAG, UMACH
C                    DIMENSIONLESS FLUX FUNCTION
      RJ(SS) =DSQRT(2*(SS-DLOG(1+SS)))*DTANH((1.5557-0.4117*
     1  DTANH(DLOG10(SMINR)))*(SS/SMINR-1)**(0.5035-0.0257*
     2  DTANH(DLOG10(SMINR))))
C
      EPS1 = 1.0D-7
      JMAX=50
      J=0
      S1 = SSIR
      S3 = SMINR
10    DSSR = (S1-S3)
      IF (DSSR.LT.(SMINR*EPS1))THEN
      CSSER = S3
      GOTO 60
      ELSE IF (J.GT.JMAX) THEN
      PRINT *, 'J SHOULD NOT EXCEED JMAX, TRY GREATER JMAX'
      STOP
      ELSE
      S2 = (S1+S3)/2
      END IF
```

```fortran
C
      SSER = S2
      EPS2 = 1.D-5
C
C                   AN IMSL INTEGRATION SUBROUTINE-DQDAG
      ERRABS = 0.0
      ERRREL = 1.0D-6
      IRULE = 6
      CALL UMACH(2, NOUT)
      CALL DQDAG (FX, SSER, SSIR, ERRABS, ERRREL,IRULE,
     1          RESULT, ERREST)
      XR=RESULT+(LR/DR)*DLOG(RJ(SSIR)/RJ(SSER))
      ERROR = DABS(XR-CXR)
C
C                       CONVERGENCE TEST
      IF (ERROR.LE.(EPS2*CXR)) THEN
      CSSER = SSER
C     WRITE (NOUT, 9999) RESULT, EXACT, ERREST, ERROR
9999  FORMAT (25(2X,'*'),/,2X,'COMPUTED=',F8.3,13X,'EXACT=',F8.3,/,
     1     2X,'ERROR ESTIMATE =', E10.3, 6X, 'ERROR =', E10.3)
      GOTO 60
      ELSE IF(XR.LT.CXR) THEN
      S1 = S2
      ELSE IF(XR.GT.CXR) THEN
      S3 = S2
      END IF
      J = J+1
      GOTO 10
C
60    RETURN
      END
C**********************************************************************
C                   DECLARE EXTERNAL FUNCTION
C**********************************************************************
```

```fortran
C
      SSER = S2
      EPS2 = 1.D-5
C
C                   AN IMSL INTEGRATION SUBROUTINE-DQDAG
      ERRABS = 0.0
      ERRREL = 1.0D-6
      IRULE = 6
      CALL UMACH(2, NOUT)
      CALL DQDAG (FX, SSER, SSIR, ERRABS, ERRREL,IRULE,
     1          RESULT, ERREST)
      XR=RESULT+(LR/DR)*DLOG(RJ(SSIR)/RJ(SSER))
      ERROR = DABS(XR-CXR)
C
C                       CONVERGENCE TEST
      IF (ERROR.LE.(EPS2*CXR)) THEN
      CSSER = SSER
C     WRITE (NOUT, 9999) RESULT, EXACT, ERREST, ERROR
9999  FORMAT (25(2X,'*'),/,2X,'COMPUTED=',F8.3,13X,'EXACT=',F8.3,/,
     1     2X,'ERROR ESTIMATE =', E10.3, 6X, 'ERROR =', E10.3)
      GOTO 60
      ELSE IF(XR.LT.CXR) THEN
      S1 = S2
      ELSE IF(XR.GT.CXR) THEN
      S3 = S2
      END IF
      J = J+1
      GOTO 10
C
60    RETURN
      END
C**********************************************************************
C                   DECLARE EXTERNAL FUNCTION
C**********************************************************************
```

```fortran
FUNCTION FX (X)
IMPLICIT REAL*8 (A-H,L,O-Z)
COMMON SMINR
FX =1/(DSQRT(2*(X-DLOG(1+X)))*DTANH((1.5557-0.4117*
1  DTANH(DLOG10(SMINR)))*(X/SMINR-1)**(0.5035-0.0257*
2  DTANH(DLOG10(SMINR)))))
RETURN
END
```

```
C******************************************************************
               PROGRAM BOMSEARCH II
C              _____
C                   EDITTED BY
C                   SHULIN ZHANG
C          ENVIRONMENTAL ENGINEERING AND SCIENCE
C             DEPARTMENT OF CIVIL ENGINEERING
C                UNIVERSITY OF ALBERTA
C
C                   OCTOBER, 1993
C
C******************************************************************
C    THIS IS A PROGRAM  DESIGNED FOR  SEARCHING  OPTIMIZED
C    PARAMETERS,  KXF, KS, DL AND SMIN, FOR CSTR TYPE BENCH
C    SCALE BIOFILM REACTORS  WITH  GIVEN BOM (AOC/BDOC) FLUX
C    AND EFFLUENT CONCENTRATION USING ERROR-IN-VARIABLES
C    TECHNIGUE (TECHNIMETRICS, 23(3): 221-31) COUPLED WITH
C    SIMPLEX METHOD (IMSL MATH/LIBRARY: 847-51).
C******************************************************************
**
C
C                   VARIABLE DECLARATION
     IMPLICIT  REAL*8  (A-H,O-Z)
     PARAMETER  (NT=9,N=4)
C              N  = NUMBER OF PARAMETERS TO BE OPTIMIZED
C              NT = NUMBER OF OBSERVATIONS
     DIMENSION  SE(NT), SS(NT), TL(NT), FLUX(NT),DJ(NT),DS(NT),
     & SEC(NT),FLUXC(NT),V(NT),X(N),XGUESS(N),
     & XLB(N),XUB(N),RXG(N-1)
     COMMON /C1/V,T,TL,FLUX,FLUXC,DJ,SE,SEC,DS,SS,RES2,DR
     EXTERNAL DBCPOL, ROSBCK, UMACH
```

```
C
C                        INPUT PHYSICAL PARAMETERS
      DR=1.0/0.5
      READ (5,*) (FLUX(I),DJ(I),SE(I),DS(I),V(I), I=1,NT)
C                             INITIALIZATIONS
C   XGUESS = (KXF, KS, DL, SMIN)
      DATA XGUESS/1.D7,6.D3,1.3D-4,10./
      DATA XLB/5.D1,4.5D3,0.1D-4,1./,XUB/1.0D8,1.0D5,1.4D-4,18./
C
C                        PRINT OUT THE INITIAL GUESS
      WRITE (6,5) XGUESS(1),XGUESS(2),XGUESS(3),XGUESS(4),
     1          XLB(1), XLB(2), XLB(3), XLB(4),
     2          XUB(1), XUB(2), XUB(3), XUB(4)
5     FORMAT (/,' THE ININTIAL GUESS ARE (',4(2X,E10.3),' )',
     1        /,' THE LOWER BOUNDS ARE   (',4(2X,E10.3),' )',
     2        /,' THE UPPER BOUNDS ARE   (',4(2X,E10.3),' )',/)
C                        SET INITIAL GUESS FOR "REAL" VALUES
      DO 1 I1=1,NT
      SEC(I1)=SE(I1)
      FLUXC(I1)=FLUX(I1)
1     CONTINUE
C
C                        SET MAXIMUM ITERATION NUMBER
      I2MAX = 200
      I2=0
3     I2=I2+1
C                        START A NEW ITERATION
C                        ALL THE BOUNDS ARE PROVIDED
      IBTYPE = 0
C                        SET ENDING CRITERIA
      FTOL = 1.D-5
      MAXFCN = 10000
C                        CALL IMSL "COMPLEX"-DBCPOL
C                        OPTIMIZATION SUBROUTINE
```

```
      CALL DBCPOL(ROSBCK,N,XGUESS,IBTYPE,XLB,XUB,FTOL,
     1       MAXFCN,X,F)
C                            PRINT RESULTS
      CALL UMACH (2, NOUT)
C                         OUTPUT OPTIMIZED PARAMETERS
      WRITE (NOUT, 7) X,F,RES2
7     FORMAT (' THE SOLUTION IS (',4(2X,D10.3),' )',//,
     1' THE FUNCTION VALUE IS ',D15.3,/,
     2' THE SUM OF RESIDUAL IS',10X, D10.3,/)
C
C                            TEST CONVERGENCE
C                            SET TOLERANT LIMIT
      EP=1.D-4
C                            CALCULATE ERRORS
      ER1 = DABS((X(1)-XGUESS(1))/XGUESS(1))
      ER2 = DABS((X(2)-XGUESS(2))/XGUESS(2))
      ER3 = DABS((X(3)-XGUESS(3))/XGUESS(3))
      ER4 = DABS((X(4)-XGUESS(4))/XGUESS(4))
C
      IF (ER1.LE.EP.AND.ER2.LE.EP.AND.ER3.LE.EP.AND.ER4.LE.EP) THEN
      GOTO 11
      ELSE IF (I2.GT.I2MAX) THEN
      PRINT *, 'TOTAL ITERATION EXCEED ',I2MAX
      GOTO 11
      ELSE
C                  CALL SUBROUTINE TO RENEW "REAL" VALUES
      CALL NEW(X(1), X(2), X(3), X(4))
C                  RENEW XGUESS
      DO 9 I3=1,N
      XGUESS(I3)=X(I3)
9     CONTINUE
      GOTO 3
      END IF
C
```

```
C                         CALCULATE BEST-FIT PROFILE
11   CALL NEW (X(1), X(2), X(3), X(4))
     XF=30000
     FK=X(1)/(XF*1000)
C                         CALCULATE K FROM OPTIMIZED KXF
C                         OUTPUT BEST-FIT PROFILE
     WRITE (6,13) T,X(1),X(2),X(3),X(4),FK
13   FORMAT (/,2X,'T=',D10.3,3X,
   1     'KXF=',D10.3,
   2     2X,'KS=',D10.3,2X,'DL=',D10.3,/,2X,'SMIN=',F8.3,
   3     2X,'K= ',E10.3,
   4     /,21(2X,'*'))
     WRITE (6,15)
15   FORMAT (/,10X, 'SE',11X,'SEC',9X,'FLUX',8X,'FLUXC',11X,'L',
   &        11X,'SS'/)
     WRITE (6,17) (SE(I4),SEC(I4),FLUX(I4),FLUXC(I4),TL(I4),SS(I4),
   &        I4=1,NT)
17   FORMAT (2X,D10.3,',',2X,D10.3,',',2X,D10.3,',',2X,D10.3,',',
   &        2X,D10.3,',',2X,D10.3,',')
     STOP
     END
C***************************************************************
C                 EXTERNAL FUNCTION TO BE MINIMIZED
C***************************************************************
     SUBROUTINE ROSBCK (N,X,F)
     IMPLICIT REAL*8   (A-H,O-Z)
     DIMENSION X(N)
     COMMON /C2/SUM
C
     CALL BOM (X(1), X(2), X(3), X(4))
     F = SUM
     RETURN
     END
```

```
C*****************************************************************
C          A SUNBROUTINE TO CALCULATE THE SUM OF SQUARED
C          RESIDUALS FOR GIVEN PARAMETERS
C*****************************************************************
      SUBROUTINE BOM (XFK, SK, DL, SMIN)
C
      IMPLICIT   REAL*8  (A-H,O-Z)
      PARAMETER (NT=9)
      DIMENSION SE(NT),SEC(NT),TL(NT),V(NT),FLUX(NT),FLUXC(NT),
     &          SS(NT),DJ(NT),DS(NT),HJ(NT)
      COMMON /C1/V,T,TL,FLUX,FLUXC,DJ,SE,SEC,DS,SS,RES2,DR
      COMMON /C2/SUM
      EXTERNAL G, GJ, GS
C
C                    SETTING VALUES FOR CONSTANTS
C
      VIS=1.003E-6
C          VIS IS THE KINEMATIC VISCOCITY OF WATER IN M2S-1
C          THE VALUE IS BASED ON AN AVERAGE TEMP OF 20OC
      SC=VIS*24*3600/DL
      E=0.36
C          E IS POROSITY, DIMENSIONLESS
      DP=3
C          DP IS DIAMETER OF GLASS BEADS IN MM
C
      DF=DL/DR
      SMINR = SMIN/SK
      T=DSQRT(SK*DF/XFK)
      TS=DSQRT(SK*DF*XFK*1000*1000)
C                    RESET SUM AS ZERO
      SUM=0.0
C                    CONSTANTS FOR PENALTY FUNCTIONS
C
C                    START DO LOOP TO CALCULATE FLUXC FOR
```

```fortran
C                          EACH GIVEN SE
      DO 22 I5=1,NT
      R=V(I5)*DP/(VIS*3600*1000)
C                                V=RECYCLE RATE IN M/H
      TL(I5)=DP/(1000.*(2.+0.644*R**0.5*SC**(1./3.))*(1+1.5*(1-E)))
      RL = TL(I5)/T
C   PRINT *, TL(I5), DF, SMIN
      FLUXCR=FLUXC(I5)/DSQRT(XFK*SK*DF*1000*1000)
      SECR=SEC(I5)/SK
      RLD = RL/DR
C
      SIGN=1+SECR-RLD*FLUXCR
      IF (SIGN.LE.0.0) THEN
      PRINT *, 'KS TOO HIGH OR DL TOO LOW OR J #',I5,' IS TOO HIGH!'
      PRINT *, '1+SS* = ', SIGN
      STOP
      END IF
C
C              START MATRIX CALCULATION
C     S1=JC*, S2=SEC*, S3=L*/D*, S4=SMIN*,S5=SQRT(KXFKSDF),S6=KS
      SUM=SUM+(G(FLUXCR,SECR,RLD,SMINR)+GJ(FLUXCR,SECR,RLD,
     &   SMINR,TS)*(FLUX(I5)-FLUXC(I5))+GS(FLUXCR,SECR,RLD,
     &   SMINR,SK)*(SE(I5)-SEC(I5)))**2/((GJ(FLUXCR,SECR,RLD,SMINR,
     &   TS)*DJ(I5))**2+(GS(FLUXCR,SECR,RLD,SMINR,SK)*
     &   DS(I5))**2)
22    CONTINUE
C
      RETURN
      END
C********************************************************************
C       A SUNBROUTINE TO RENEW THE "REAL" VALUES FOR J AND SE
C********************************************************************
      SUBROUTINE NEW (XFK, SK, DL, SMIN)
C
```

```
      IMPLICIT  REAL*8  (A-H,O-Z)
      PARAMETER (NT=9)
      DIMENSION SE(NT),SEC(NT),TL(NT),V(NT),FLUX(NT),FLUXC(NT),
     &      SS(NT),DJ(NT),DS(NT)
      COMMON /C1/V,T,TL,FLUX,FLUXC,DJ,SE,SEC,DS,SS,RES2,DR
      EXTERNAL G, GJ, GS
C
C                       SETTING VALUES FOR CONSTANTS
C
      VIS=1.003E-6
C             VIS IS THE KINEMATIC VISCOCITY OF WATER IN M2S-1
C             THE VALUE IS BASED ON AN AVERAGE TEMP OF 20OC
      SC=VIS*24.*3600./DL
      E=0.36
C             E IS POROSITY, DIMENSIONLESS
      DP=3
C             DP IS DIAMETER OF GLASS BEADS IN MM
C
      DF=DL/DR
      SMINR = SMIN/SK
      T=DSQRT(SK*DF/XFK)
      TS=DSQRT(SK*DF*XFK*1000*1000)
C                       RESET RES2 AS ZERO
      RES2=0.0
C                START DO LOOP TO CALCULATE FLUXC FOR
C                       EACH GIVEN SE
      DO 33  I6=1,NT
      R=V(I6)*DP/(VIS*3600.*1000.)
C                       V=RECYCLE RATE IN M/H
      TL(I6)=DP/(1000.*(2.+0.644*R**0.5*SC**(1./3.))*(1+1.5*(1-E)))
      RL = TL(I6)/T
      FLUXCR=FLUXC(I6)/DSQRT(XFK*SK*DF*1000*1000)
      SECR=SEC(I6)/SK
      RLD=RL/DR
```

```fortran
C                 START MATRIX CALCULATION
C      S1=JC*, S2=SEC*, S3=L*/D*, S4=SMIN*,S5=SQRT(KXFKSDF),S6=KS
       FLUXC(I6)=FLUX(I6)-(G(FLUXCR,SECR,RLD,SMINR)+GJ(FLUXCR,
     &    SECR,RLD,SMINR,TS)*(FLUX(I6)-FLUXC(I6))+GS(FLUXCR,
     &    SECR,RLD,SMINR,SK)*(SE(I6)-SEC(I6)))*GJ(FLUXCR,
     &    SECR,RLD,SMINR,TS)*DJ(I6)**2/((GJ(FLUXCR,SECR,RLD,SMINR,
     &    TS)*DJ(I6))**2+(GS(FLUXCR,SECR,RLD,SMINR,SK)*
     &    DS(I6))**2)
       SEC(I6)=SE(I6)-(G(FLUXCR,SECR,RLD,SMINR)+GJ(FLUXCR,SECR,
     &    RLD,SMINR,TS)*(FLUX(I6)-FLUXC(I6))+GS(FLUXCR,SECR,
     &    RLD,SMINR,SK)*(SE(I6)-SEC(I6)))*GS(FLUXCR,SECR,RLD,
     &    SMINR,SK)*DS(I6)**2/((GJ(FLUXCR,SECR,RLD,SMINR,
     &    TS)*DJ(I6))**2+(GS(FLUXCR,SECR,RLD,SMINR,SK)*
     &    DS(I6))**2)
       SS(I6) = SEC(I6)-TL(I6)*FLUXC(I6)/(DL*1000)
       RES2 = RES2+(SE(I6)-SEC(I6))**2
33     CONTINUE
C
       RETURN
       END
C
C*******************************************************************
**
C                 DECLARE EXTERNAL FUNCTIONS
C*******************************************************************
C
C*******************************************************************
       FUNCTION G(S1,S2,S3,S4)
C      S1=JC*, S2=SEC*, S3=L*/D*, S4=SMIN*,S5=SQRT(KXFKSDF),S6=KS
C*******************************************************************
       IMPLICIT  REAL*8 (A-H,O-Z)
C
       G=(S1**2/2)-((S2-S3*S1)-DLOG(1+S2-S3*S1))*DTANH((1.5557-0.4117*
     &   DTANH(DLOG10(S4)))*((S2-S3*S1)/S4-1)**(0.5035-0.0257*
```

```fortran
     &  DTANH(DLOG10(S4))))**2
C
      RETURN
      END
C**********************************************************************
      FUNCTION GJ(S1,S2,S3,S4,S5)
C     S1=JC*, S2=SEC*, S3=L*/D*, S4=SMIN*,S5=SQRT(KXFKSDF),S6=KS
C**********************************************************************
      IMPLICIT  REAL*8  (A-H,O-Z)
C
      GJ=S1/S5+(S3/S5)*(S2-S3*S1)/(1+S2-S3*S1)*
     &  DTANH(DGAMA(S4)*((S2-S3*S1)/S4-1)**DBETA(S4))**2+
     &  ((S2-S3*S1)-DLOG(1+S2-S3*S1))*
     &  2*DTANH(DGAMA(S4)*((S2-S3*S1)/S4-1)**DBETA(S4))*
     &  DSECH(DGAMA(S4)*((S2-S3*S1)/S4-1)**DBETA(S4))**2*
     &  DBETA(S4)*DGAMA(S4)*((S2-S3*S1)/S4-1)**(DBETA(S4)-1)*
     &  S3/(S4*S5)
C
      RETURN
      END
C**********************************************************************
      FUNCTION GS(S1,S2,S3,S4,S6)
C     S1=JC*, S2=SEC*, S3=L*/D*, S4=SMIN*,S5=SQRT(KXFKSDF),S6=KS
C**********************************************************************
      IMPLICIT  REAL*8  (A-H,O-Z)
C
      GS=(1/S6)*((S3*S1-S2)/(1+S2-S3*S1))*
     &  DTANH(DGAMA(S4)*((S2-S3*S1)/S4-1)**DBETA(S4))**2-
     &  ((S2-S3*S1)-DLOG(1+S2-S3*S1))*
     &  2* DTANH(DGAMA(S4)*((S2-S3*S1)/S4-1)**DBETA(S4))*
     &  DSECH(DGAMA(S4)*((S2-S3*S1)/S4-1)**DBETA(S4))**2*
     &  DBETA(S4)*DGAMA(S4)*((S2-S3*S1)/S4-1)**(DBETA(S4)-1)*
     &  (1/(S4*S6))
C
```

```fortran
      RETURN
      END
C*********************************************************************
      FUNCTION DGAMA(S4)
C     S4=SMIN*
C*********************************************************************
      IMPLICIT  REAL*8  (A-H,O-Z)
C
      DGAMA=1.5557-0.4117*DTANH(DLOG10(S4))
C
      RETURN
      END
C*********************************************************************
      FUNCTION DBETA(S4)
C     S4=SMIN*
C*********************************************************************
      IMPLICIT  REAL*8  (A-H,O-Z)
C
      DBETA=0.5035-0.0257*DTANH(DLOG10(S4))
C
      RETURN
      END
```

Output Sample for CMBR Biofilm Reactors

COMPUTATION OUTPUT FOR OZONATED WATER

PARAMETERS	(KXF	KS	D	SMIN)
THE INITIAL GUESS IS	(0.100E+08	0.600E+04	0.130E-03	0.100E+02)
THE LOWER BOUND IS	(0.500E+02	0.450E+04	0.100E-04	0.100E+01)
THE UPPER BOUND IS	(0.100E+09	0.100E+06	0.140E-03	0.180E+02)

THE SOLUTION IS (0.995E+08   0.457E+04   0.321E-04 0.119E+02)

THE FUNCTION VALUE IS   0.209E+02

THE SOLUTION IS (0.507E+08   0.448E+05   0.140E-03   0.142E+02)

THE FUNCTION VALUE IS   0.256E+02

THE SOLUTION IS (0.570E+08   0.456E+05   0.132E-03   0.142E+02)

THE FUNCTION VALUE IS   0.258E+02

THE SOLUTION IS (0.675E+08   0.513E+05   0.127E-03   0.141E+02)

THE FUNCTION VALUE IS   0.258E+02

THE SOLUTION IS (0.718E+08   0.547E+05   0.127E-03   0.143E+02)

THE FUNCTION VALUE IS   0.258E+02

THE SOLUTION IS (0.718E+08   0.547E+05   0.127E-03   0.143E+02)

THE FUNCTION VALUE IS   0.258E+02

THE FINAL SOLUTION IS:

τ = 0.220E-03   KXF= 0.718E+08 KS= 0.547E+05 D= 0.127E-03
SMIN= 14.256 K= 0.239E+01

********* ********* ********* ********* ********* ********* *********
 SE   SEC   FLUX   FLUXC   L   SS

4.46E+01   5.17E+01   1.35E+04   1.15E+04   1.06E-04   4.21E+01
7.31E+01   5.85E+01   1.15E+04   1.32E+04   1.05E-04   4.77E+01
2.41E+02   2.40E+02   5.56E+04   5.59E+04   1.05E-04   1.94E+02
2.76E+02   2.95E+02   7.85E+04   6.88E+04   1.05E-04   2.39E+02
1.92E+02   2.01E+02   5.06E+04   4.68E+04   1.05E-04   1.63E+02
3.18E+02   3.40E+02   8.66E+04   7.92E+04   1.05E-04   2.75E+02
1.94E+01   1.95E+01   2.78E+03   2.77E+03   1.05E-04   1.72E+01
1.11E+02   1.02E+02   2.23E+04   2.35E+04   1.05E-04   8.25E+01
1.65E+02   1.27E+02   2.56E+04   2.94E+04   1.05E-04   1.03E+02

APPENDIX 4: APPLICATION OF X* IN PROCESS DESIGN - AN EXAMPLE

The following is an example which demonstrates how a typical curve of percentage BOM removal versus dimensionless detention time (X^*) can be used for designing a biofilm filter.

Assumptions

The following assumptions are provided based on typical values presented in Tables 2-1 and 2-3:

- Average Influent AOC = 250 µg acetate C/L

- Media Diameter d_{p-60} = 1.25 mm (i.e. α=5000 m^{-1})

- Average AOC Diffusivity D = 4×10^{-5} m^{2}d^{-1} and D_f=0.5D = 2×10^{-5} m^{2}d^{-1}

- kX_f/K_s = 20 d^{-1}

- Typical curve of % Removal vs X^* as per Figure 2-8

It should be noted that the influence of temperature on process performance has be implied in the given values of kinetic parameters and substrate diffusivity. More real-time information is required to develop the relationship between temperature and the values of kinetic parameters and substrate diffusivity.

Design Objective

The objective of the design is to determine the detention times (θ) required for desired effluent AOC concentrations of 50 and 25 mg acetate C/L respectively.

Calculation

By definition in Chapter 2:

$$X^* = \theta \alpha D_f / \tau$$ (1)

Equation (1) can be rearranged as

$$\theta = (\tau / \alpha D_f) X^*$$ (2)

By definition in Chapter 2:

$$\tau = [D_f/(kX_f/K_s)]^{(1/2)} = (2\times10^{-5}\,m^2d^{-1}/20d^{-1})^{(1/2)} = 10^{-3}\,m$$

Substitute the values of τ, α, and D_f into equation (2)

$$\theta = [(10^{-3}\,m/(5000\,m^{-1}\times2\times10^{-5}\,m^2d^{-1})]X^* = 0.01X^* \text{ (d)} \qquad (3)$$

For desired effluent AOC of 50 μg acetate C/L

$$\text{\% Removal} = 100\%\times(250-50)/250 = 80\%$$

From the curve in Figure 2-8, X* value of approximately 1.5 is required for 80% removal. Using equation (3),

$$\theta = 0.01X^* \text{ (d)} = 0.01\times1.5\times60\times24 \text{ (min)} = 21.6\ min$$

For desired effluent AOC of 25 μg acetate C/L

$$\text{\% Removal} = 100\%\times(250-25)/250 = 90\%$$

From the curve in Figure 2-8, X* value of approximately 2.5 is required for 90% removal. Using equation (3),

$$\theta = 0.01X^* \text{ (d)} = 0.01\times2.5\times60\times24 \text{ (min)} = 36.0\ min$$

Results

A biofilter with detention time of 21.6 min is required to achieve a effluent concentration of 50 μg acetate C/L. A 67% increase of detention time to 36.0 min is required to achieve effluent concentration of 25 μg acetate C/L or additional 10% of removal.